**Optimization of scalaBle rEaltime modeLs and functIonal testing for e-drive ConceptS**

**EUROPEAN COMMISSION**
**Horizon 2020**
**GV-07-2017**
**GA # 769506**

| | | |
|---|---|---|
| **Deliverable No.** | OBELICS D7.5 | |
| **Deliverable Title** | Optimization of OBELICS test procedures | |
| **Deliverable Date** | 2018-05-30 | |
| **Deliverable Type** | REPORT | |
| **Dissemination level** | Public (PU) | |
| **Written By** | Yousef Firouz (VUB)<br>Sahar Khaleghi (VUB)<br>Edoardo Locorotondo (UNIFI)<br>Lorenzo Berzi (UNIFI)<br>Roland Platz (FHG-LBF)<br>Jürgen Nuffer (FHG-LBF)<br>Matthias Rauschenbach (FHG-LBF) | 2018-04-30<br>2018-04-30<br>2018-04-30<br>2018-04-30<br>2018-04-30<br>2018-04-30<br>2018-04-30 |
| **Reviewed by** | Thilo Bein (FHG-LBF)<br>Tomaž Katrašnik (UL) | 2018-05-25<br>2018-05-25 |
| **Approved by** | Horst Pfluegl (AVL) – Project Coordinator | 2018-05-28 |
| **Status** | Final | 2018-05-29 |

## Contents

## Figures

## Tables

## Publishable Executive Summary

# 1. Purpose of the document

The purpose of this document is to develop test methodologies from previous and current battery characterization procedures of partners and use them together with the future outcome of WP2 in order to standardize test protocols among partners. The introduced test methodologies in this report are developed based on the international standardization community (IEC, ISO) and in particular based on CEN-CENELEC. Partners involved in this deliverable, summarized their test procedure for battery cell characterization and battery pack safety tests. Furthermore, the standard specific tests and procedures for offline and online parameter identification purposes have been gathered. This deliverable will investigate on automated methods and procedures for parameter identification of physical and/or empiric models of batteries as well as the online state estimation such as state of charge (SoC).

## 1.1 Document Structure

1. Introduction
2. Battery cell characterization and identification test procedure (VUB)
3. Battery pack characterization and safety test procedure (FHG-LBF)
4. State estimation (UNIFI)
5. Creating Real World related methods for electric vehicles (UNIFI)

## 1.2 Deviations from original Description in the Grant Agreement Annex 1 Part A

### 1.2.1 Description of work related to deliverable in GA Annex 1 – Part A

**Task 7.2: Optimization of OBELICS test procedures as a common test tool among the partners (LEAD: VUB, Partners: UNIFI, FHG) [M1-8]**
Optimization of developed test methodologies in WP2 and converting them into standardized test protocols among partners. Proposal to present adapted test procedure to the international standardization community (IEC, ISO) and in particular to CEN-CENELEC, who is responsible for adopting international standards as European standards, the actual drafting of standards now mostly being performed on a global level. Following the proper procedures, this proposal will take the shape of a New Work Item Proposal.
This task will allow investigating on reliable and automated methods and procedures for parameter identification of physical and/or empiric models of batteries (state of charge and health, lifetime, etc.).
**UNIFI** will contribute with optimization of the test procedures for OBELICS according to the results of former WPs. Guidelines for the integration of such data in a reliability and availability assessment framework will also be provided.
**FhG** will contribute to defining the most appropriate test procedures from safety point of view.

### 1.2.2 Time deviations from original planning in GA Annex 1 – Part A

There are no deviations with respect to the timing of this deliverable.

### 1.2.3 Content deviations from original plan in GA Annex 1 – Part A

There are no deviations from the Annex 1 – Part A with respect to the content.

# 2 Introduction

Battery Characterization tests are the most important step towards the modelling, performance analysis, aging and safety measurement. Due to confidentiality and/or safety issues there is no access to the exact material's parameters or cell configuration. For this reason, the battery is considered as a black box and characterization tests will be performed in order to parametrize the assigned model which simulates battery behaviors. The aim of this document is to establish a harmonized testing protocol for the cell testing procedures. This document starts with the battery cell, as the very basic and essential component, characterization test procedures. All the standard tests which need to be performed on the cells have been categorized and some test's parameters have been suggested based on the previous experiences.

In next part of the document, the characterization and safety test procedures related to the battery pack have been listed. As energy storage system (battery pack) contributes highly to the overall mass and cost of the vehicle it has to undergo severe multi-physical testing for guaranteeing a high level of system reliability and safety.

All mentioned steps regarding testing the cells and battery pack will lead to battery modeling and online state estimation. Online parameter identification helps to have an accurate estimation of the battery status and correct functioning of battery monitoring and management system (BMS).

In case of battery cell characterization, this document is organized to follow a chronological order. Thus, it begins with the cell connections suggestions; then it follows with the BOL characterization testing, the periodic check-ups and finally the EOL characterization testing. This document focuses on the detailed description of test procedures and specific sequences of tests as a function of the characterization testing. Most of the sequences described here will be included in the detailed description of several test procedures that will be defined within WP2. Therefore, this report is not representing official OBELICS test procedure nor state of the art test procedure which is used by partners. Rather, this report presenting the regular standard-based test procedures which already have been utilized by involved partners.

# 3 Battery cell characterization and identification test procedures

## 3.1 Definitions

- **Beginning of Life – BOL**: At BOL a procedure is foreseen to determine the cell characteristics at the beginning of any testing work. The characteristics of the cell at BOL will be determined with some performance characterization tests and a Short-IPIT for the electrochemical characterization. This is due to the fact that cells could be stored before use which could lead to ageing and also change in their material properties.

- **Actual Capacity – Cact:** Describes the capacity (Ah) that can be discharged until EODV on discharge at C/3 and 25°C from a completely charged cell that was charged at a current rate of C/3 and at 25°C (CCCV). This gives the reference to the irreversible loss of capacity over the ageing. The rest time between charging and discharging is 30 min. It is calculated as the mean value of results from 2 measurements (according to the capacity tests in sections 3.5.3, 3.7.1.3, 3.7.2.3 and 3.8.3).

- **Initial Reference Capacity – Cinit:** It is the actual capacity, expressed in Ampere-hours, at the Begin-of-Life of the battery (as described in section 3.5.3).

- **Nominal Capacity – Cnom:** This is the capacity, expressed in Ampere-hours, stated by the manufacturer at specific conditions.

- **C-Rate:** Coefficient of the nominal capacity of the battery (expressed in $h^{-1}$) determines the charging or discharging current value so, the time needed to perform a complete charge or discharge. Example: If a Current of $I = 5A$ is used in a system with a nominal capacity of $C_{nom} = 1Ah$, then we have: C-rate $= \frac{Current}{C_{nom}} = \frac{5A}{1Ah} = 5\ h^{-1}$). In the test performed, the current reference will be maintained constant in relation to the nominal capacity of the battery. According to the values given by the ISO 12405-2 and the IEC 62660-1 for BEV applications, the C-rate will be C/3 which corresponds to $I = \text{C\_rate}/3$.

- **Checkup – CU:** A checkup contains a determined sequence of characterization tests. It is supposed to check the performance of the battery under test periodically and to obtain some useful parameters for other purposes, like: modelling, validation, comparison, etc.

- **Maximum Voltage (Charge Voltage Limit) – CVL:** The CVL is the maximum allowed charge voltage value, proposed by the battery manufacturer.

- **Minimum Voltage (Discharge Voltage Limit) – DVL:** The DVL is the minimum battery voltage value, proposed by the battery manufacturer.

- **End of Charge Voltage – EOCV:** Cut-off voltage for constant current charging and constant voltage charging, given by the battery manufacturer.

- **End of Discharge Voltage – EODV:** Cut-off voltage is the minimum voltage value reached in a discharge process given by the battery manufacturer.

- **End of Life – EOL:** EOL, according to the standard ISO 12405-1/2, is the condition of a battery at which its actual capacity has lowered to a value of 80% or less of the initial capacity of the battery. It is defined as the point in time when the properties of the cell show that the cell cannot be used for the given purpose (maintain a specific driving range in automotive applications). In this work the actual capacity will be measured according to the capacity test procedure, defined in sections 3.5.3, 3.7.1.3, 3.7.2.3 and 3.8.3.

- **End of Test – EOT:** In the cases in which, even before reaching the EOL, the cycling cannot be performed, the test will be ended. When a battery test is finished due to any possible reason than what has been specified in EOL paragraph, one can say the battery has reached its EOT or an EOT condition.

- **Energy Roundtrip Efficiency**: The energy roundtrip efficiency is calculated as the ratio between the charged and the discharged energy. It can be calculated as follows:

$$\eta(\%) = \frac{Energy\ DCH}{Energy\ CHA} = \frac{E_{DCH}(Wh)}{E_{CHA}(Wh)} \cdot 100$$

Equation 3-1 Energy roundtrip efficiency

- **Equilibrium Voltage:** The voltage measured at the rest time in concrete state conditions (temperature, SOC …).

- **Full equivalent cycles – FEC:** In cases in which the cycling is performed with a DOD inferior to 100%, the FEC represents the number of equivalent cycles at 100% DOD, in order to compare cell degradation with the same amount of Ah throughput (charged and discharged Ah). $FEC = (Number\ of\ cycles * DOD)$ of each cycling type.

- **Hybrid Pulse Power Characterization – HPPC:** A test procedure, consisting of pulse trains, whose results are used to calculate pulse power and energy capabilities of the cell. The internal resistance values are also obtained as an indicator of the power capabilities of the cell.

- **Impedance Parameter Identification Test – IPIT:** Routinely the electric cell properties will be investigated with the electrochemical impedance spectroscopy (EIS).

- **Open-Circuit Voltage – OCV:** The OCV is defined as the voltage measured between terminals of the cell at rest since a certain period (depending on the stabilization of the voltage) with no load connected to it. The OCV changes with the SOC and the temperature.

- **Reference current – Iref:** In the test performed in this project, the current reference will be maintained constant in relation to the nominal capacity of the battery.

- **Remaining useful life – RUL:** Describes the ageing of the battery scaled from the 100% to the EOL. Thus, at the BOL the remaining useful life will be RUL=100% and at the EOL it will be RUL=0%.

$$RUL(\%) = 100.(1 - \frac{\Delta C}{1 - EOL})$$

Equation 3-2: Calculation of RUL

- **Room temperature – RT:** Room temperature is defined as T = 25 °C (± 1°C). Tests at RT have to be done in temperature chambers.

- **Standard Charge – S-CHA:** The standard charge is the charging procedure that will be used in most characterization tests. It is thought to completely recharge the battery following a CC-CV procedure with the reference current value defined before (C/3). In **Error! Reference source not found.** the charging procedure can be seen:

Table 3-1: Standard charge procedure

| Step | Action | Current (A) | Limit |
|---|---|---|---|
| 1 | CC CHA | (C/3) | > EOCV |
| 2 | CV CHA | 1 | <0.05 C-Rate |
| 3 | Pause | 0 | 30 min |

- **State of Health – SOH (First Life):** Describes the ageing of the battery. The SOH is defined as follows:

$$SOH = 100\% - \Delta C$$

Equation3-3: SOH

**At the BOL, the state of health will be SOH=100% and at the EOL, it will be SOH=80%.**

- **Capacity Fade – ΔC:** The loss of capacity measured as a function of time of ageing test with respect to the initial capacity. The capacity fade is calculated by the given formula, where $t_0$ is the value at the beginning of the test and $t_1$ is the value at a given point in time.

$$\Delta C\,(\%) = 100 \cdot \left(1 - \frac{C_{act}(t_1)}{C_{act}(t_0)}\right)$$

Equation 3-4: Capacity Fade (ΔC)

## 3.2 Introduction:

This part of the report focuses on establishing a consistent testing protocol for the cell testing procedures.
It begins with the cell reception procedure and continues with the cell connections suggestions; then it will be progressed with the BOL characterization testing, the periodic checkups and finally the EOL characterization testing.
**Error! Reference source not found.**, shows the chronological test sequence, beginning with the cell reception and continuing with the test schedule corresponding to each task (ageing, extreme conditions testing…).
Furthermore, there is focus on the comprehensive description of test procedures and specific sequences of tests as the purpose of the characterization testing. Finally, it is worth to mention that on each test, the SOC levels are calculated according to the actual reference capacity values obtained in the capacity test, while the C-rates are maintained constant as explained before, in section 3.1

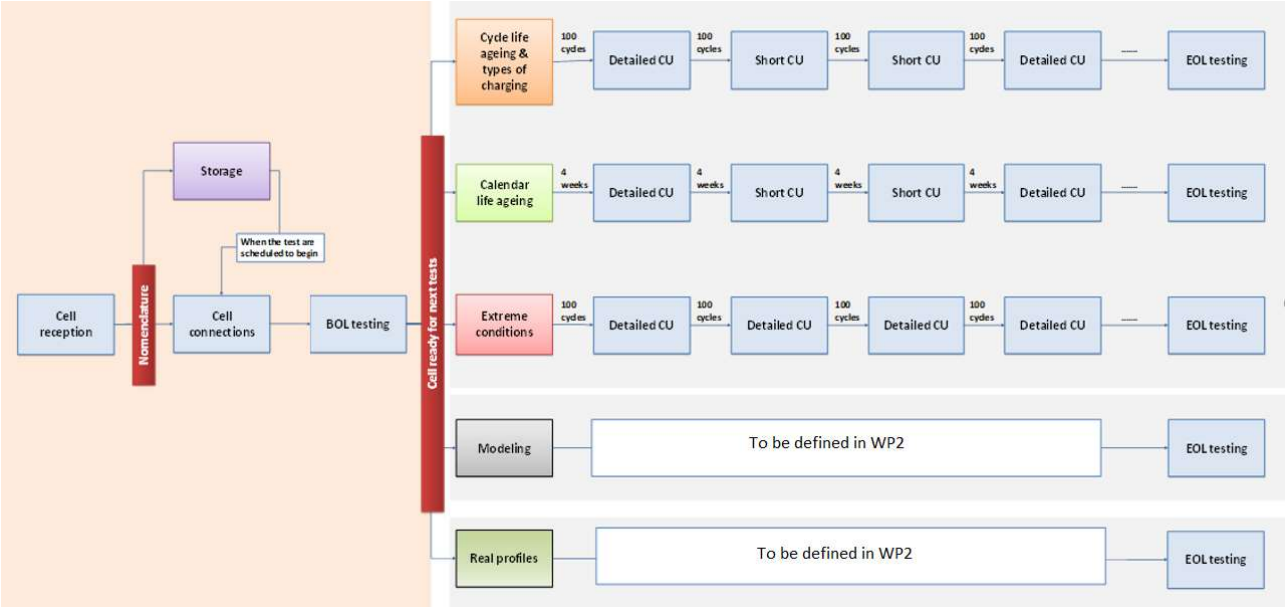


Figure 3-1: Chronological sequence to be followed during the battery testing

## 3.3 Cell Reception

Having manufactured the cells, some criteria might be specified to ensure a high comparability level among various centers involved in the battery testing. Thus, some information related to the cell reception procedure is collected regarding the nomenclature, cell storage conditions before testing and cell pre-conditioning.

### 3.3.1 Nomenclature

The nomenclature of cells should represent some information about them such as:

- Cell type/chemistry (NMC, LFP, LTO, …)
- Cell consecutive number (from 1 to XXX) + batch number: (XXXBX)
- Test type:
    - First Life Cycling Ageing Tests: FLC
    - First Life Storage Ageing Tests: FLS
    - Modelling Tests: M
    - Validation tests: V
    - …

So, the nomenclature that will be used could follow the following format:

NMC-XXXBX-FLC

Cells used for second life (after first life ageing is finished), may also include extra labels added to the previous nomenclature, such as SLS (Second Life Storage or calendar ageing) or SLC (Second Life Cycling ageing).

### 3.3.2 Storage before testing

In terms of storage before testing (and also for long-term storage) some consideration has been taken into account: (As NMC cells (FIAT 500e) have been considered for OBELICS use cases, all numbers mentioned in section 3 refers to NMC batteries)

- Cells will be delivered at 50 % SOC and a voltage of 3.7 V
- Cells must be stored in dry conditions at 25°C. (20-25°C)
- Cells must be stored at 50 % SOC (actual capacity) and a voltage of 3.7 V
- Cells must be charged after 3 months to 50 % SOC and a voltage of 3.7 V
- Cells must be stored in the blister in which they will be delivered

After the storage period, when the cells are intended to be used for experimentation, the connectors will be mounted (Section 3.4) and the BOL testing (Section 3.5) will be performed as shown in **Error! Reference source not found.**.

### 3.3.3 Cell pre-conditioning

In this case, an electrical formation is not essential. All cells will have the same formation and electrical treatment. The cells will be shipped at 50 % SOC and 3.7 V.

### 3.3.4 Storage between tests

Considering the storage between tests (less than one week), it has been determined that the cells should not be stored at SOC levels below 20% and voltage below 3.5V. In this case, removing the connectors before storing the cells and storing them in the blisters is not obligatory. For the period of longer than a week, cells must be stored at 50 % SOC (of the actual capacity) and at a voltage of 3.7 V (Section 3.3.2).

## 3.4 Cell Connections

Ensuring the data reproducibility and reliability, it is critical that the current and voltage wires are connected to the cells correctly. Once the cell reception procedure is completed, the following steps must be taken to mount the cell connectors appropriately before the BOL testing. In this way, when the whole procedure is concluded, the cells will be organized for the BOL test sequence as well as, for any characterization or ageing test procedure.

### 3.4.1 Description

The wire length is depending on the location of the equipment in the laboratory. In addition, the required wire diameter depends on the current rates to be used. The dimensions of the wires could lead to losses so, the cell connection criteria should be considered before the start of any measurement.
For this reason, the connection bench should be designed in a way that an ideal connection with minimum resistance, as well as non-additional heating, will be achieved. Moreover, the connection bench must allow the connections to be done easily, quickly and reliably, and reducing any risks for short-circuiting the cells.

### 3.4.2 Connectors

Terminals are then placed between two nickel plates and copper plates with holes, allowing attachment of the connection wires directly to the cell terminals (**Error! Reference source not found.**). The contact between terminal and nickel plates must be faultless. To make it possible, a dynamometric key could be used so that, the torque applied can be controlled (5Nm).
All small holes between the terminal and used connection bars have been filled with special conducting paste. The layer of the conductive paste should be placed as it is indicated in **Error! Reference source not found.** in order to assure large contact surface area and low resistance between the cell terminals and fixture.

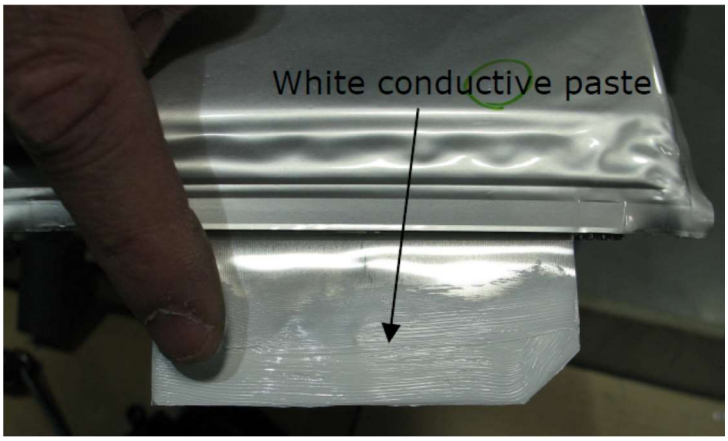


Figure 3-2: White conductive paste applied to the cell terminal

The number of holes in each tab must be 3, since it is recommended not to make current and voltage measurements at the same point to avoid voltage drops due to the current circulation through the terminals; one will be made in the nickel plates and the other one will be in the terminals of the cell (to measure the voltage directly from the cell terminals). Apart from those two holes, another extra hole is located on the nickel plates to mount the connectors that will be used to perform the IPIT tests as it can be seen in **Error! Reference source not found.**

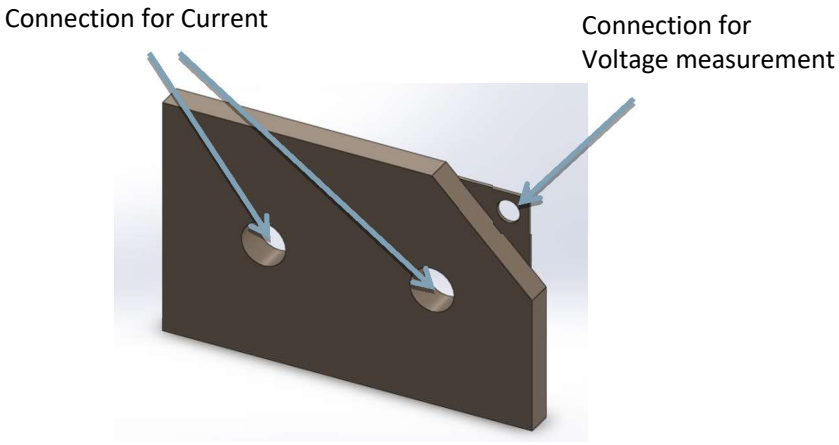


Figure 3-3: Nickel plates with holes for current and the terminal with the hole for voltage measurement

Furthermore, it is proposed to use connectors like those which shown in **Error! Reference source not found.** (as the purpose of comfort). The wires from the battery test station used for voltage sensing could have an outlet connector and connected to a socket coming from the cell terminal easily.

Figure 3-4: XT-60 Connector

Advantages of optimal connection, where higher discharge capacities are measured, would be that complete charge is ensured by means of the CC mode, improving the process efficiency and lower deviation between measurements. This is especially true for higher current rates. For frequently changed cells, calendric ageing cells, a connection of the current cables should also be used to minimize the stress at the cell connectors (**Error! Reference source not found.**). The influence of the resistance and heat generation of the connectors can be neglected up to 200A.

Figure 3-5: Connectors to be used for current cables

### 3.4.3 Low resistance electrical connection verification test

To evaluate connection quality of the cell terminals, the voltage drop between terminal of the cell and the current cables has to be measured, so that resistance of connectors can be assessed. In this case, as the resistance value should be very low, the quantities should be made by measuring the voltage drop during a short CC discharge. Either way, those measurements have to be performed on every cell in order to ensure correct connection. Furthermore, the measured resistance values should be clarified.

### 3.4.4 Cables

It is recommended to twist the wires of the load cable together, also twisted them internally, and keep them separate from wires of the voltage sensing cable to avoid coupling effects between load cable and voltage sensing cables (during the Short-IPIT tests).
Twisting the cables reduces the induced currents formed on a cable pair while exposing to a magnetic field (origin of which could also be the current circulating through a conductor). Therefore, it is important to twist the current cables of the EIS meter to decrease the generated electromagnetic interference (EMI); additionally, twisting the voltage cables can increase their immunity against magnetic fields. In this way, the accuracy of the measurements is enhanced. In **Error! Reference source not found.**, it is illustrated how the cable pairs have to be twisted.

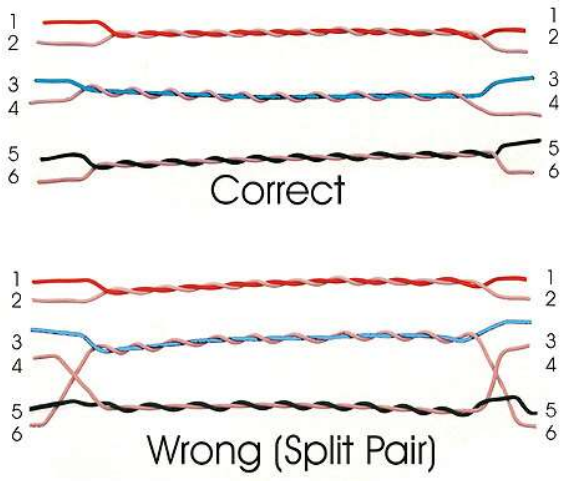

Figure 3-6: Illustration of inappropriate (lower) and proper (upper) cable twisting

## 3.5 BOL Testing

As mentioned in section 3.4, the cell connections should be mounted before the start of any ageing or modelling task and every cell has to be subjected to the BOL test sequence. The test sequence that should be followed is defined afterward. Then, each test procedure included in the test sequence is explained in detail. Notice that on each test, the SOC levels are calculated according to the actual capacity values obtained from the capacity test, while the C-rates are maintained constant as explained before in section 3.1.

### 3.5.1 BOL Test Sequence

The test sequence to be followed in this step is illustrated in **Error! Reference source not found.**.

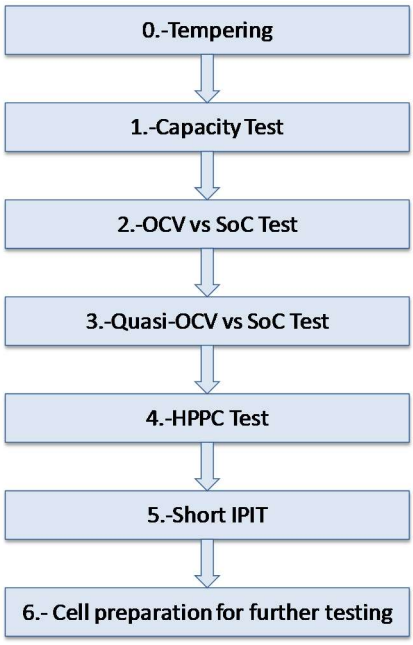


Figure 3-7: BOL test sequence

The test sequence initiates with a tempering process and it follows with 5 different test procedures and the results will be used as the reference for check-ups made during cycling and calendar ageing tasks. Finally, the preparation procedure is proposed to make the cell ready for the subsequent test procedure. The time required for the whole BOL test sequence is about 185h.

### 3.5.2 Tempering process

The test sequence has to start with a tempering process to ensure reducing the measurement and operation noise introduced on the results so that the comparability of the obtained results will be enhanced. It's worth to say that this process is not assumed as a test procedure exactly, rather some concrete considerations regarding the temperature measurements of the cells. In this way, three issues should be considered: the temperature measurements, the temperature control and the tempering procedure itself.

#### 3.5.2.1 Temperature measurements

The temperature will be measured by means of one thermocouple on each cell. This thermocouple must be located at the cell point. Some non-committal measurements with the thermal camera will be made by VUB in a preliminary phase to ensure where is the location of the hottest point on the surface of cells. The measurements will be repeated several times during the ageing of the cells to ensure that the hottest point continues to be the same or it gets changed during the ageing process.

Some measurements suggest that the hottest point of the cell will be the lower side of the cell. In each case, the mentioned non-committal measurements of the cell will allow checking of the hottest point and tracking evolution of thermal behaviour of the cell.

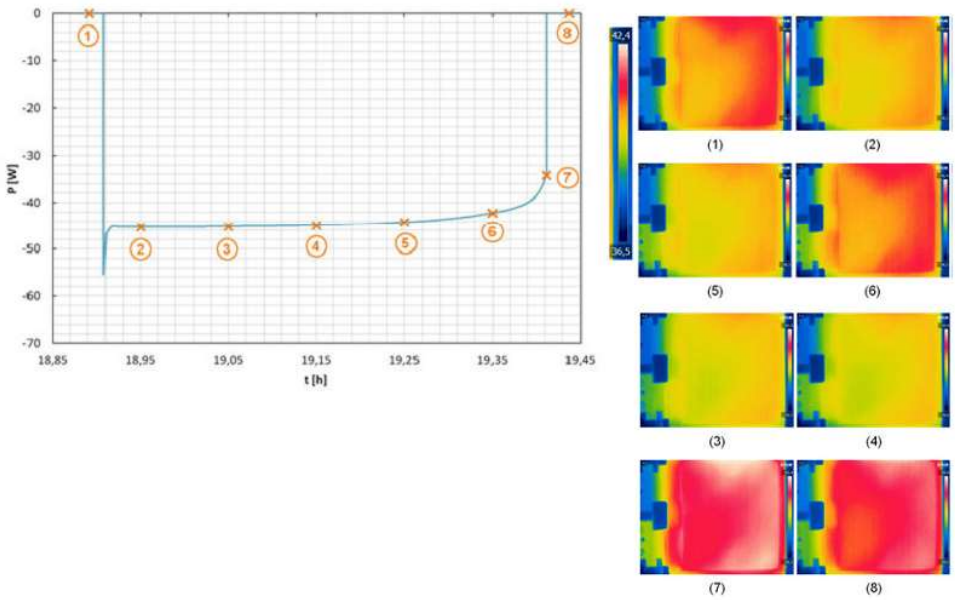


Figure 3-8: Measurements of cell temperature on commercial cells.

### 3.5.2.2 Temperature Control

As the cells don't face stress during the test procedures, it is not expected to observe high heat-generation. Therefore, to avoid the disregarding the real temperature of the cell, the climate chamber has to be set to 25°C for each test in the test sequence.

### 3.5.2.3 Tempering procedure

There is no specific procedure to follow for the tempering. However, it has been arranged that before any test sequence, if the temperature of the cell has achieved the desired 25°C, a rest period of 30min should be applied. So that, a suitable relaxation of the cell temperature is ensured.

### 3.5.3 Capacity test

The initial reference capacity will be measured at 25°C (after the tempering procedure). The determination of the capacity will start with a standard charge (as described in section 3.1). Then, after a pause period of 30 minutes, a discharge down to the EODV will be made, followed by a pause period of 30 minutes.

Table 3-2: Capacity test procedure

| Step | Action | Current (A) | Limit |
|---|---|---|---|
| 1 | Standard CHA | (C/3) | |
| 2 | PAU | 0 | 30 min |
| 3 | DCH | (C/3) | < EODV |
| 4 | PAU | 0 | 30 min |
| 5 | Repeat steps 1-4 | | 2 times |

Finally, another standard charging will be done. The steps will be repeated 2 times to measure the real capacity of the cell correctly. The capacity test lasts approximately 7x 2 = 14 hours.

#### 3.5.3.1 Analysis and documentation

During this phase, the following parameters have to be logged every 1 second:

- Cell Voltage $(V)$
- Cell Current $(A)$
- Charged/Discharged capacity $(Ah)$ on each charge/discharge step
- Charged/Discharged energy $(Wh)$ on each charge/discharge step
- Cell Temperature (°C)

The following results should be documented and analysed:

- Current, voltage and cell temperature versus time at each discharge test and standard charge.
- Discharged capacity in $Ah$, energy in $Wh$ and average power in $W$, at each discharge test.
- Charged capacity in $Ah$, energy in $Wh$ and average power in $W$, at each standard charge following each discharge test.
- Energy round trip efficiency at each discharge test.
- Discharged energy in $Wh$ as a function of SOC at each discharge test (in % of nominal capacity).
- The EODV of all available cell voltage measuring points for all performed discharge tests.
- Determined C/3 nominal capacity which is taken as the basic value for all further discharge current requirements.

### 3.5.4 OCV vs SOC test procedure

This procedure is used to specify the equilibrium voltage – DOD characteristic for a comparison of the Open Circuit Voltage (OCV) of the Cell at BOL and EOL. This cell's characteristic is also required for battery modelling. The equilibrium voltage for each SOC and both charge and discharge curves is determined as the value of the voltage measured after a 3-hour pause.
In order to determine the amount of Ah needed to be charged or discharged to establish a fixed SOC, the capacity value obtained in the previous capacity test for each cell will be used, respectively.
The time required for the OCV vs. SOC test is approximately 135 h.

**Table 3-3: OCV vs SOC test procedure**

| Step | Action | Current (A) | Limit |
|---|---|---|---|
| 1 | Standard charge (25°C) | (C/3) | |
| 2 | Pause (OCV Determination) | 0 | 3h |
| 3 | Discharge | (C/3) | ΔDOD=5% |
| 4 | Pause (OCV Determination) | 0 | 3h |

| | | | |
|---|---|---|---|
| 5 | Repeat 4. - 5. until EODV | | EODV |
| 6 | Pause (OCV Determination) | 0 | 3h |
| 7 | Charge | (C/3) | ΔDOD=5% |
| 8 | Pause (OCV Determination) | 0 | 3h |
| 9 | Repeat 7. - 8. until EOCV | | EOCV |

#### 3.5.4.1 Analysis and documentation

During this test, at least the following parameters have to be logged every 1 second:

- Cell Voltage $(V)$.
- Cell Current $(A)$.
- Charged/Discharged capacity $(Ah)$ on each charge/discharge step.
- Charged/Discharged energy $(Wh)$ on each charge/discharge step.
- Cell Temperature (°C).

The following results should be documented and analysed:

- Determination of the OCV-DOD Characteristic for each discharge step
- Determination of the OCV-DOD Characteristic for each charging step
- Determination of the OCV-DOD Characteristic for the average of each DOD step

### 3.5.5 HPPC test procedure

The purpose of the Hybrid Pulse Power Characterization Test (HPPC) is to measure the charge and discharge resistances and consequently the charge and discharge power of the cells at different SOCs, with different C-rates. It will characterize the cell at the BOL, the EOL and during the ageing tests. In detail, different discharge resistances, charge resistances, discharge powers and charge powers will be determined.
The test profile used in this case involves a pulse train with several discharge and charge pulses at different C-rates (0.5C, 1C, 1.5C, 2C and 2.5C) all calculated based on the nominal capacity of the cell which has been presented in **Error! Reference source not found.**. In this way, since the power capabilities of the cell are measured at different C-rates, the comparability between the various generations of the batteries will be ensured (that's why the current values are referred to the C-rate).

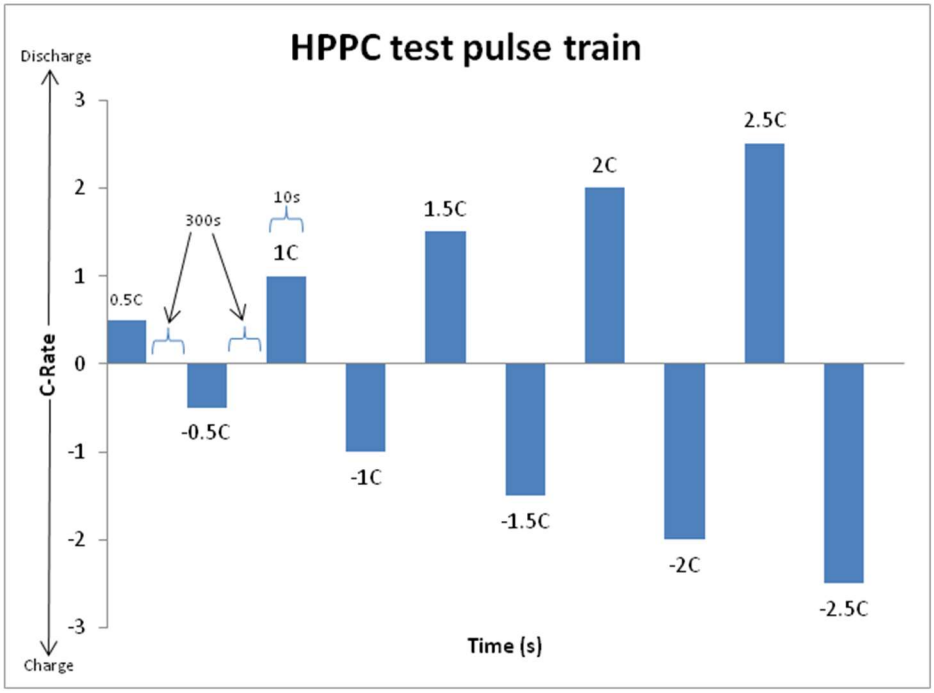


Figure 3-9: HPPC test pulse train

Every HPPC test will be performed at 25°C. The SOC in which the measurement is to be done needs to be fixed Ah-based, by means of the capacity value measured in the capacity test (see section 3.5.3). The time course of the pulse train according to the HPPC test is summarised in Table 3-45.

Table 3-4: HPPC test pulse train

| Time increment (s) | Accumulated Time (s) | Process |
|---|---|---|
| 10 | 10 | DCH 0,5C |
| 300 | 310 | PAU |
| 10 | 320 | CHA 0,5C |
| 300 | 620 | PAU |
| 10 | 630 | DCH 1C |
| 300 | 930 | PAU |
| 10 | 940 | CHA 1C |
| 300 | 1240 | PAU |
| 10 | 1250 | DCH 1,5C |
| 300 | 1550 | PAU |
| 10 | 1560 | CHA 1,5C |
| 300 | 1860 | PAU |
| 10 | 1890 | DCH 2C |
| 300 | 2190 | PAU |

| | | |
|---|---|---|
| 10 | 2200 | CHA 2C |
| 300 | 2500 | PAU |
| 10 | 2510 | DCH 2.5C |
| 300 | 2810 | PAU |
| 10 | 2820 | CHA 2.5C |
| 300 | 3120 | PAU |

Finally, the HPPC test procedure can be seen in table 3-6.

It takes approximately 10 hours to perform the HPPC test.

**Table 3-5: HPPC test pulse train**

| Step | Action | Current (A) | Limit |
|---|---|---|---|
| 1 | Standard Charge (25°C) | (C/3) | |
| 2 | PAU | 0 | 30 min |
| 3 | DCH | (C/3) | SOC (%) = 80, 50, 20 |
| 4 | PAU | 0 | 30 min |
| 5 | HPPC | | |
| 6 | Repeat steps 3-5 at SOC 80 %, 50%, 20% | | |

#### 3.5.5.1 Analysis and documentation:

During this test, at least the following parameters should be logged every 1 second during the pause periods and during the charge/discharge periods and every 10ms during the pulses:

- Cell Voltage $(V)$.
- Cell Current $(A)$.
- Charged/Discharged capacity $(Ah)$ in each charge/discharge step.
- Charged/Discharged energy $(Wh)$ in each charge/discharge step.
- Cell Temperature (°C).

The following results have to be documented and analysed:

- Charge and discharge power for 1s and 10s for every charge and discharge pulse in function of SOC.
- Charge and discharge resistance for 1s and 10s for every charge and discharge pulse as well as the overall resistance as a function of SOC.

### 3.5.6 Short-IPIT procedure

The “Short-IPIT” tests will be performed at different values of SOC and fixed on an Ah-basis to acquire information about the electrochemical properties of the cells during the ageing process. This test procedure uses the capacity value determined from the capacity test (see section 3.5.5).

To perform the Impedance parameterisation correctly, the following properties should be considered:

- Frequency Range from $f_{max} = 5\ kHz$ to $f_{min} = 5\ kHz$
- Frequency Distribution: 8 Frequencies / Decade
- Uideal = $8\ mV$
- The measurement has to be performed in temperature chambers at a constant temperature of 25 °C.

Before each IPIT, the cells have to be charged with the standard charge procedure (see section 3.1) at 25°C.
The time required for the whole test is 10 hours approximately.
In Table 3-67 specifications of the test procedure that should be followed are listed.

**Table 3-6: Short-IPIT test procedure**

| Step | Action | Limit | $\mathbf{f_{min}}$ | $\mathbf{f_{max}}$ | Current (A) |
|---|---|---|---|---|---|
| 1 | Standard Charge (25°C) | | | | (C/3) |
| 2 | Discharge to SOC = 80% | ΔDOD = 20 % | | | (C/3) |
| 3 | Pause | 30 min | | | 0 |
| 4 | Spectra @ 80% SOC | 1 h | 5 mHz | 5 kHz | Few mA |
| 5 | Discharge to SOC = 50% | ΔDOD = 30 % | | | (C/3) |
| 6 | Pause | 30 min | | | 0 |
| 7 | Spectra @ 50% SOC | 1 h | 5 mHz | 5 kHz | Few mA |
| 8 | Discharge to SOC = 20% | ΔDOD = 30 % | | | (C/3) |
| 9 | Pause | 30 min | | | 0 |
| 10 | Spectra @ 20% SOC | 1 h | 5 mHz | 5 kHz | Few mA |

#### 3.5.6.1 Analysis and documentation

During this test, at least the following parameters have to be logged every 1 second:

- Cell Voltage $(V)$.
- Cell Current $(A)$.
- Charged/Discharged capacity $(Ah)$ on each charge/discharge step.
- Charged/Discharged energy $(Wh)$ on each charge/discharge step.
- Cell Temperature (°C).

The following results have to be documented and analysed:

- Real Part of the Impedance $(RE(z))$
- Imaginary Part of the Impedance $(Im(z))$

- Cell Voltage ($U$)
- AC-Current ($IAC$)
- DC-Current ($IDC$)
- 0 C-Rate DC Spectra at = 20%, 50%, 80% SOC.

### 3.5.7 Cell preparation for further testing

To finish the whole test sequence, a standard charging (as described in section 3.1) should be performed to recharge the cell completely after the tests have been completed. Once the cell is recharged fully, it has to be discharged to the SOC in which the following test has to start (Ah-based discharge, calculated with the results obtained in the capacity test as described in section 3.5.3). In this way, it is ensured that this SOC is always obtained at 25°C.

## 3.6 Further testing: SOH & EOL definitions

The cells are ready for further tests, once BOL characterization has been achieved. The concrete procedures indicated in **Error! Reference source not found.**

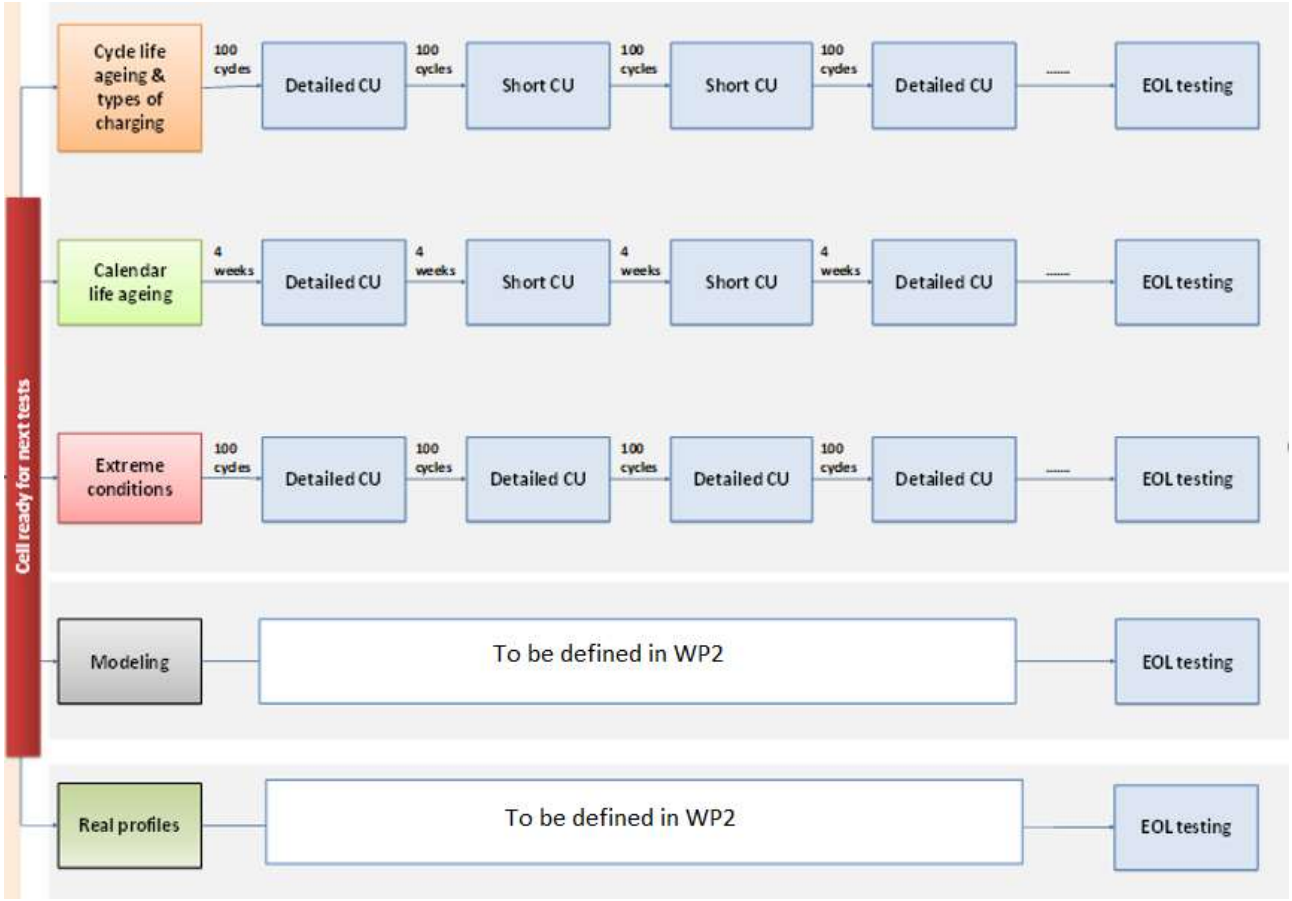


Figure 3-10: Test sequences to be performed

### 3.6.1 Quasi-OCV vs SOC test procedure

The "Quasi-OCV" approach is used as a time-efficient method to analyze the characteristic of the open circuit voltage over the state of charge. The measurement starts with a fully charged cell, which is discharged to EODV

with a small current (C/5 C-Rate). The current rate is assumed to be small enough for the voltage measured to be considered as "quasi-OCV". After this step, the cell is charged with the same current rate up to the EOCV. Thus, two individuals "OCV vs SOC" curves, corresponding to both charging and discharging phases are obtained, which in many cases are different due to hysteresis effects of the cell.
The time required for this test is approximately 14 hours.

**Table 3-7: Quasi-OCV vs SOC test procedure**

| Step | Action | Current (A) | Limit |
|---|---|---|---|
| 1 | Standard Charge (25°C) | (C/3) | |
| 2 | Discharge | (C/5) | < EODV |
| 3 | Pause | 0 | 10min |
| 4 | Charge | (C/5) | > EOCV |

#### 3.6.1.1 Analysis and documentation

During this test, at least the following parameters have to be logged every 1 second:

- Cell Voltage $(V)$.
- Cell Current $(A)$.
- Charged/Discharged capacity $(Ah)$ on each charge/discharge step.
- Charged/Discharged energy $(Wh)$ on each charge/discharge step.
- Cell Temperature (°C).

The following results have to be documented and analysed:

- Calculation of the "Quasi-OCV" as the average of the two voltage curves over Depth of Discharge.
- Discharged and charged capacity $Ah$.
- dV/dQ curve.
- "Quasi-OCV" Characteristic over DOD.

## 3.7 Periodic Check-ups -SOH Characterization

Some check-ups have to be performed during various procedures to control the cells' behaviour and to characterize the degradation mechanisms. The frequency of the SOH characterisation check-ups will differ depending on the testing task.
In view of the tests involved in each check-up, two types of test have been identified. First, short check-ups (see section 3.7.1) have to be performed to obtain basic information of the cell. After that, the detailed check-ups (see section 3.7.2) have also to be performed to gain comprehensive information about the cell. (To provide further insight of cells ageing behaviour.)
The sequence corresponding to each check-up type will be defined in this section. Finally, every test will be described in detail. Notice that on each test, the SOC levels are calculated according to the actual capacity values which obtained in the capacity test (section 3.7.1.3 or 3.7.2.3), while the C-rates are maintained constant as explained before, in section 3.1

### 3.7.1 Short check-ups

As mentioned before, the short check-ups will be part of a test sequence which will provide the "basic information" needed for modelling and checking the performance of cells.

#### 3.7.1.1 Short check-up test Sequence

**Error! Reference source not found.** indicates the test sequence to be followed

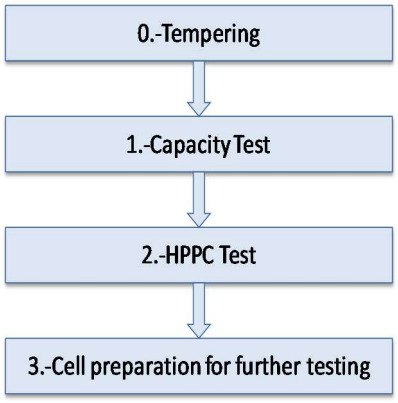


Figure 3-11: Short checkup test sequence

The entire test sequence commences with a tempering process and it is followed by 2 different test procedures. Finally, the "cell preparation procedure" is proposed, in order to make the cell ready for the next test procedure. The required time for the Short check-up test sequence is about 24h.

#### 3.7.1.2 Tempering process

Three issues have to be considered while tempering process: the temperature measurements, temperature control and the tempering procedure itself (see sections 3.5.2.1 to 3.5.3).

#### 3.7.1.3 Capacity test

The capacity will be measured at 25°C (after the tempering procedure). The determination of the capacity will start with a standard charge (section 3.1). Then, after a pause period of 30 minutes, a discharge down to the EODV will be made, subsequently a pause period of 30 minutes should be considered again. Finally, another standard charge will be done. Those steps will be repeated 2 times to measure the real capacity of the cell correctly.

The capacity test lasts 7 x 2 = 14 hours approximately.

Table 3-8: Capacity test procedure

| Step | Action | Current (A) | Limit |
|---|---|---|---|
| 1 | Standard CHA | (C/3) | |
| 2 | PAU | 0 | 30 min |
| 3 | DCH | (C/3) | < EODV |
| 4 | PAU | 0 | 30 min |
| 5 | Repeat steps 1-4 | | 2 times |

#### 3.7.1.4 Analysis and documentation:

During this test, at least the following parameters have to be logged every 1 second:

- Cell Voltage $(V)$.
- Cell Current $(A)$.
- Charged/Discharged capacity $(Ah)$ on each charge/discharge step.

- Charged/Discharged energy ($Wh$) on each charge/discharge step.
- Cell Temperature (°C).

The following results have to be documented and analysed:

- Current, voltage and cell temperature versus time at each discharge test and standard charge.
- Discharged capacity in $Ah$, energy in $Wh$ and average power in $W$, at each discharge test.
- Charged capacity in $Ah$, energy in $Wh$ and average power in $W$, at each standard charge following each discharge test.
- Energy round trip efficiency at each discharge test.
- Discharged energy in $Wh$ as a function of SOC at each discharge test (in $\%$ of nominal capacity).
- The EODV of all available cell voltage measuring points for all performed discharge tests.
- Determined $C/3$ nominal capacity which is taken as the basic value for all further discharge current requirements.

#### 3.7.1.5 HPPC test procedure

Hybrid Pulse Power Characterization Test (HPPC) is aimed to measure the charge and discharge resistances as well as the charge and discharge power of the cells at the variant state of charges and C-rates. This will characterise the cell at the BOL, the EOL and during the ageing tests. Specifically, the different discharge resistances, charge resistances, discharge powers and charge powers will be determined. The test profile used in this case involves a pulse train with several discharge and charge pulses at different C-rates as shown in **Error! Reference source not found.**12. (0.5C, 1C, 1.5C, 2C and 2.5C. those all calculated with the nominal capacity of the cell. In this way, the power capabilities of the cell at different C-rates are measured, which has resulted in the comparability between various generations of batteries (that's why the current values are referred to the C-rate). Every HPPC test will be performed at 25°C.

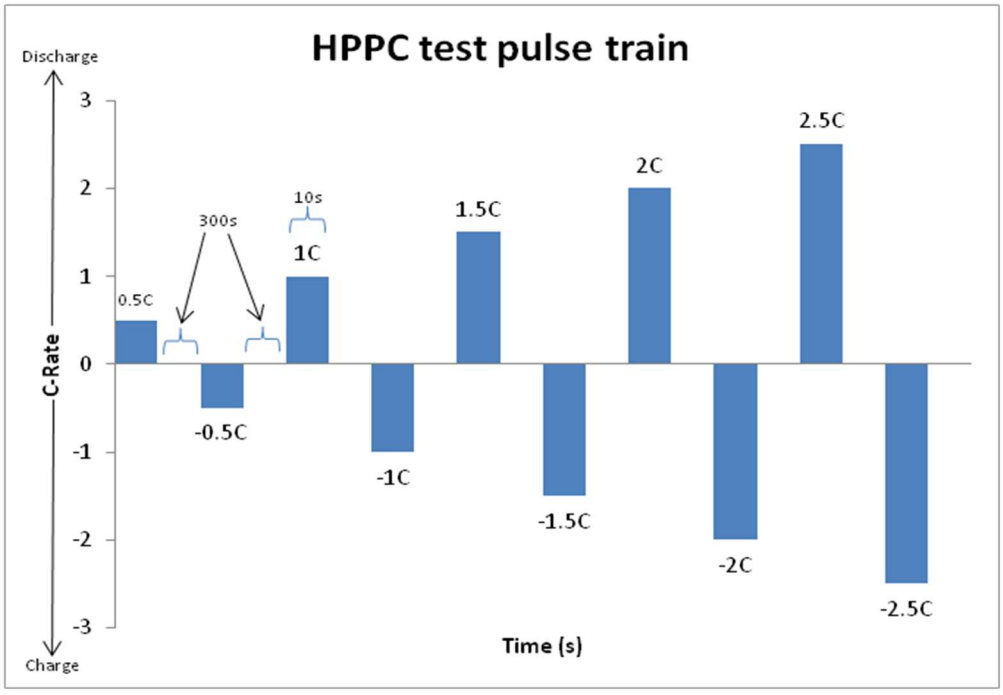

Figure 3-12: HPPC test pulse train

The SOC in which the measurement is to be done needs to be fixed Ah-based, by means of the capacity value measured during the capacity test (see section 3.7.1.3). The time course of the pulse train according to the HPPC test is summarised in Table 3-99.

Table 3-9: HPPC test pulse train

| Time increment (s) | Accumulated Time (s) | Process |
|---|---|---|
| 10 | 10 | DCH $0{,}5C$ |
| 300 | 310 | PAU |
| 10 | 320 | CHA $0{,}5C$ |
| 300 | 620 | PAU |
| 10 | 630 | DCH 1C |
| 300 | 930 | PAU |
| 10 | 940 | CHA 1C |
| 300 | 1240 | PAU |
| 10 | 1250 | DCH 1,5C |
| 300 | 1550 | PAU |
| 10 | 1560 | CHA 1,5C |
| 300 | 1860 | PAU |
| 10 | 1890 | DCH 2C |
| 300 | 2190 | PAU |
| 10 | 2200 | CHA 2C |
| 300 | 2500 | PAU |
| 10 | 2510 | DCH 2.5C |
| 300 | 2810 | PAU |
| 10 | 2820 | CHA 2.5C |
| 300 | 3120 | PAU |

The HPPC test procedure is listed in Table 3-100. It takes approximately 10 hours to perform the HPPC test.

Table 3-10: HPPC test procedure

| Step | Action | Current (A) | Limit |
|---|---|---|---|
| 1 | Standard Charge (25°C) | $(C/3)$ | |
| 2 | PAU | 0 | 30 min |
| 3 | DCH | $(C/3)$ | SOC (%) = 80, 50, 20 |

| | | | |
|---|---|---|---|
| 4 | PAU | 0 | 30 min |
| 5 | HPPC | | |
| 6 | Repeat steps 3-5 at SOC 80 %, 50%, 20% | | |

#### 3.7.1.6 Analysis and documentation

During this test, at least the following parameters have to be logged every 1 second during the pause periods and during the charge/discharge periods and every 10ms during the pulses:

- Cell Voltage $(V)$.
- Cell Current $(A)$.
- Charged/Discharged capacity $(Ah)$ on each charge/discharge step.
- Charged/Discharged energy $(Wh)$ on each charge/discharge step.
- Cell Temperature (°C).

The Following results have to be documented and analysed:

- Charge and discharge power for 1s and 10s for every charge and discharge pulse in function of SOC.
- Charge and discharge resistance for 1s and 10s for every charge and discharge pulse as well as the overall resistance as a function of SOC.

#### 3.7.1.7 Cell preparation for further testing

To accomplish the whole test sequence, a standard charging (according to section 3.1) has to be performed to recharge the cell completely after the tests have been performed. Once the cell is fully recharged, it has to be discharged to the SOC in which the following test has to start (Ah-based discharge, calculated with the results obtained in the latest capacity test of the cell). In this way, it is ensured that this SOC is always reached at 25°C.

### 3.7.2 Detailed check-ups

Some detailed check-ups will be achieved by extending the “basic information” obtained in the short check-ups. As the duration of the detailed check-ups will be longer, these check-ups will be performed less frequently, thus the degrading of the cell on exhaustive testing tasks will be avoided. The specific frequency of the detail check-ups depends on the type of experiment.

#### 3.7.2.1 Detailed check-up test Sequence

The test sequence which will be followed can be seen in 3-13.

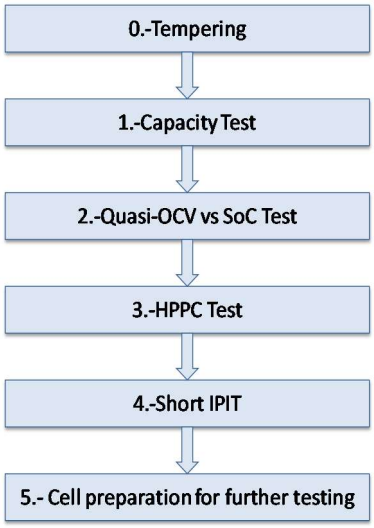


Figure 3-13: Detailed checkup test sequence

At first, a tempering process is done and it will be followed by 4 different test procedures. In the end, the preparation procedure is proposed, in order to make the cell ready for the next test procedure.
The time required for the detailed check-up test sequence is about 50h.

#### 3.7.2.2 Tempering process

Three topics have to be considered during tempering process: the temperature measurements, temperature control and the tempering procedure itself (see sections 3.5.2.1 to 3.5.2.3).

#### 3.7.2.3 Capacity test

The capacity will be measured at 25°C (after the tempering procedure). The determination of the capacity will start with a standard charge (section 3.1). Then, after a pause period of 30 minutes, a discharge down to the EODV will be made, followed by a pause period of 30 minutes. Finally, another standard charge will be done. Those steps will be repeated 2 times to measure the real capacity of the cell correctly.
The capacity test lasts approximately 7 x 2 = 14 hours.

Table 3-11: Capacity test procedure

| Step | Action | Current (A) | Limit |
|---|---|---|---|
| 1 | Standard CHA | (C/3) | |
| 2 | PAU | 0 | 30 min |
| 3 | DCH | (C/3) | < EODV |
| 4 | PAU | 0 | 30 min |
| 5 | Repeat steps 1-4 | | 2 times |

#### 3.7.2.4 Analysis and documentation

During this test, at least the following parameters have to be logged every 1 second:

- Cell Voltage $(V)$.
- Cell Current $(A)$.

- Charged/Discharged capacity ($Ah$) on each charge/discharge step.
- Charged/Discharged energy ($Wh$) on each charge/discharge step.
- Cell Temperature (°C).

Following results have to be documented and analyzed:

- Current, voltage and cell temperature versus time at each discharge test and standard charge.
- Discharged capacity in $Ah$, energy in $Wh$ and average power in $W$, at each discharge test.
- Charged capacity in $Ah$, energy in $Wh$ and average power in $W$, at each standard charge following each discharge test.
- Energy round trip efficiency at each discharge test.
- Discharged energy in $Wh$ as a function of SOC at each discharge test (in % of nominal capacity).
- The EODV of all available cell voltage measuring points for all performed discharge tests.
- Determined C/3 nominal capacity which is taken as the basic value for all further discharge current requirements.

#### 3.7.2.5 Quasi-OCV vs SOC test

The "Quasi-OCV" approach is considered as a time-efficient method to analyse the open circuit voltage characteristic over the state of charge. The measurement starts with a fully charged cell, which is discharged to EODV with a small current (C/5 C-Rate). The current rate is assumed to be small enough for the voltage measured to be considered as "quasi-OCV". After this step the cell is charged with the same current rate up to the EOCV. Thereby, two individuals "OCV vs SOC" curves, corresponding to both charging and discharging are obtained, which in many cases are different due to hysteresis effects of the cell.
The required time for this test is 14 hours approximately.

**Table 3-12: Quasi-OCV vs SOC test procedure**

| Step | Action | Current (A) | Limit |
|---|---|---|---|
| 1 | Standard Charge (25°C) | (C/3) | |
| 2 | Discharge | (C/5) | < EODV |
| 3 | Pause | 0 | 10min |
| 4 | Charge | (C/5) | > EOCV |

#### 3.7.2.6 Analysis and documentation

During this test, at least the following parameters have to be logged every 1 second:

- Cell Voltage ($V$).
- Cell Current ($A$).
- Charged/Discharged capacity ($Ah$) on each charge/discharge step.

- Charged/Discharged energy ($Wh$) on each charge/discharge step.
- Cell Temperature (°C).

The following results have to be documented and analysed:

- Calculation of the "Quasi-OCV" as the average of the two voltage curves over Depth of Discharge.
- Discharged and charged capacity $Ah$.
- dV/dQ curve.
- "Quasi-OCV"Characteristic over DOD.

#### 3.7.2.7 HPPC test procedure

The purpose of the Hybrid Pulse Power Characterization Test (HPPC) is to measure the charge and discharge resistances and consequently the charge and discharge power of the cells at different SOCs, and with different C-rates. This will characterise the cell at the BOL, the EOL and during the ageing tests. Specifically, different discharge resistances, charge resistances, discharge powers and charge powers will be determined.
The test profile used in this case consists of a pulse train with several discharge and charge pulses at different C-rates (0.5C, 1C, 1.5C, 2C and 2.5C, all calculated based on the nominal capacity of the cell as presented in **Error! Reference source not found.**14. In this way, the power capabilities of the cell at different C-rates are measured, ensuring the comparability between the various generations of the batteries (that's why the current values are referred to the C-rate).
Every HPPC test will be performed at 25°C [1].

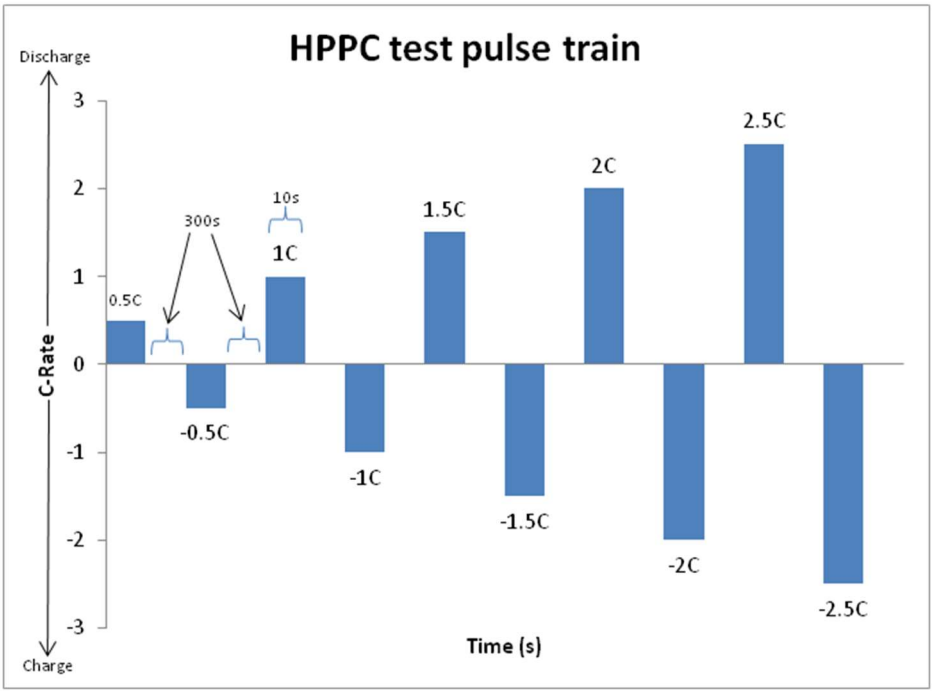


Figure 3-14: HPPC test pulse train

[1] HPPC test will be done at 25ºC for most tests.

The SOC in which the measurement is to be done needs to be fixed Ah-based, by means of the capacity value measured in the capacity test (see section 3.7.2.3).
The time course of the pulse train according to the HPPC test is summarised in table 3-13.

**Table 3-13: HPPC test pulse train**

| Time increment (s) | Accumulated Time (s) | Process |
|---|---|---|
| 10 | 10 | DCH 0,5C |
| 300 | 310 | PAU |
| 10 | 320 | CHA 0,5C |
| 300 | 620 | PAU |
| 10 | 630 | DCH 1C |
| 300 | 930 | PAU |
| 10 | 940 | CHA 1C |
| 300 | 1240 | PAU |
| 10 | 1250 | DCH 1,5C |
| 300 | 1550 | PAU |
| 10 | 1560 | CHA 1,5C |
| 300 | 1860 | PAU |
| 10 | 1890 | DCH 2C |
| 300 | 2190 | PAU |
| 10 | 2200 | CHA 2C |
| 300 | 2500 | PAU |
| 10 | 2510 | DCH 2.5C |
| 300 | 2810 | PAU |
| 10 | 2820 | CHA 2.5C |
| 300 | 3120 | PAU |

Finally, the HPPC test procedure is shown in
Table 3-144. It takes approximately 10 hours to perform the HPPC test.

**Table 3-14: HPPC test procedure**

| Step | Action | Current (A) | Limit |
|---|---|---|---|
| 1 | Standard Charge (25°C) | (C/3) | |
| 2 | PAU | 0 | 30 min |
| 3 | DCH | (C/3) | SOC (%)=80, 50, 20 |
| 4 | PAU | 0 | 30 min |
| 5 | HPPC | | |
| 6 | Repeat steps 3-5 at SOC 80 %, 50%, 20% | | |

### 3.7.2.8 Analysis and documentation:

During this test, at least the following parameters have to be logged every 1 second during the pause periods and during the charge/discharge periods and every 10ms during the pulses:

- Cell Voltage $(V)$.
- Cell Current $(A)$.
- Charged/Discharged capacity $(Ah)$ on each charge/discharge step.
- Charged/Discharged energy $(Wh)$ on each charge/discharge step.

- Cell Temperature (°C).

The following results have to be documented and analysed:

- Charge and discharge power for 1s and 10s for every charge and discharge pulse in function of SOC.
- Charge and discharge resistance for 1s and 10s for every charge and discharge pulse as well as the overall resistance as a function of SOC.

#### 3.7.2.9 Short-IPIT procedure

To accomplish information about the electrochemical properties of the cells during the ageing process, those Short IPIT tests will be performed at different SOCs fixed Ah-based, by means of the capacity value determined from the capacity test.
To perform the Impedance parameterisation correctly, the following properties have to be considered:

- Frequency Range from $f_{max} = 5\ kHz$ to $f_{min} = 5\ kHz$
- Frequency Distribution: 8 Frequencies / Decade
- Uideal = 8 mV
- The measurement has to be performed in temperature chambers at the constant temperature of 25 °C.

Before every IPIT the cells have to be charged with the standard charge procedure (see section 3.1) at 25°C.
The time required for the whole test is 10 approximately hours.
The test procedure to be followed is listed in Table 3-155.

**Table 3-15: Short-IPIT test procedure**

| Step | Action | Limit | fmin | fmax | Current (A) |
|---|---|---|---|---|---|
| 1 | Standard Charge (25°C) | | | | (C/3) |
| 2 | Discharge to SOC = 80% | ΔDOD = 20 % | | | (C/3) |
| 3 | Pause | 30 min | | | 0 |
| 4 | Spectra @ 80% SOC | 1 h | 5 mHz | 5 kHz | Few mA |
| 5 | Discharge to SOC = 50% | ΔDOD = 30 % | | | (C/3) |
| 6 | Pause | 30 min | | | 0 |
| 7 | Spectra @ 50% SOC | 1 h | 5 mHz | 5 kHz | Few mA |
| 8 | Discharge to SOC = 20% | ΔDOD = 30 % | | | (C/3) |
| 9 | Pause | 30 min | | | 0 |
| 10 | Spectra @ 20% SOC | 1 h | 5 mHz | 5 kHz | Few mA |

#### 3.7.2.10 Analysis and documentation

During this test, at least the following parameters have to be logged:

- Real Part of the Impedance $Re(Z)$
- Imaginary Part of the Impedance $Im(Z)$
- Cell Voltage $(U)$
- AC-Current $(IAC)$

- DC-Current $(IDC)$
- 0 C-Rate DC Spectra at = 20%, 50%, 80% SOC.

#### 3.7.2.11 Cell preparation for further testing

To complete the whole test sequence, a standard charge (according to section 3.1) has to be performed to recharge the cell completely after performing the tests. Once the cell is fully recharged, it has to be discharged to the SOC, in which the following test has to start (Ah-based discharge, calculated with the results obtained in the latest capacity test of the cell). In this way, it is ensured that this SOC is always reached at 25°C.

## 3.8 EOL Testing

Finally, before the cells are retired for the second life ageing or simply moved away from operation, some EOL test have to be performed. So, the baseline reference values for the second life can be set, and some extra details are obtained for the study of the first life ageing.
Notice that on each test, the SOC levels are calculated according to the actual capacity values obtained in the capacity test, while the C-rates are maintained constant, as explained before in section 3.1.

### 3.8.1 EOL Test Sequence

The test sequence to be followed is depicted in 3-15.

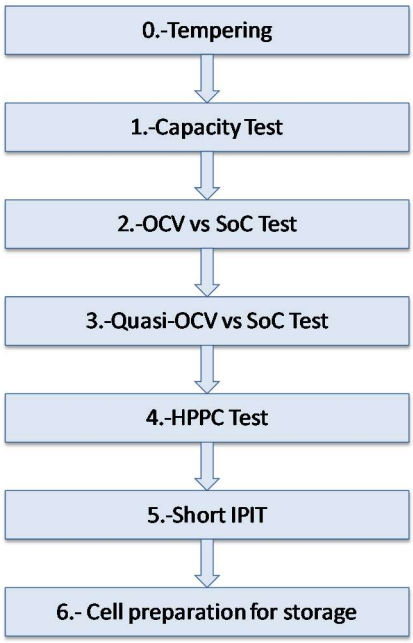


Figure 3-15: EOL test sequence

The whole test sequence begins with a tempering process and it follows with 5 different test procedures; their results will be the reference for the check-ups made during cycling and calendar ageing tasks.
The time required for the whole EOL test sequence is about 185h.

### 3.8.2 Tempering process

Three criteria have to be considered: the temperature measurements, temperature control and the tempering procedure itself (see sections 3.5.2.1 to 3.5.2.3).

### 3.8.3 Capacity test

The capacity will be measured at 25°C (after the tempering procedure). The determination of the capacity will start with a standard charge (section 3.1). Then, after a pause period of 30 minutes, a discharge down to the EODV will be made, followed by a pause period of 30 minutes. Finally, another standard charge will be done. Those steps will be repeated 2 times to correctly measure the real capacity of the cell.
The capacity test lasts 7 x 2 = 14 hours approximately.

**Table 3-16: Capacity test procedure**

| Step | Action | Current (A) | Limit |
|---|---|---|---|
| 1 | Standard CHA | (C/3) | |
| 2 | PAU | 0 | 30 min |
| 3 | DCH | (C/3) | < EODV |
| 4 | PAU | 0 | 30 min |
| 5 | Repeat steps 1-4 | | 2 times |

#### 3.8.3.1 Analysis and documentation

During this test, at least the following parameters have to be logged every 1 second:

- Cell Voltage $(V)$.
- Cell Current $(A)$.
- Charged/Discharged capacity $(Ah)$ in each charge/discharge step.
- Charged/Discharged energy $(Wh)$ in each charge/discharge step.
- Cell Temperature (°C).

The following results have to be documented and analysed:

- Current, voltage and cell temperature versus time at each discharge test and standard charge.
- Discharged capacity in $Ah$, energy in $Wh$ and average power in $W$, at each discharge test.
- Charged capacity in $Ah$, energy in $Wh$ and average power in $W$, at each standard charge following each discharge test.
- Energy round trip efficiency at each discharge test.
- Discharged energy in $Wh$ as a function of SOC at each discharge test (in % of nominal capacity).
- The EODV of all available cell voltage measuring points for all performed discharge tests.
- Determined $C/3$ nominal capacity which is taken as the basic value for all further discharge current requirements.

### 3.8.4 OCV vs SOC test procedure

The equilibrium voltage is determined by this procedure– DOD characteristic for a comparison of the Open Circuit Voltage (OCV) of the Cell at BOL and EOL. This characteristic of the cell is also needed for battery modelling.
The equilibrium voltage for each SOC and both charge and discharge curves are determined as the value of the voltage measured after a 3-hour pause.
In order to clarify the amount of $Ah$ needed to be charged or discharged to establish a fixed SOC, the capacity value obtained in the previous capacity test for each cell will be used, respectively.
The time required for the OCV vs. SOC test is 135 h approximately.

**Table 3-17: OCV vs SOC test procedure**

| Step | Action | Current (A) | Limit |
|---|---|---|---|
| 1 | Standard charge (25°C) | (C/3) | |
| 2 | Pause (OCV Determination) | 0 | 3h |
| 3 | Discharge | (C/3) | ΔDOD=5% |
| 4 | Pause (OCV Determination) | 0 | 3h |
| 5 | Repeat 4. - 5. until EODV | | EODV |
| 6 | Pause (OCV Determination) | 0 | 3h |
| 7 | Charge | (C/3) | ΔDOD=5% |
| 8 | Pause (OCV Determination) | 0 | 3h |
| 9 | Repeat 7. - 8. until EOCV | | EOCV |

#### 3.8.4.1 Analysis and documentation

During this test, at least the following parameters have to be logged every 1 second:

- Cell Voltage $(V)$.
- Cell Current $(A)$.
- Charged/Discharged capacity $(Ah)$ on each charge/discharge step.
- Charged/Discharged energy $(Wh)$ on each charge/discharge step.
- Cell Temperature (°C).

The following results have to be documented and analysed:

- Determination of the OCV-DOD Characteristic for each discharge Step
- Determination of the OCV-DOD Characteristic for each charge Step
- Determination of the OCV-DOD Characteristic for the average of each DOD step

### 3.8.5 Quasi-OCV vs SOC test

The “Quasi-OCV” approach is considered as a time-efficient method to analyse the characteristic of the open circuit voltage over the state of charge. The measurement starts with a fully charged cell, which is discharged to EODV with a small current (C/5 C-Rate). The current rate is assumed to be small enough for the voltage

measured as “quasi-OCV”. After this step, the cell is charged with the same current rate up to the EOCV. Thus, two individuals “OCV vs SOC” curves, corresponding to both charging and discharging are obtained, which in many cases are different due to hysteresis effects of the cell.
The time requires for this test is 14 hours approximately.

**Table 3-18: Quasi-OCV vs SOC test procedure**

| Step | Action | Current (A) | Limit |
|---|---|---|---|
| 1 | Standard Charge (25°C) | (C/3) | |
| 2 | Discharge | (C/5) | < EODV |
| 3 | Pause | 0 | 10min |
| 4 | Charge | (C/5) | > EOCV |

#### 3.8.5.1 Analysis and documentation

During this test, at least the following parameters have to be logged every 1 second:

- Cell Voltage $(V)$.
- Cell Current $(A)$.
- Charged/Discharged capacity $(Ah)$ on each charge/discharge step.
- Charged/Discharged energy $(Wh)$ on each charge/discharge step.
- Cell Temperature (°C).

The following results have to be documented and analysed:

- Calculation of the “Quasi-OCV” as the average of the two voltage curves over Depth of Discharge.
- Discharged and charged capacity $Ah$.
- dV/dQ curve.
- “Quasi-OCV” Characteristic over DOD.

### 3.8.6 HPPC test procedure

Purpose of the Hybrid Pulse Power Characterization Test (HPPC) is to measure the charge and discharge resistances and also the charge and discharge power of the cells at a different state of charges, and with different C-rates. This will characterise the cell at the BOL, the EOL and during the ageing tests. In detail, different discharge resistances, charge resistances, discharge powers and charge powers will be determined.
The test profile used in this case consists of a pulse train with several discharge and charge pulses at different C-rates (0.5C, 1C, 1.5C, 2C and 2.5C, all calculated with the nominal capacity of the cell as shown in Figure 3-166. In this way, the power capabilities of the cell at different C-rates are measured, ensuring the comparability between the various generations of the batteries (that’s why the current values are referred to the C-rate).
Every HPPC test will be performed at 25°C.

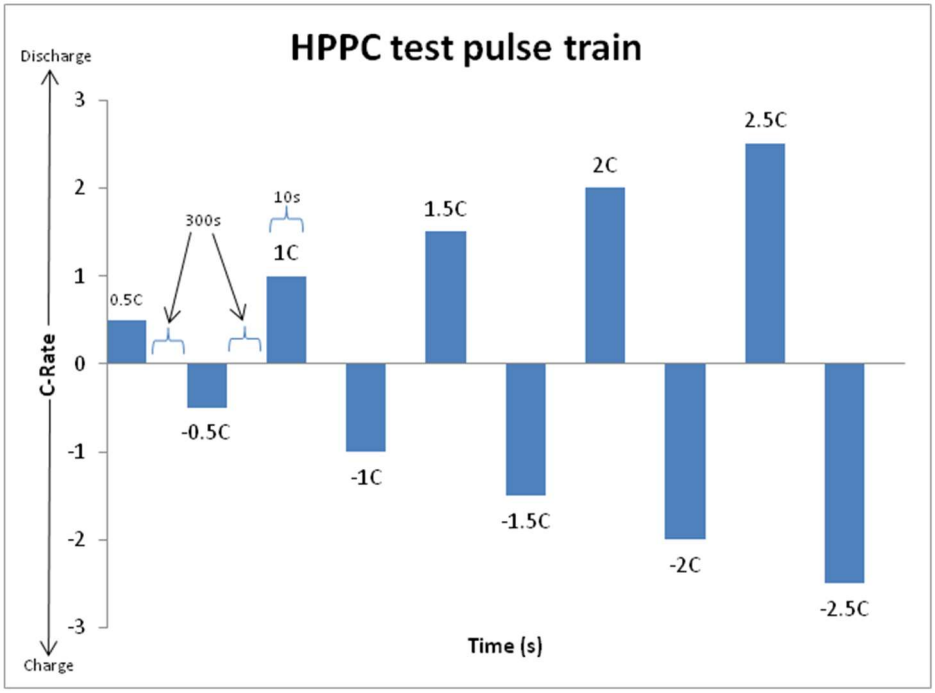


Figure 3-16: HPPC test pulse train

The SOC in which the measurement done needs to be fixed Ah-based, by means of the capacity value measured in the capacity test (see section 3.8.3).
The time course of the pulse train according to the HPPC test is summarised in Table 3-1919.

Table 3-19: HPPC test pulse train

| Time increment (s) | Accumulated Time (s) | Process |
|---|---|---|
| 10 | 10 | DCH 0,5C |
| 300 | 310 | PAU |
| 10 | 320 | CHA 0,5C |
| 300 | 620 | PAU |
| 10 | 630 | DCH 1C |
| 300 | 930 | PAU |
| 10 | 940 | CHA 1C |
| 300 | 1240 | PAU |
| 10 | 1250 | DCH 1,5C |
| 300 | 1550 | PAU |
| 10 | 1560 | CHA 1,5C |
| 300 | 1860 | PAU |
| 10 | 1890 | DCH 2C |
| 300 | 2190 | PAU |

| | | |
|---|---|---|
| 10 | 2200 | CHA 2C |
| 300 | 2500 | PAU |
| 10 | 2510 | DCH 2.5C |
| 300 | 2810 | PAU |
| 10 | 2820 | CHA 2.5C |
| 300 | 3120 | PAU |

The HPPC test procedure can be seen in Table 3-200. It takes approximately 10 hours to perform the HPPC test.

**Table 3-20: HPPC test procedure**

| Step | Action | Current (A) | Limit |
|---|---|---|---|
| 1 | Standard Charge (25°C) | (C/3) | |
| 2 | PAU | 0 | 30 min |
| 3 | DCH | (C/3) | SOC(%)=80, 50, 20 |
| 4 | PAU | 0 | 30 min |
| 5 | HPPC | | |
| 6 | Repeat steps 3-5 at SOC 80 %, 50%, 20% | | |

#### 3.8.6.1 Analysis and documentation

During this test, at least the following parameters have to be logged every 1 second during the pause periods and during the charge/discharge periods and every 10ms during the pulses:

- Cell Voltage $(V)$.
- Cell Current $(A)$.
- Charged/Discharged capacity $(Ah)$ on each charge/discharge step.
- Charged/Discharged energy $(Wh)$ on each charge/discharge step.
- Cell Temperature (°C).

The following results have to be documented and analysed:

- Charge and discharge power for 1s and 10s for every charge and discharge pulse in function of SOC.
- Charge and discharge resistance for 1s and 10s for every charge and discharge pulse as well as the overall resistance as a function of SOC.

### 3.8.7 Short-IPIT procedure

The Short IPIT tests will be performed at different SOCs fixed Ah-based, by means of the capacity value determined from the capacity test to achieve information about the electrochemical properties of the cells during the ageing process.

To perform the Impedance parameterisation properly, the following properties have to be considered:

- Frequency Range from $f_{max} = 5\ kHz$ to $f_{min} = 5\ kHz$
- Frequency Distribution: 8 Frequencies / Decade
- Uideal = $8\ mV$
- The measurement has to be performed in temperature chambers at constant temperature of 25 °C.

Before every IPIT, the cells have to be charged with the standard charging procedure (see section 3.1) at 25°C.

The time required for the whole test is approximately 10 hours.

The test procedure that has to be followed can be seen in Table 3-211.

**Table 3-21: Short-IPIT test procedure**

| Step | Action | Limit | fmin | fmax | Current (A) |
|---|---|---|---|---|---|
| 1 | Standard Charge (25°C) | | | | (C/3) |
| 2 | Discharge to SOC = 80% | ΔDOD = 20 % | | | (C/3) |
| 3 | Pause | 30 min | | | |
| 4 | Spectra @ 80% SOC | 1 h | 5 mHz | 5 kHz | Few mA |
| 5 | Discharge to SOC = 50% | ΔDOD = 30 % | | | (C/3) |
| 6 | Pause | 30 min | | | 0 |
| 7 | Spectra @ 50% SOC | 1 h | 5 mHz | 5 kHz | Few mA |
| 8 | Discharge to SOC = 20% | ΔDOD = 30 % | | | (C/3) |
| 9 | Pause | 30 min | | | 0 |
| 10 | Spectra @ 20% SOC | 1 h | 5 mHz | 5 kHz | Few mA |

#### 3.8.7.1 Analysis and documentation

During this test, at least the following parameters have to be logged:

- Real Part of the Impedance $(Re(Z))$

- Imaginary Part of the Impedance $Im(Z)$
- Cell Voltage $U$
- AC-Current $IAC$
- DC-Current $IDC$
- 0 C-Rate DC Spectra at = 20%, 50%, 80% SOC.

### 3.8.8 Cell preparation for storage

To finish the whole test sequence, a standard charging (section 3.1) should be performed to recharge the cell completely after performing the tests. Once the cell is fully recharged, it has to be discharged to 50% SOC at C/3 rate (Ah-based discharge, calculated with the results obtained in the capacity test) to make the cell ready for storage). In the particular case of cells intended for post-mortem analysis, it will be further determined whether they have to be stored at 100% SOC or 0% SOC, depending on some preliminary results.

## 3.9 Test duration Summary

A summary on the duration of the characterisation tests described in this section is shown in Table 3-222.

**Table 3-22: Summary of the duration of the different test sequences**

| Test type | Duration (h) | BOL | SOH short | SOH detailed | EOL |
|---|---|---|---|---|---|
| Capacity | 14 | ✓ | ✓ | ✓ | ✓ |
| OCV vs SOC | 135 | ✓ | | | ✓ |
| Quasi-OCV vs SOC | 14 | ✓ | | ✓ | ✓ |
| HPPC | 10 | ✓ | ✓ | ✓ | ✓ |
| Short IPIT | 10 | ✓ | | ✓ | ✓ |
| Total ≈ | | 185 h | 24 h | 50 h | 185 h |

# 4 Battery pack characterization and safety test procedure

## 4.1 Introduction

In currently available Battery Electric Vehicles (BEVs), the rechargeable energy storage system (RESS) contributes highly to the overall mass and cost of the vehicle. Hence, its validation is a critical part of the overall product development process. In this context the RESS has to undergo severe multi-physical testing for guaranteeing a high level of system reliability and safety.

The term “safety” in context of the HV battery falls into three major sections [1]:

- Structural safety
- Electrical safety
- Safety against fire and explosion

At LBF, a wide range of methodologies is available for the 1st and the 2nd section, since LBF has a longstanding experience in structural durability evaluation of passive components as well as recent experience in the evaluation of E/E systems. The latter section can only be evaluated indirectly but not be addressed experimentally at LBF, since the test facilities do not allow the destructive testing of HV batteries.

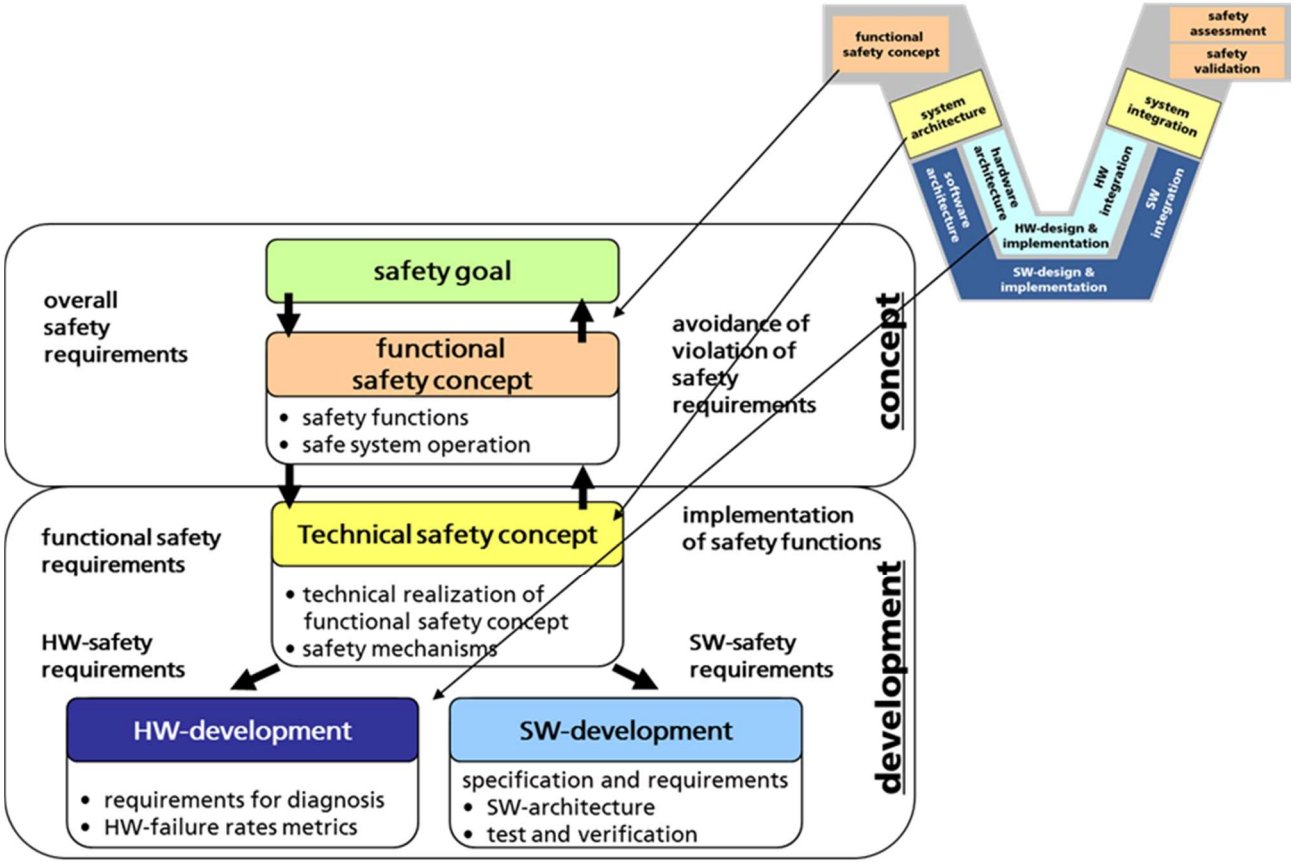


**Figure 4-1: Safety life cycle, derived from and in accordance with the safety life cycle described in ISO 26262**

Several standards apply when dealing with the evaluation of the safety of the HV battery, depending on the market that applies. For the EU, ECE R94/12 dealing with uniform provisions concerning the approval of vehicles with regard to the protection of the occupants in the event of a frontal collision, as well as ECE R95

(Uniform provisions concerning the approval of vehicles with regard to the protection of the occupants in the event of a lateral impact) shall be mentioned. In the USA, FMVSS 305 (Electric-powered vehicles: electrolyte spillage and electrical shock protection) applies. For other countries, similar regulations can be found [1].
In general, it is important to mention that the safety of the battery must be evaluated in the context of the holistic system, meaning the vehicle topology.
Since 2011, the standard ISO 26262 [2] describes the state of the art for E/E Systems in vehicles. The evaluation of the methodologies necessary to assess the safety can be derived from this standard regarding the electrical, chemical, mechanical and functional safety. The safety life cycle, as described in the standard, can be seen in Figure 4-1. It is important to mention that in general the safety concept covers all stages of the development and evaluation process, and different measures must be undertaken in each step. The “item definition”, for example, covers the functions, the interfaces, mission conditions (e.g. environmental conditions).
Based on these pre-assumptions, LBF methodology covers a holistic approach along the vehicle topology. The experimental and numerical methods applied during the development process deliver data which are used to feed the so-called probabilistic FMEA (probFMEA) in order to reach a holistic system evaluation.

## 4.2 Test rig for safety and reliability investigation

### 4.2.1 Specifications of the test stand

At Fraunhofer LBF, testing high-voltage (HV) battery systems for BEV takes place in a multi-physical test environment specifically developed for this purpose. This setup consists of three major components: a multi-axis simulation table (MAST) to apply mechanical loads, a vehicle energy system (VES) to apply electrical loads and a climatic chamber to superimpose thermal loads for the battery during testing, Figure 4-2. The MAST design is based on a hexapod with six servo-hydraulic actuators. The general motion of the upper platform of the hexapod comprises three translational and three rotational degrees of freedom and is defined using rigid body kinematics. This makes the MAST particularly suitable for testing systems which are exited through their inertial forces. The deformation states like bending and torsion (eigenmode) of the HV-battery are not directly implied from the test rig but produced by the accelerations of the platform.
A highly automated system continuously monitors the test, thus makes it possible to reproduce a realistic system test in the lab. The specification of the system enables platform motion and accelerations in all six degrees of freedom and covers a frequency range of up to 200 Hz. The maximum supported mass is 1,000 kg. The VES is capable of bi-directional loading of the battery with 290 kW having system limits at 800 V and 600 A on the DC-bus. In order to meet the requirements with regard to environmental simulation, the climatic chamber allows a temperature range from about -40 °C to 80 °C with a relative humidity above the freezing point of up to 95 %. The average cooling rate in the chamber is at 4 K/min.

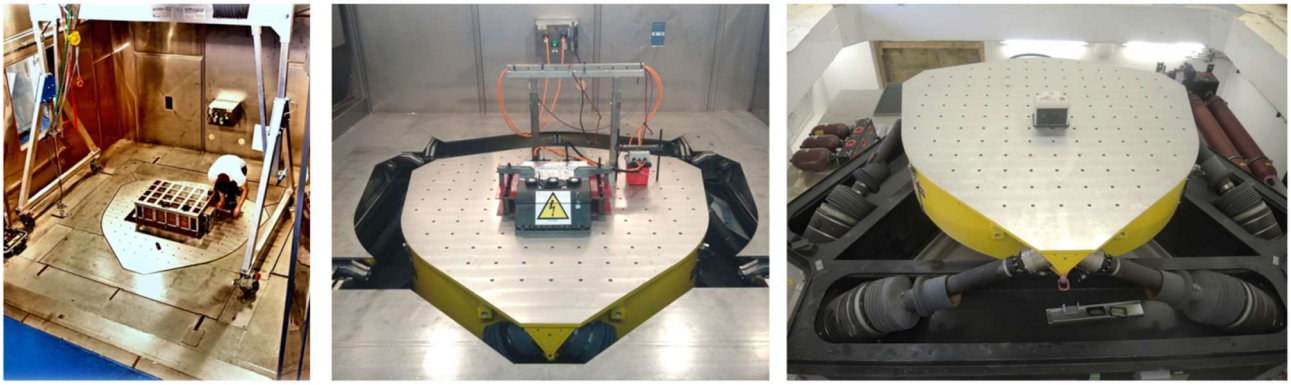

Figure 4-2: Multi-physical test environment for HV-Battery testing at Fraunhofer LBF

Each HV-battery under characterization test encounters varying and specific test profiles within the range of the above mentioned mechanical, electrical and thermal loading conditions. Usually, the test profiles are specified by the LBF or by clients under the advice of the LBF. The effects of the tests on the HV-battery are measured also by means of mechanical, electrical and thermal measures. On the mechanical side, acceleration and force sensors as well as strain gauges at various exposed locations on or inside the housing are used to evaluate the HV-battery system's dynamic behavior. On the electrical and thermal side, the battery-management-system (BMS) gives information about the voltage, current, state of charge (SoC), and temperature on the cell, module and system level of the HV-battery. What is more, property values of the vehicle like speed, odometer etc., property values of the electric motor like power, stator temperature etc., and property values of the inverter like DC-capacitor temperature, housing temperature etc. can be experimentally simulated by hardware in the loop (HiL) investigations with the test environment.

### 4.2.2 Safety concept of the test rig

The test environment's safety concept satisfies the requirement up to the hazard level 6 without fire and explosions but with possible debris. Figure 4-3 shows the safety concept realized at Fraunhofer LBF for HV-battery testing. The testing room's oxygen level is reduced to 3 % during tests by inerting nitrogen. To reduce the risk of fire, the room can be also purged with carbon dioxide or liquid nitrogen. Oxygen and carbon dioxide is measured permanently as well as the temperature in the testing room. In case of emergency, an exhaust in-site installation with an air vent and a bursting disc ensures that the gases flow to the outside, an electrical lock keeps the door of the test room closed.

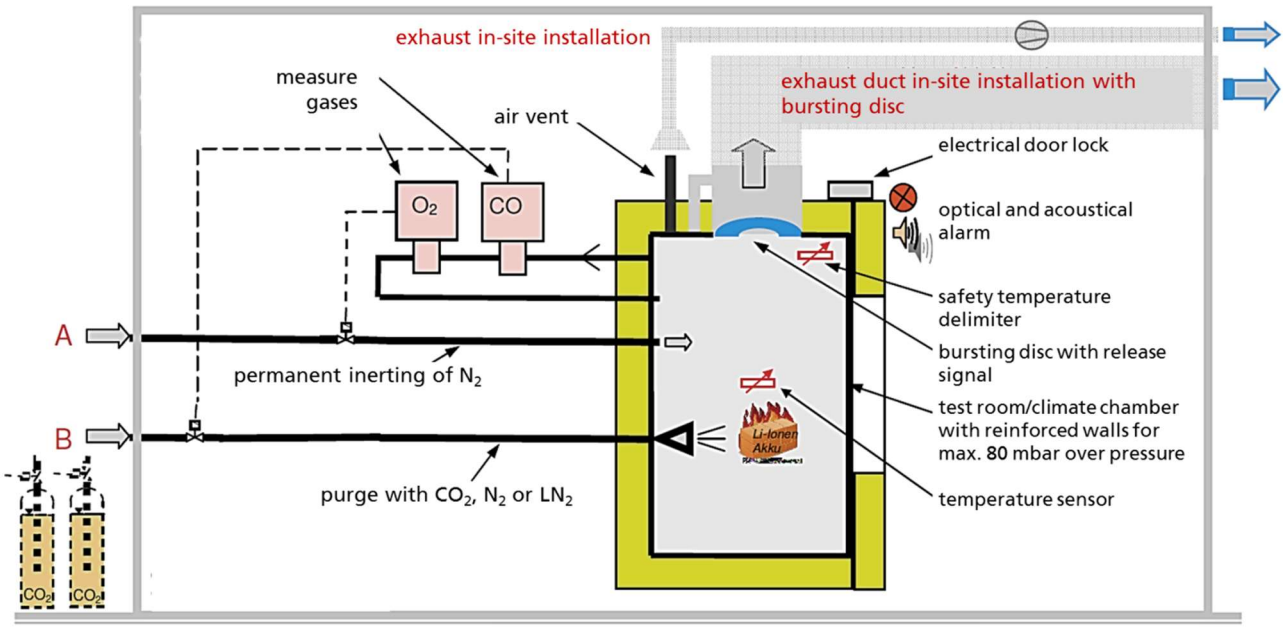


Figure 4-3: Safety concept for HV-Battery testing at Fraunhofer LBF

## 4.3 Safety test procedure

The infrastructure available at LBF enables for reliability and safety assessment of battery systems. In this framework, the following procedures are available and under current scientific development at LBF:

a) Derivation of operational loads from test drives
b) Acceleration techniques in order to reduce test time and effort
c) Transfer of real mechanical loading to experimentally simulated and time-shortened mechanical loading by MAST

d) Derivation and monitoring of safety-relevant parameters during experimental evaluation and Introduction of these parameters into overall safety assessment tools like probFMEA

These procedures will be described in the following:

### 4.3.1 Derivation of operational loads from test drives

The vehicle dynamics and its implications on the RESS are resulting from longitudinal, transverse and vertical along with rotational mechanical loading. To identify these loads, test drives are necessary. The BEVs under testing are a Nissan Leaf, BMW i3 and a Tesla Model S, all owned by LBF. The testing procedure leads to significant cost and time reduction of RESS system validation and help battery and vehicle developers to propel the overall development process.
Fraunhofer LBF uses a controlled route around Darmstadt with representative regular traffic conditions. Accidental maneuvers that causes abusive loads are explicitly excluded from that consideration. The excitations due to route disturbances are superimposed with regular mechanical loads that are evolved from driving on the route. By virtue of the roughness present on the route which deviates from normal geometric conditions, additional forces with random and distinct transient characteristics may occur. The basic stresses evolved from driving on the route are then superimposed with high-frequency additional loads with random phase position. Figure 4-4 gives a rough idea of the data collection process by Fraunhofer LBF from the route around Darmstadt to retrieve information about deterministic and stochastic driving maneuvers of LBF's test BEV and the data processing to get, eventually, data about the actual mechanical loading.

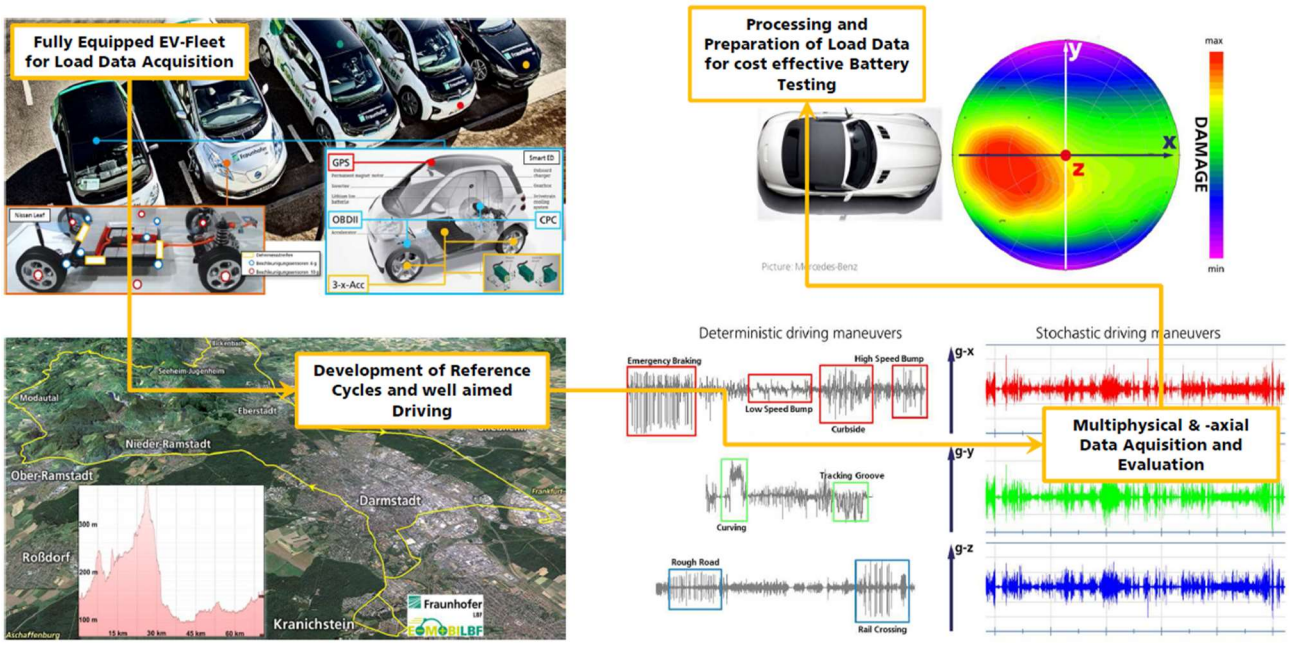


**Figure 4-4: Overview of LBF's test BEV, test route, driving maneuvers and data processing for mechanical load data.**

Route disturbances and irregularities like cobblestones, potholes or railway ties cause an uncorrelated relationship between the individual forces in the HV-battery components and therefore an irregular state of stress. These stresses can no longer be mathematically expressed in a deterministic way, but by using non-deterministic approaches with statistics and probability. The statistical properties are described through constants and characteristics – in case that the random processes are constant at least for a certain time interval and thus they exhibit quasi-stationary property.

The random loads play a decisive role for inertia excited components and mounting points on the vehicle, especially for the relation between mechanical loads and stresses. The stresses of a variety of components like fuel tanks, exhaust systems, electrical systems or wire harness with respect to their dimensions as well as inertia and stiffness properties are described by the acceleration variables of a random oscillation and also the eigenfrequencies and eigenmodes of the structure. Such processes can be favorably discussed in the frequency domain. The Power Spectral Density (PSD) is the decisive input for vibration tests with well-known electromagnetic shakers which are derived from the assumption of a pure random load.
Normally, a complete and comprehensive mechanical testing for the battery system of BEVs with all its components is not possible because the deterministic load cases are mostly not considered in the random vibration tests for all parts of the RESS. For example, the housing including its connection to the body, the coolant lines and the contact terminals are quite relevant and cannot be neglected. Therefore, the RESS of BEVs are tested at Fraunhofer LBF with complete operational loads using random vibration loading and low-frequency operational loads in an environment specifically developed for this purpose. The LBF has pursued the possibility for realistic operational load simulation for electrical storage systems in automotive applications. It is necessary to record mechanical operational loads from drive tests which are then transferred to test sequences used in laboratory testing. These drive tests can be carried out in special test tracks – so-called proving grounds (PG) – and then subsequently reduced to replicate operating load conditions which are relevant. The automotive manufacturers have their own test tracks which take into consideration the rough road conditions in a range of different frequencies, and also their own share of longitudinal and transverse dynamic driving conditions. Sometimes public roads are used for the determination of irregular loads and race tracks are used for the deterministic load related to lateral and longitudinal dynamics.
The RESS in BEV is commonly referred to as a high-voltage (HV) battery system. The HV-Battery is an assembly of electrically interconnected cells or modules with their own support structure and subjected to complex, multiphysical loads which are significantly influenced by mechanical, electrical and thermal variables. Electric and thermal operational characteristics as well as the loads to individual cells and modules are managed by the Battery Management System (BMS) using internal sensors and a cooling system according to defined parameters, Figure 4-5. This ensures a safe and reliable operation of the HV-battery in BEV.

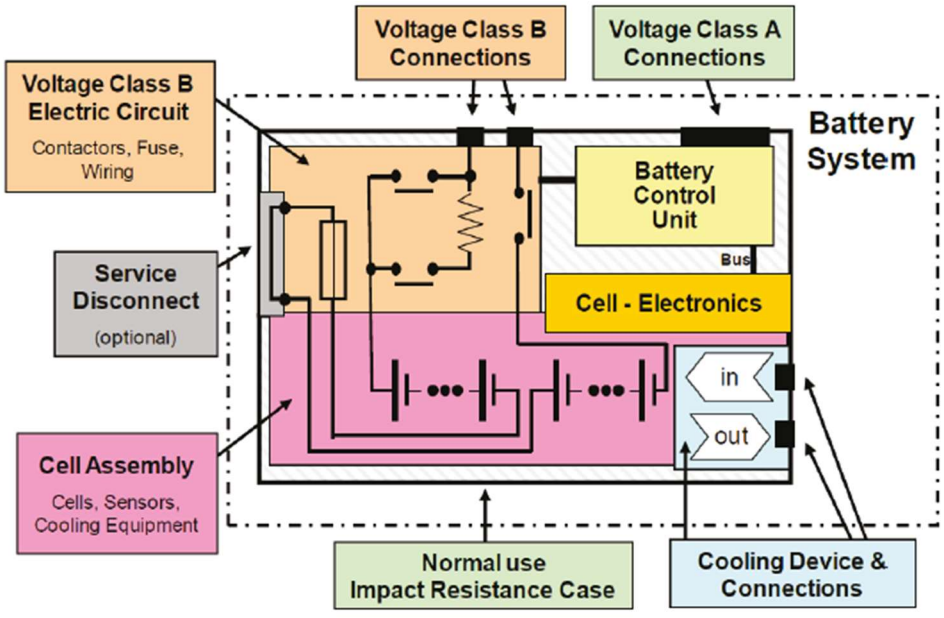


**Figure 4-5: Typical configuration of a battery system with integrated Battery Control Unit (BCU), [3].**

### 4.3.2 Acceleration techniques in order to reduce test time and- effort

In the framework of HV-battery testing, acceleration-time sequences measured by the manufacturer at various system points during testing at proving grounds can be used for testing in the lab. System points are preferably the mounting locations on the battery or fixations to the vehicle, along with several locations inside the battery housing to characterize and control the dynamic behavior. The accelerations measured at mounting points of the battery are used as a reference for the battery tests on the MAST. The acceleration-time sequence for the test is considered to the same frequency as in a test track. The elimination of stops and approach distances between individual test drive sections reduces the time for laboratory testing significantly compared to test track, Figure 4-6, [4].

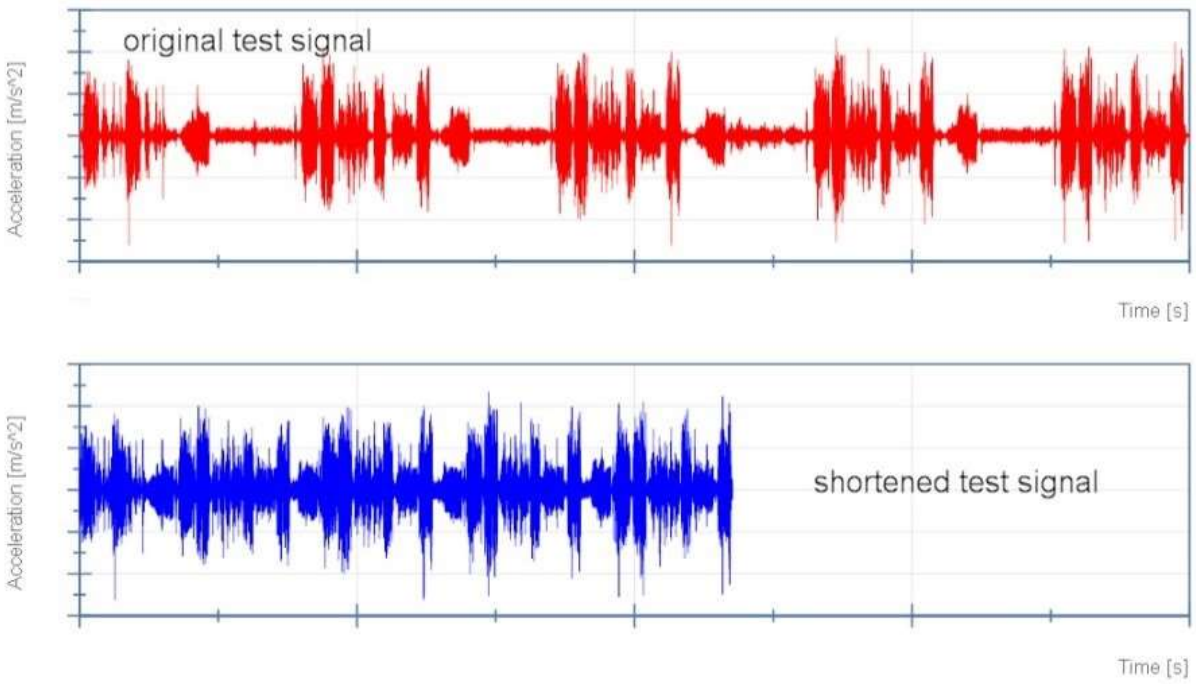


**Figure 4-6: Comparison of an original and shortened test signal [4].**

The underlying assumption of this process – the transferability of accelerations with respect to accumulated damage due to vibration amplitudes – is not valid for a complex system which consists of several individual masses and inertias like the HV-battery. The HV-battery is an inertially excited vibrating system whose mechanical stresses are expressed using frequencies and energies. Using accelerations for applying the well-known concept of accumulated damage effects is not really possible for a complex HV-battery which is made from many individual elements and components providing mass and stiffness. The battery is a flexible system which is loaded by inertia effects. Because of that, stress and damage effects cannot be computed by spectrum based accumulation but has to consider the frequency domain and those frequencies which introduce dominant power. Therefore, the time-domain is transformed piecewise into the frequency-domain using the Fast Fourier Transformation (FFT) where the power signal corresponding to each section is analyzed separately. From the computed individual terms of signal sections, criteria can be developed to serve as a reference to the PSD at a defined level of e.g. 90 %. The idea of the identification procedure is roughly depicted in Figure 4-7. For more details, refer to [4].

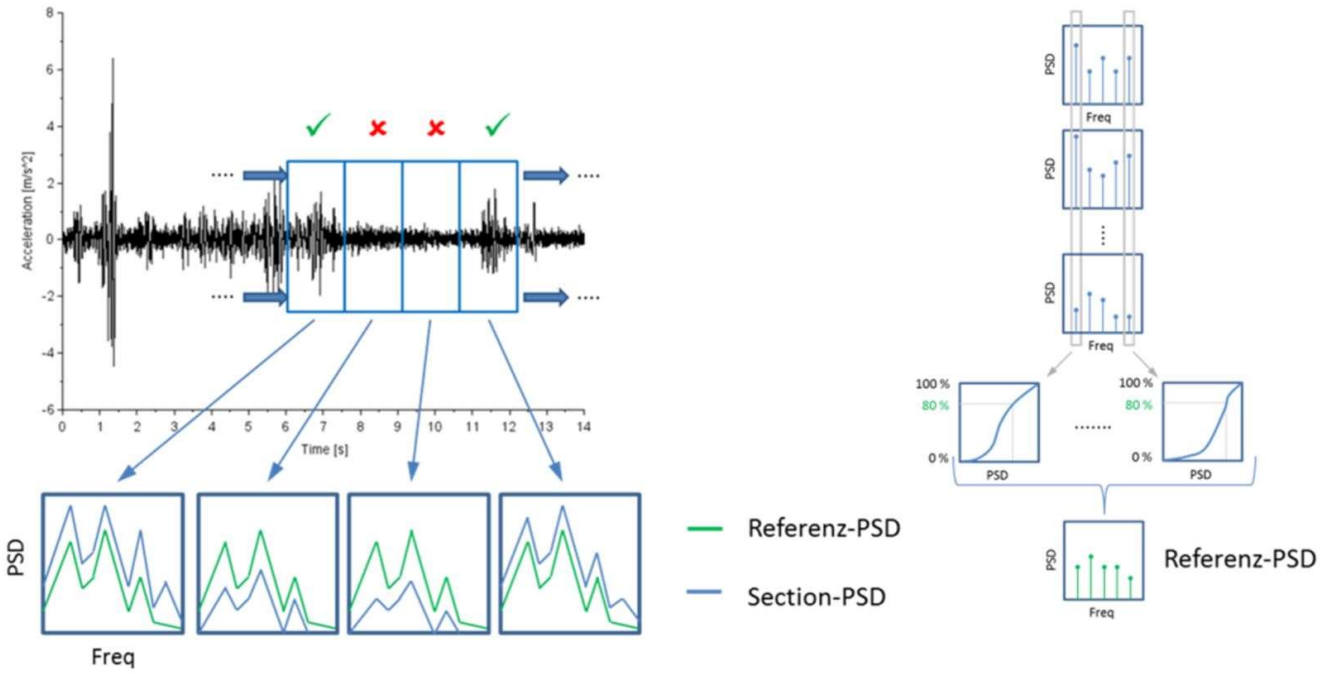


Figure 4-7: Identification of time-sections with low load introduction depending on PSD-spectra [4].

### 4.3.3 Transfer of real mechanical loading to experimentally simulated and time-shortened mechanical loading by MAST

In order to replicate a measured time history series, the response characteristics of the mechanical systems should be known by test drives, see Figure 4-4. There is maybe a need to perform phase shift and/or amplitude corrections to collect the effects of superimposed signals with varied frequencies and phase angles. However, the simple utilization of a target signal does not lead to the desired response corresponding to the target. Figure 4-8 depicts the generation of a drive file by using an inverted system model approach [5]. The system behavior is initially determined using system identification. The inversion of the identified inertia, stiffness and damping matrices provide the inverted system model. The result of the inverse model imposed on the target is the resultant drive file. This is expressed as demand on the real mechanical system.

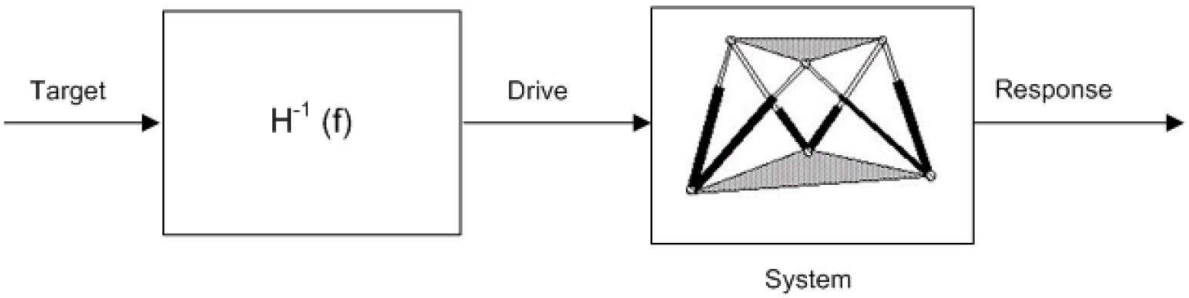


Figure 4-8: Schematic drive-file generation using an inverted system model [5]

In practice, however, model inaccuracies and nonlinearities inevitably lead to deviation from target and a response which cannot be treated as an acceptable solution. Therefore, the cascaded control loop is employed where the system response is compared to the target and the existing error is fed back into the inverted system model, Figure 4-9. The calculated result is amplified and superimposed on the previous drive signal until the response signal nearly matches the target. The number of iterations required depends on the amplification factor, the individual iteration and the quality of the previously identified system model.

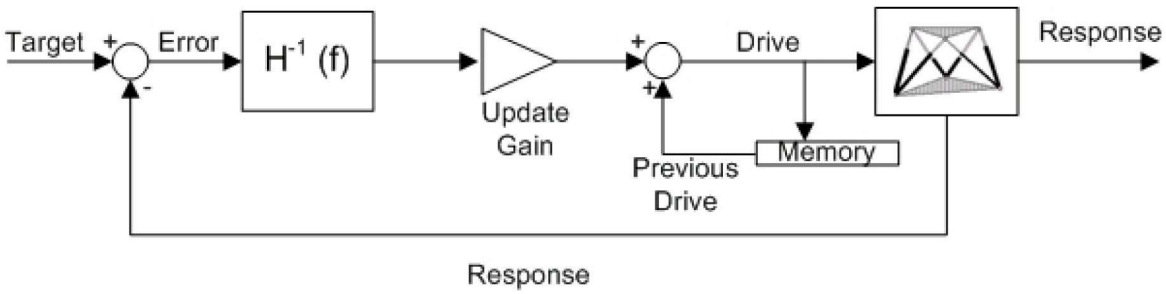


Figure 4-9: Control cascade for drive-file-generation [5].

The quality of the system identification is evaluated by the coherence of the responses against the demand signal. Noisy responses indicate small coherence and an inadequate system model. In principle, all six degrees of freedom of the HV-battery system, consisting of three translations and three rotations have to be covered with at least six uniaxial accelerations. The coherence between signals ranges between a maximum of one, indicating perfect correlation, and a minimum of zero indicating no correlation. The coherences observed are summarized in Figure 4-10, using multiple coherences. Multiple-coherence over the entire frequency range should be larger than 0.8.

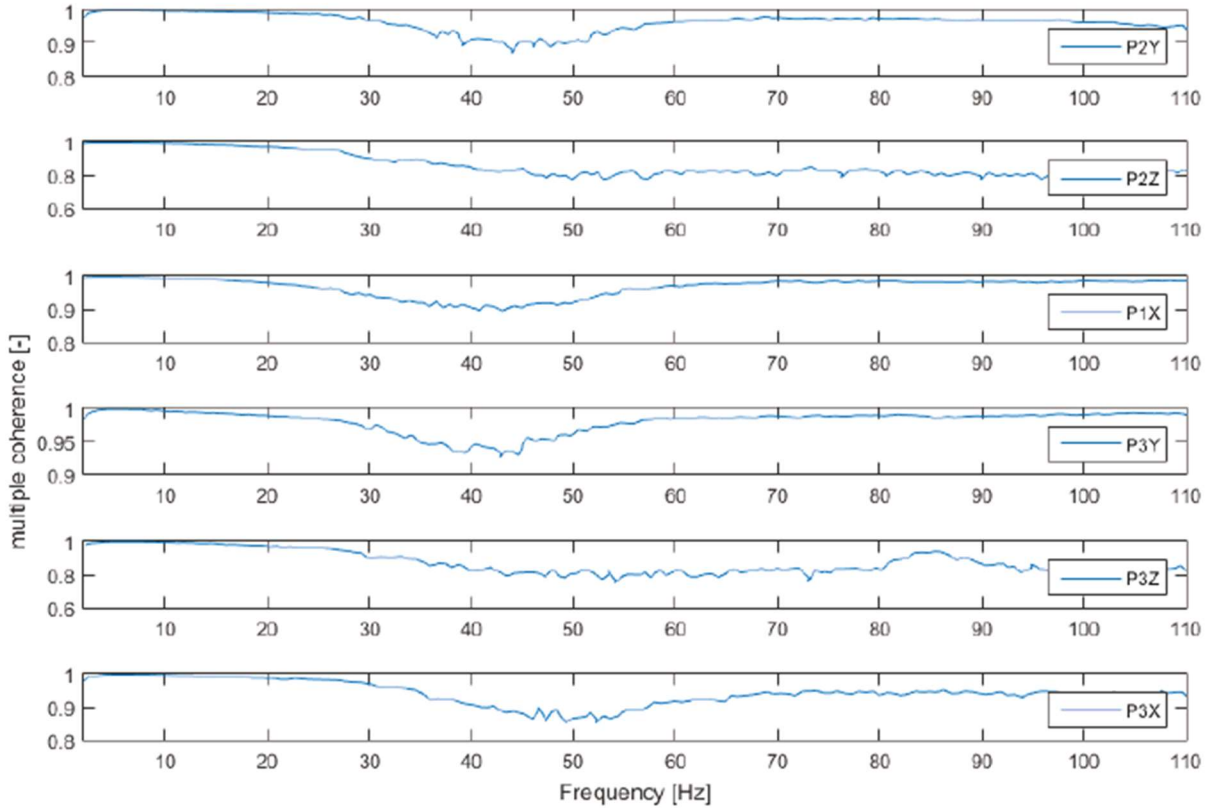

Figure 4-10: Multiple coherence between demand and response signals of individual accelerometers over the excitation frequency range

The iterated signals are classified and checked for consistency in order to ensure that stresses during test remain consistent with stresses during real driving conditions. This is done by comparison as it is shown in Figure 4-11 of the filtered response signals (depicted in red) with the target signals (filtered signal depicted green and unfiltered signal depicted blue).

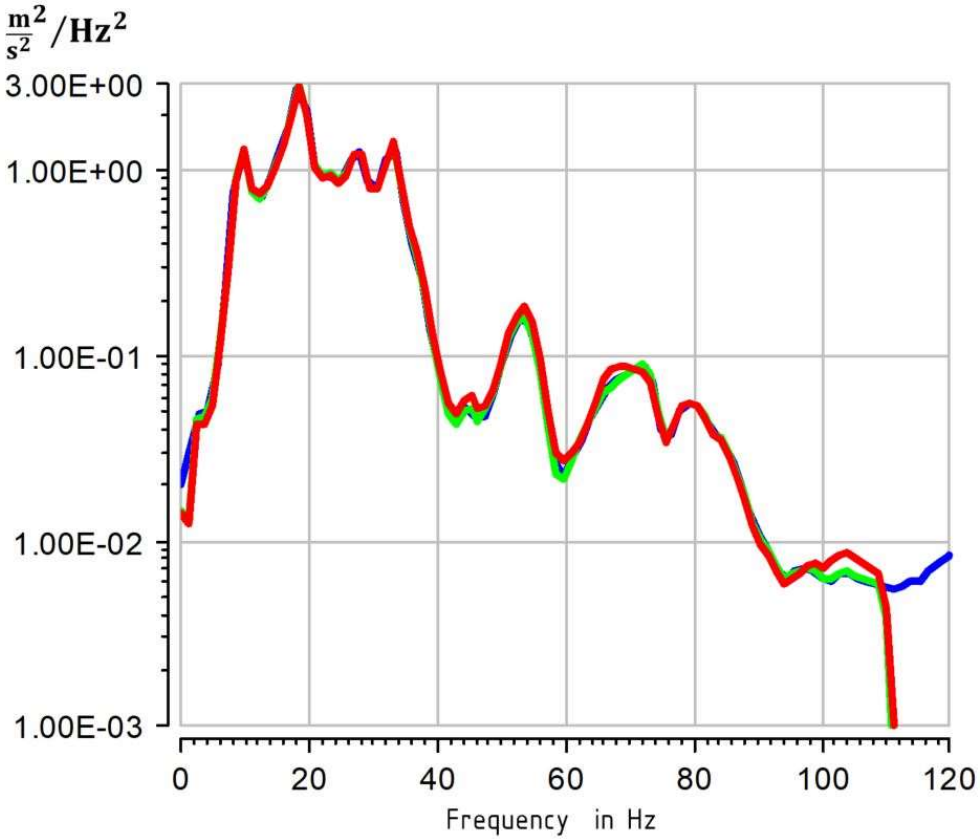


Figure 4-11: Multiple coherence between demand and response signals of individual accelerometers over the excitation frequency range

### 4.3.4 Derivation and monitoring of safety-relevant parameters during experimental evaluation and Introduction of these parameters into overall safety assessment tools like probFMEA

The approach of multi-domain, system-integrated battery testing enables the revision and verification of the functionality and behavior intended in the system design. On the test bench, the co-functioning components actually operate together under realistic loads and surrounding conditions. Furtherly, with additionally applied measuring equipment and sensors, as well as wide-ranged recording and evaluation, the concise system function can be assessed and verified, eventually.

Thereby, for safety and reliability it is of importance to observe, whether the system is operating robustly and flawlessly under regular operating conditions and modes, as well as under extreme scenarios and conditions. This allows for an assessment whether the system operates as desired concerning primary properties as electrical performance, as well as secondary characteristics, such as controllable heat generation and sufficient heat removal. Based on this, the appropriateness of the implemented recording and monitoring of the operational loads in the target system can be validated. For this, based on the recordings of the full set of data in

the test facility, it can be interpreted, whether the data recorded and observed under regular operation provide an information profile, which is sufficient for a safe and flawless operation.

As well, the functional concept of the battery system and its ability of co-functioning with the vehicle drive train can be displayed in a near-realistic way.
Furthermore, the reliability and safety-relevant properties of single components can be implicitly verified or, if present, error-proneness are possible to be investigated. At the end of a sufficiently long and intense test campaign with full coverage of potential adverse influences, it can be assumed, that the parts and the implemented design are accordingly robust. This can be interpreted as a certain minimum level of reliability of the parts under the applied stresses and loads.

In addition to the observations of flaws and damage under extreme reference scenarios described above, injection of faults is of high relevance in order to show, that the system is behaving or acting in a desired and specified way. For both, the robustness against extreme influences as well as specified failure occurrences, the localization of relevant failure locations and phenomena is strongly supported by analytical failure analyses, such as the FMEA in general. For this, it brings along criteria and details of which critical parts to test or inspect concerning specific phenomena or properties. This contributes to defining the data to be observed, faults to be injected during the test and details to be examined during and after the test run.

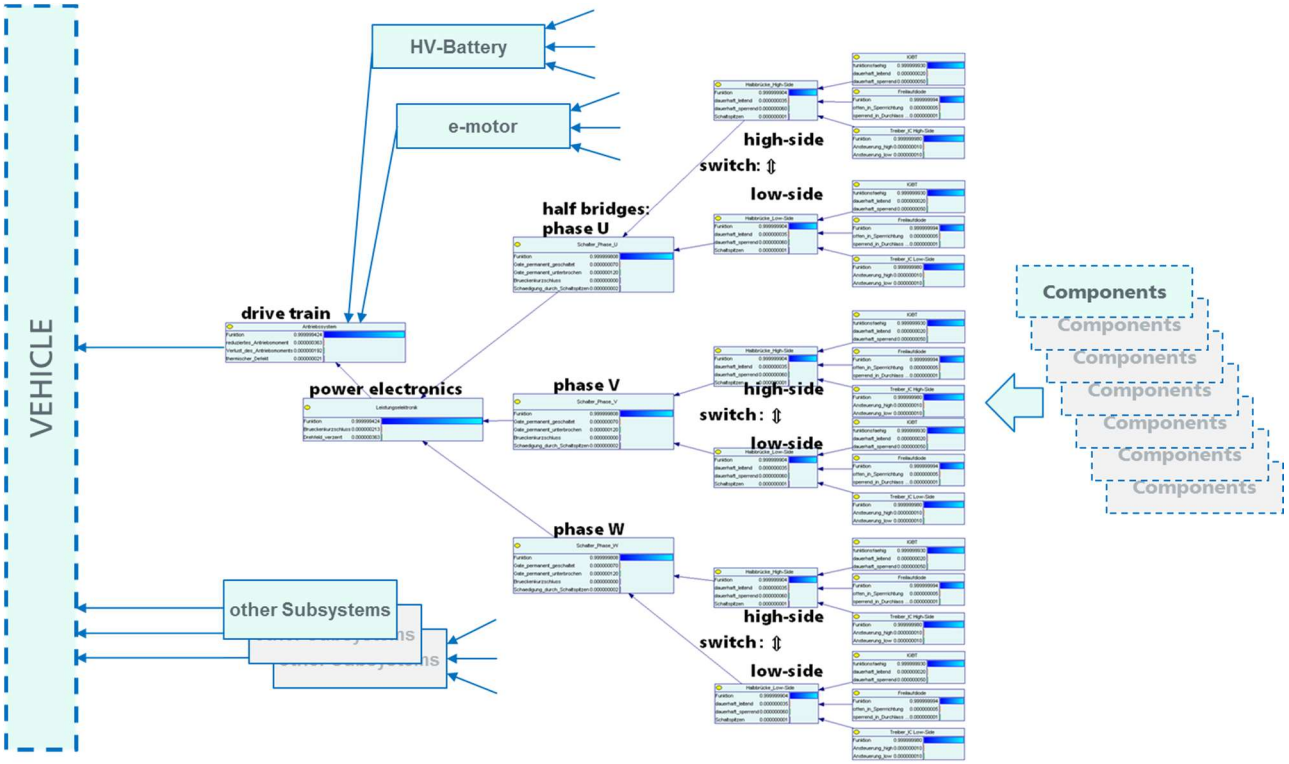


**Figure 4-12: Excerpt from the probabilistic FMEA (probFMEA) as a basis for holistic system reliability and safety assessment**

The information obtained by the evaluation of the test campaign, in return, is useful to reduce uncertainty in the appraisal performed in analytical failure analyses, e.g. FMEA, and probFMEA, especially. In OBELICS, the probFMEA will serve as the major tool for the assessment of the holistic system (vehicle topology) covering failure mechanisms from the subcomponents of the powertrain in general and from the battery specifically, Figure 4.12. This concept was presented in [6]. During the elaboration of the failure analysis databases, the majority of assumptions on the correct behavior of components implicitly are based on the premise of the overall structural integrity and robustness of the system as a whole. To substantiate this assumption, an

accordingly intense testing provides verification for this fundamental prerequisite. Further, in case of revelation of flaws, the estimation of the probability of the failure mode can be refined and uncertainty can be reduced. The conditions which promoted the failure and its consequences can be evaluated and inserted into the database. Additionally, fault injection can serve for the verification of the effectiveness of failure diagnosis, as well as the correct triggering of derated operation or safety mechanisms, in general, within the boundaries of a non-destructive operation.

### 4.3.5 Role of the presented methods within OBELICS

Within the project, the here presented measures interact with other activities in the following way:

1) Experimental data generation for feeding the models developed in WP 2 and 3 (with or without reference to safety aspects, depending on the demands of the model)
2) Integration of the probFMEA as a tool to interconnect the OBELICS activities to the demands of ISO 26262.
3) Creating demands for testing and test facilities in WP 4 in order to gain realistic and useful reliability and/or safety relevant data.
4) Collecting and structuring information of the use cases with regard to performance and/or safety metrics.

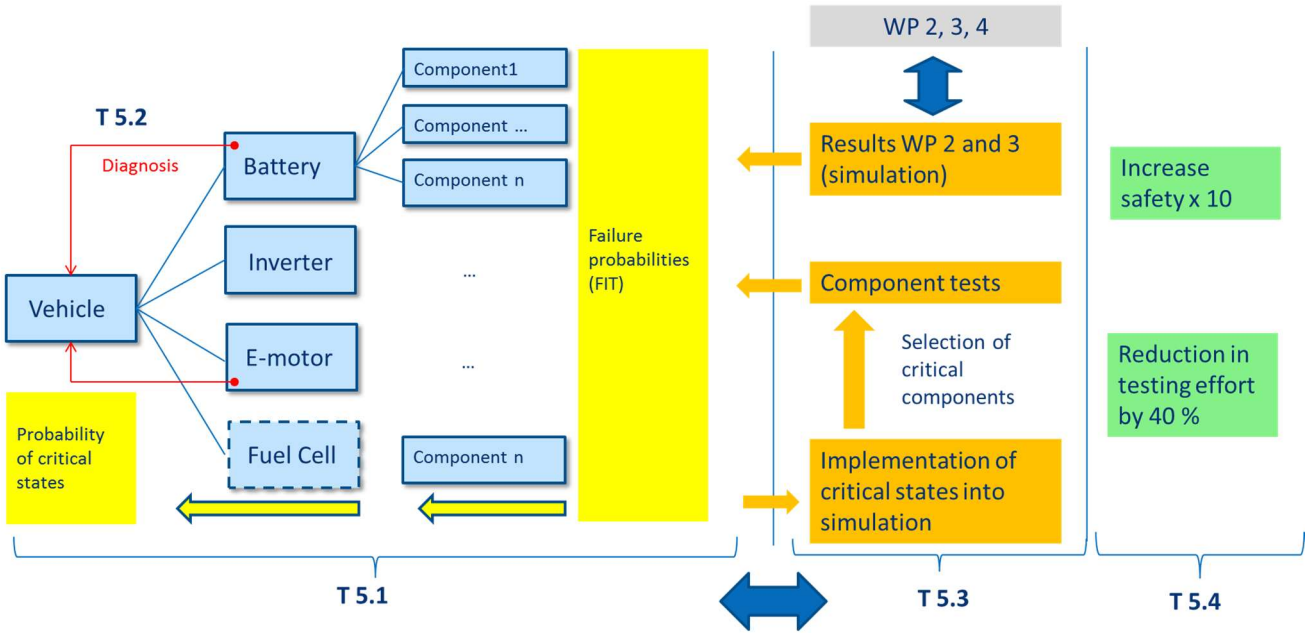


**Figure 4-13: Workflow for safety-relevant tasks within the OBELICS project**

Fig. 4-13 gives an overview of the interactions and workflows of different tasks in WP 5 (where the safety analysis is mainly performed) to other WPs and activities. One major aspect regarding the safety evaluation is to create proper safety-relevant data which shall be converted into a FIT (Failure-in-time) – rate as an input quantity for the probFMEA. In so far, the battery is one part of the power train contributing to the overall safety of the powertrain and the vehicle. In order to increase the safety on system level, measures may be introduced on battery or on a system level, depending on the failure mode. These assumptions underline the earlier statement that the safety of the battery is to be evaluated on the system (vehicle) level.

# 5 State estimation

Performance and Safety International (European and Extra-European) standards define a set of acceptable criteria to ensure that the battery system (lithium type) is safe and suitably efficient when installed on Hybrid or Electric Vehicle (HEV, EV). In particular, performance test procedures allow the estimation of actual battery state and its parameter identification. These data define cost and quality of battery (in terms of singe cell, module and battery systems) and they are also fundamental to define weight, reduction of space, and in conclusion they are useful to safety when battery is storing and delivering energy on an HEV or EV, so they should be periodically monitored. State of Art of battery state estimation proposes solutions that can be performed online, then on board the vehicle, or through laboratory tests, in this case using the test procedures proposed by the International Standards. For these test, current and voltage supplied/absorbed by battery and temperature (surrounding, battery surface or internal temperature) are the main inputs which are used for battery state estimation. In literature there are different definitions of battery state; the main parameters which should be continuously monitored are the following:

- **State Of Charge (SOC):** is the percentage of residual capacity respect to battery nominal capacity.
- **Open Circuit Voltage (OCV):** is the battery voltage measured when no load is attached.
- **State Of Health SOH:** is usually defined as a vector which contains the degradation over time (aging) of some parameters such as internal resistance and capacity.
  1. **Capacity Fade:** is the percentage of maximum available capacity of aged battery respect to new.
  2. **Internal Resistance:** is the percentage of internal resistance of aged battery respect to new.
- **State Of Function (SOF):** is the ability of the battery to support a particular application in its current state. This concept is mainly used to identify online if the battery can be used to power the application in its current SOC and SOH.

In this chapter, state estimation methods for lithium battery are discussed during test procedure, highlighting their requirements: definition of input measurements data and accuracy of respective sensors, sample time, and environmental conditions.

## 5.1 State of Charge and Open Circuit Voltage

Open Circuit Voltage (OCV) is considered as main battery identification parameter because its value is strongly related to State Of Charge (SOC), and the estimation of OCV-SOC curve function is very useful to obtain not only a robust SOC estimation, but a robust SOH estimation too. A classical method for SOC estimation is the integral current measurement at a defined sample time (in literature Ampere-hour Counting method). However, this method can be used if current sensor is more accurate and sample time is little; moreover, initial estimation SOC must be corrected. Implementing only Ampere Count method for online SOC estimation on board EV could present high estimation error. So, to improve battery state estimation accuracy, BMS should be able to simulate internally the charge and discharge processes using a battery physical model. Thevenin equivalent circuit model of battery is usually used because it should solve the compromise between computational cost and accuracy to simulate battery discharging process and its electrical properties. An example of Thevenin equivalent circuit is shown in Figure 5-1. The Open Circuit Voltage value defines Thevenin ideal voltage generator and it is related to SOC. Using an opportune model-based observer, e.g. Kalman Filter, SOC should be estimated minimizing its mean square error, so optimizing SOC estimation. Thanks to OCV-SOC curve, algorithm can correct the current integral errors during runtime. In this case calibration OCV-SOC is necessary before algorithm runs. Moreover, OCV is not sensitive to surrounding and battery internal temperature [7], [8]. In particular in [8] it was proven that OCV value changed less than 10 mV as temperature passed from -10℃ to 50℃. The pulse charge and discharge test under room temperature can be performed to calibrate this curve. An example of this test is shown in [9] and [10], where is called Pulse power characterization profile, using for battery internal resistance estimation too. Another example of pulse charge and discharge test is shown in Figure 5-2: under this test, the cell was first completely charged, rested for 2 h and then subjected to ten discharge pulses interspersed by 1 h rest phases till the cell was completely discharged. Subsequently, the cell was charged using ten charge pulses interspersed by 1 h rest phases till the cell was completely charged. The cell was then allowed to rest for 13 h.

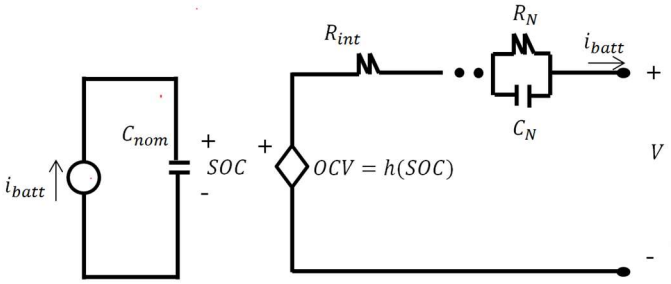


Figure 5-1: An example of battery model using Thevenin equivalent model circuit.

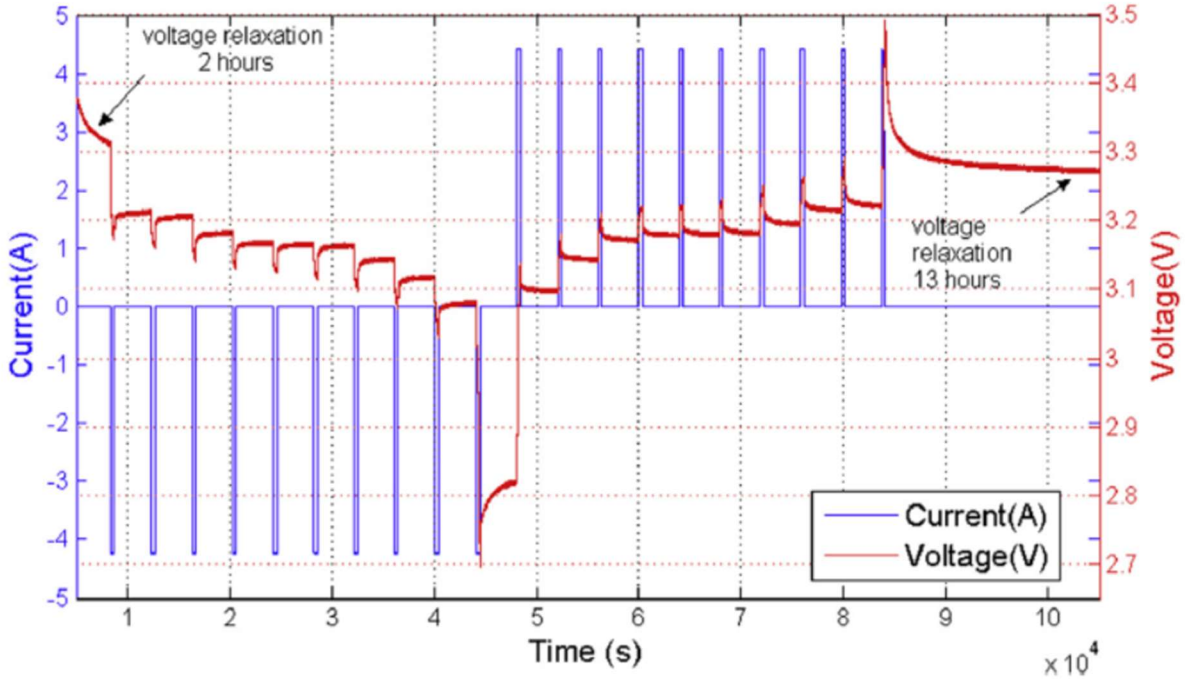


Figure 5-2: An example of Pulse discharge and charge test (is similar to pulse power test described in [9]) to calibrate OCV-SOC curve and analyze voltage relaxation effect of a LFP cell [11].

Using profile test shown in Figure 5-2, it is noticeable that battery voltage relaxes to approximately reach its OCV after a period of rest; this phenomena, called *Voltage relaxation effect* should be added to battery Thevenin circuit using one RC block. In [11], [12], [13], [14] complete voltage relaxation time is major of 1 hour, and it changes depending on battery SOC. Indeed, voltage relaxation time is less between the [20, 80] % of SOC compared to when the SOC was near 0% or 100%, as seen in Figure 5-2. From the pulse discharge and charge test, OCV should be plotted with respect to the SOC choosing a time of rest. Obviously, OCV measurement is more accurate if time of rest chosen for the test is longer, as seen in Figure 5-3. OCV should be measured in correlation with actual SOC in pulse discharging phase and in pulse charge phase, observing hysteresis phenomena which is present in lithium batteries. In Figure 5-3 it is noticeable that the hysteresis effect is correlated with the long voltage relaxation time, with the level of hysteresis decreasing with the rest period. Chosen an appropriate time of rest of the test, is reported an example of OCV-SOC curve with hysteresis effect in Figure 5-4.

In lithium battery, especially LFP, curve is extremely flat in the middle area for the SOC, e.g. the voltage gradient of the LFP OCV-SOC curve shown in Figure 5-4 is of the order of 0.1 V in the window of [20%, 80%] of SOC. Even a small error in voltage measurement, would lead to extremely inaccurate results in this area, thus it occurs that OCV-SOC calibration should be accurately estimated.

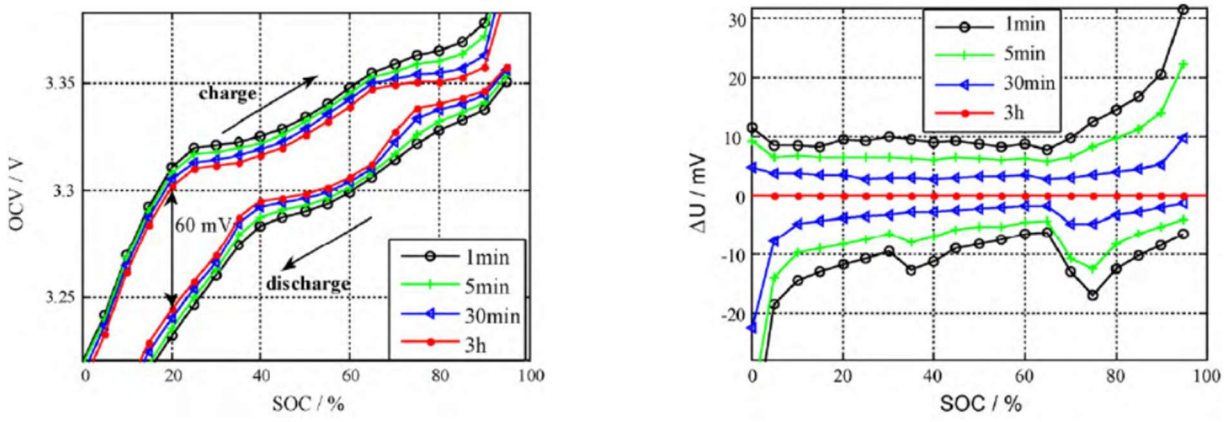


Figure 5-3: OCV-SOC of a LFP cell curves plotted at various rest period on the left; OCV estimation error at various rest period on the right [12].

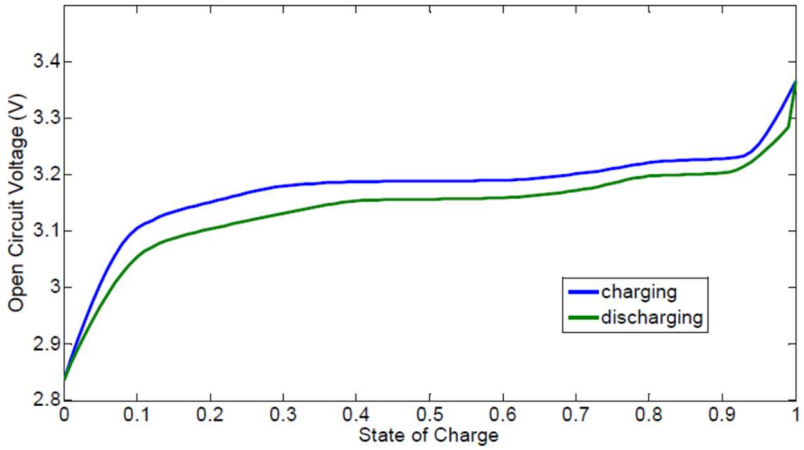


Figure 5-4: Flat OCV-SOC correlation for a LFP cell [11].

## 5.2 State of Health

The State of Health (SOH) defines the performances related to the condition of the battery in beginning of life; it is a parameter used to predict the "end of life" and battery aging. Battery performance parameters which degrade with battery aging are mainly two:

- **Capacity Fade:** battery rated capacity decreases over time, thus the maximum available energy stored by aged battery becomes less.
- **Internal resistance:** battery internal resistance increases over time; this increase causes a drop in the power that can be extracted / injected from / into the battery, thus a power fade for aged battery and the decrease of the battery charge/discharge maximal current intensity.

SOH estimation of a battery is an extremely complicated task, since there are many factors that interact with each other affecting the overall performance of the battery. The factors that most influence the battery are the following:

- The charge and discharge C-rate to which battery is subjected;
- Environmental temperature;
- Depth of Discharge (DOD) and Charge (DOC) to which battery is subjected;
- Self-discharge;

In [15] it was confirmed that environmental temperature was a major factor contributing to aging acceleration in the real world. So, it is important to specify environmental test condition and charge/discharge current profile.
In the next sub-chapters, it is discussed not only the test profile applied for SOH estimation, but the possibly method to estimate battery SOH analyzing their input and constraint condition requirements.

### 5.2.1 Capacity Fade

Battery capacity test procedure is described in according to international standard ISO 12405 and represented in [9], [10]. Test consists of standard charge and discharge test at a constant current, interspersed by a rest period. This test is conducted at different C-rate charging and discharging phase to have consistent battery capacity estimation. Moreover, this test should be conducted at different temperature (room temperature, -18°C, 0°C, 40°C) to observe in particular battery's performance under extreme temperature. It's noticeable in Figure 5-5 that capacity estimated under extreme temperatures is more different respect to capacity reference [16]. Consequently, it is important that test is conducted at least once at room temperature.

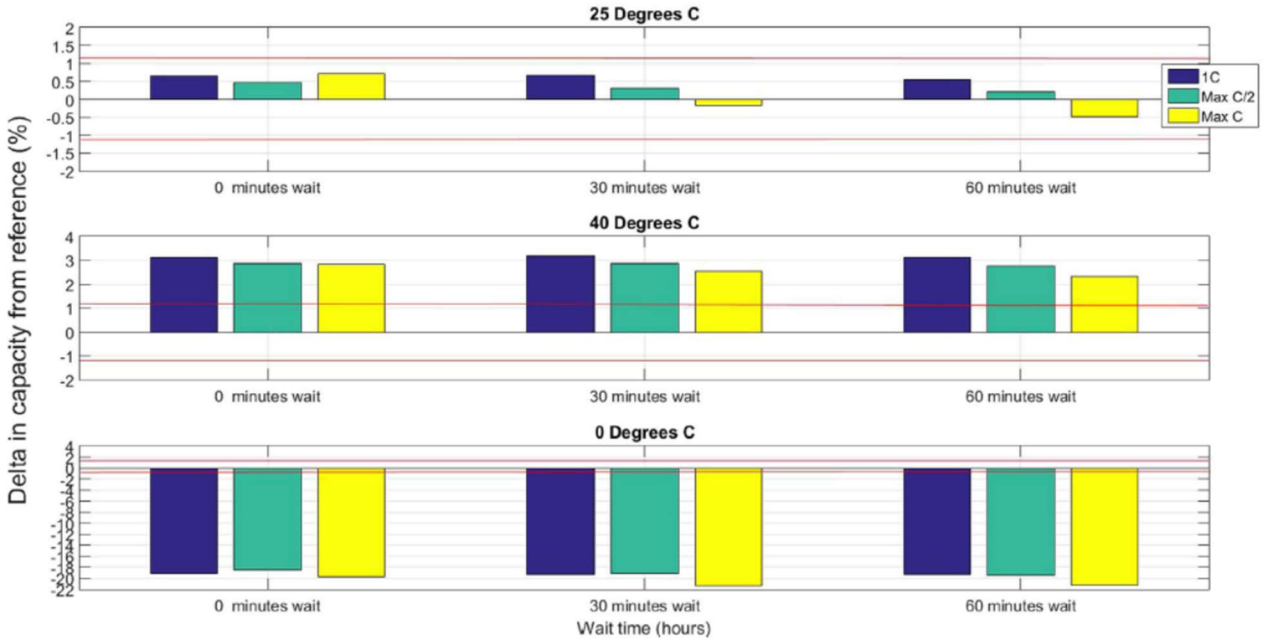


Figure 5-5: Capacity estimated for a LFP cell under different capacity test varying charge/discharge rate, rest period and environmental temperature [16].

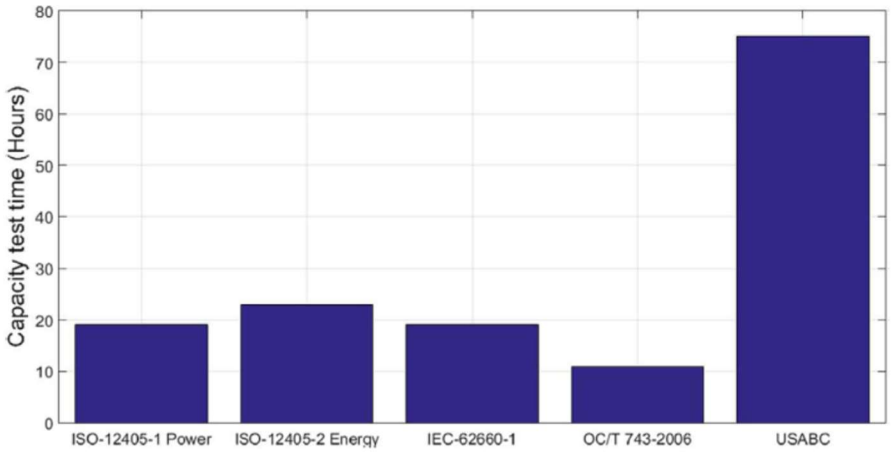


Figure 5-6: Capacity test durations within international standards [16].

Classical method for capacity estimation is the integral current calculation (Ampere Count method) during complete standard charge or standard discharge phase. This method can be used if current sensor is more accurate and sample time is little; moreover, initial estimation SOC must be corrected. Then, capacity estimation performed by standard test procedure takes a long time, as shown in Figure 5-6. Recently, in [7] and in [17] it was proven which battery rated capacity can be estimated by identifying known features of the OCV-SOC curve. In [17] this new capacity estimation method is called *Improved Ampere Count*. In Figure 5-7 is represented Ah-V

curve (SOC is replaced by accumulated capacity in Ah and V is replaced by OCV) of LFP cell at its different phase of life. From Figure 5-7 it's clearly noticeable that Ah-V curve exhibits some particular features which quite not sensitive respect to battery SOH are. In this way, recognizing a specific feature (e.g. feature highlighted in Fig. 8), it's possible to identify a known SOC level. Moreover, feature highlighted in Figure 5-7 could be analyzed by its slope: indeed, aged cell, assumes a flatter curve than new cell. Consequently, an Incremental Capacity Analysis of Ah-V curve [7], [17] can be conducted to estimate SOH by feature's slope, computing step by step numeric derivative of Ah-V curve (ICA curve) as shown in Figure 5-8. Once cell ICA curve is reproduced in the feature of interest (found in the definite voltage of interest), Ampere-count method is used to analyze the whole feature, i.e. integral of ICA curve is calculated and finally results is proportioned by capacity accumulated of the new cell in this voltage of interest (Figure 5-9). Indeed, measuring area instead of only peak maximum amplitude provides more accurate results because the integration process acts as an average of whole feature. It is observed that a reduction of the area consists of a reduction in the accumulated capacity among the two voltage limits, thus in proportion, a capacity loss and so SOH degradation.

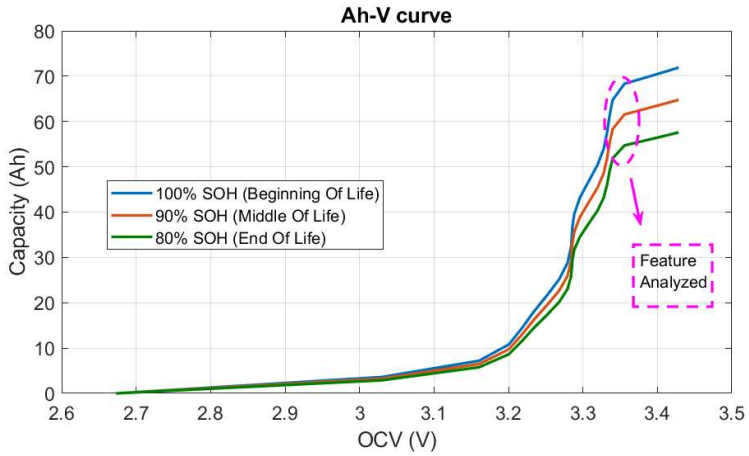


**Figure 5-7 Ah-V curves of LFP cell at different SOHs and the particular feature's curves analyzed in [17].**

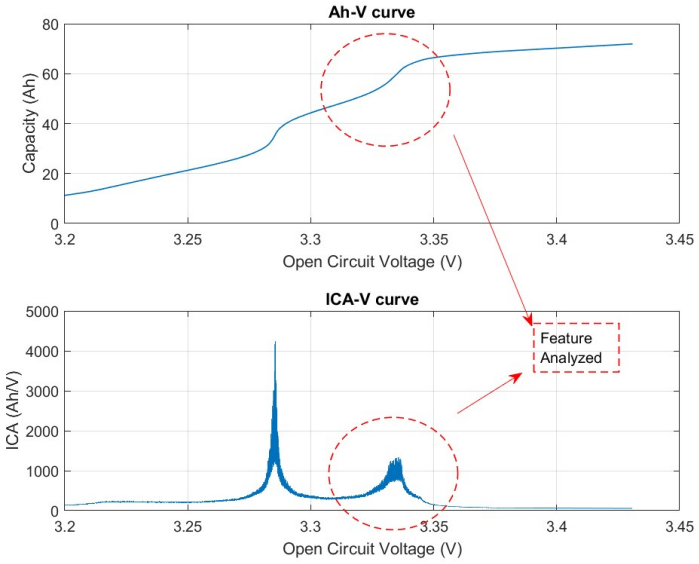


**Figure 5-8: ICA curve and its construction before numerical derivation [17].**

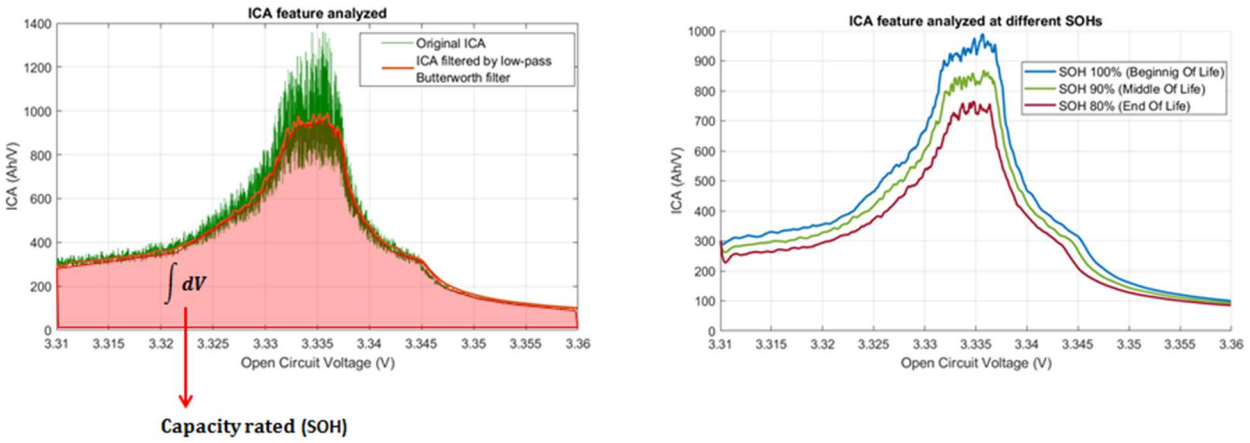


**Figure 5-9: ICA curve reproduced and integration process to obtain SOH information by comparison capacity rated between aged and new cell on the left; ICA curve at different battery phase of life [17].**

This novel approach allows to estimate battery rated capacity online and on-board vehicle; moreover it can accelerate energy capacity measurement because requires only a partial recharge, e.g. it requires recharging phase from 65% to 90% of SOC to identify slop feature in [17] and estimate SOH. Moreover, this method can be used during all battery's life, because Ah-V feature analyzed is always present during its life. However, improved Ampere-Count method elaborates an accurate SOH estimation if OCV and current values during phase recharge are accurately measured. Consequently, this method requires a more accurate OCV-SOC calibration and current and voltage measurement should be acquired at a sample time order of 1 s.

### 5.2.2 Internal Resistance and Power Fade

Battery internal resistance is the parameter which defines battery performance: voltage drop, power dissipated in heat, maximal charge and discharge current and finally battery efficiency depends by this parameter. Internal resistance value strongly depends on battery SOC and surface (or internal) temperature: in [18] and in [19] it is proven that battery internal resistance value increases when temperature decreases and at low SOC values. In particular this effect is shown in Figure 5-10, where in [17] it's realized a surface function $\Upsilon(SOC, Temp_{sur})$, which returns the value of cell internal resistance in function of the *SOC* and the surface temperature $Temp_{sur}$.

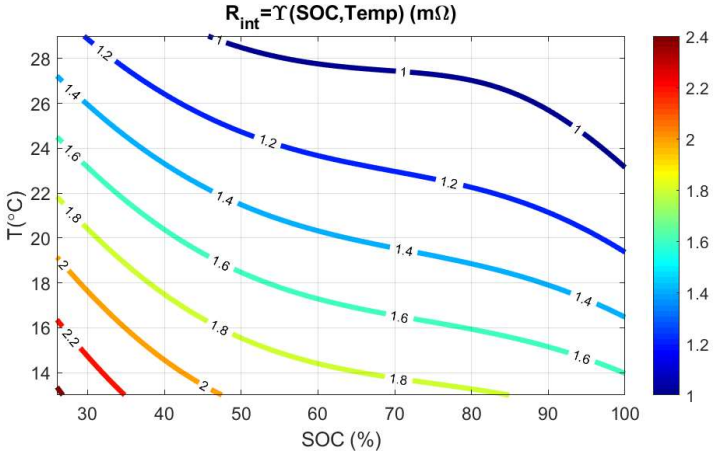


**Figure 5-10: Analytical surface function internal resistance for LFP cell [17].**

The pulse power test shown in [9], [10], which combines the PNGV / Freedom Car "Hybrid Pulse Power Characterization Test" and the EUCAR "Internal Resistance, Open Circuit Voltage, and Power Determination Test", is used for internal resistance identification and in general for battery Thevenin model's parameter identification shown in Figure 5-1. Defining the equations on battery model circuit's loop:

$$\begin{cases} \dot{SOC}(t) = \dfrac{1}{C_{nom}} i_{batt}(t) \\ \dot{v}_1(t) = \dfrac{v_1(t)}{R_1 C_1} + \dfrac{1}{C_1} i_{batt}(t) \\ \vdots \\ \dot{v}_N(t) = \dfrac{v_N(t)}{R_N C_N} + \dfrac{1}{C_N} i_{batt}(t) \\ v(t) = OCV(t) + R_{\text{int}} i_{batt}(t) + v_1(t) + \ldots + v_N(t) \end{cases}$$

**Equation 5-1: Time continuous battery model circuit.**

Battery voltage $V_{model}$ can be estimated solving system (Equation 5-1). The identification of parameters $(R_0, R_1, C_1, \ldots, R_N, C_N)$ should be computed minimizing the error between measured and simulated voltage profile. The classical error function chosen to be minimized is the following:

$$\varepsilon = \sum_{k=1}^{M} (V_{measured,k} - V_{model,k})^2$$

**Equation 5-2: Least Square Error function is chosen as performance index to be minimized.**

Last equation corresponds to the parameter identification based on Least Square Method; *M* represents the end of time test. This method should be used at various SOC values during pulse power test in order to analyze relationship between model's parameter and SOC. Moreover, it is suggested to conduct test at different room temperature in order to realize an appropriate surface function or look-up table which relates model's parameter with SOC and temperature at a sampling frequency of least 0.1 Hz. As already mentioned, battery model has a generic number $n$ of RC groups, where $n$ is usually 1 or 2 to avoid excessive complexity of the model. The Figure 5-11 shows the comparison between experimental and simulated voltage for $n$=1 and $n$=2 at the end of discharge and charge pulse. The comparison shows that both models present rather acceptable results, but the 2 RC group model gives very good result even during the first part of the considered transient. Indeed the 2 RC group model uses one RC group to capture the short-term relaxation dynamics and the other RC group to capture long-term relaxation dynamics.

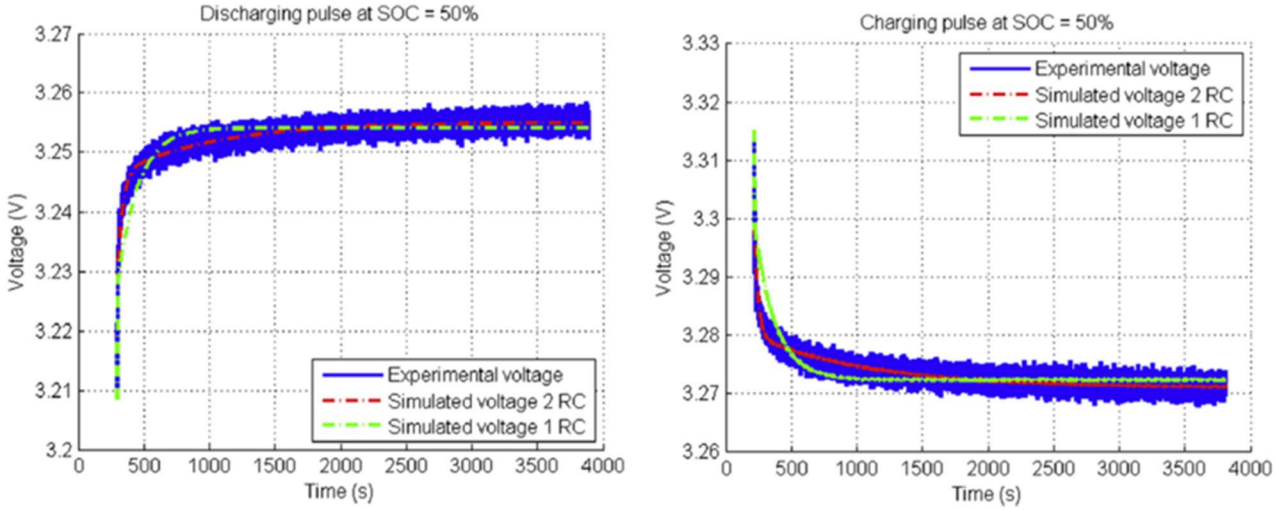


**Figure 5-11: Voltage behavior after a discharge process (on the left) and charge process (on the right) [11].**

An alternative method is the online battery model's parameter identification defined *Recursive Least Square* method [19], [20]: at each sample time *kT*, the set of parameters $(R_0, R_1, C_1, \ldots, R_N, C_N)$ are recursively

estimated minimizing the performance index (Equation 5-2) which *M*= *kT*. The estimation approach of this algorithm is similar to Kalman Filter, where the state of process is represented by the model's parameter. To enhance recursively estimation parameters by varying of actual operating conditions of the battery, e.g. the sudden passage from a discharge to a charge phase (regenerative brake), parameter λ ∈ [0,1] called *forgetting factor* is inserted in performance index (Equation 5-3):

$$\varepsilon = \sum_{k=1}^{M} \lambda^{M-k} (V_{measured,k} - V_{model,k})^2$$

**Equation 5-3 Recursive Least Square with Forgetting Factor performance index**

The voltage estimation error squares committed are weighted according to the distance from the current time *kT*. The voltage estimation errors more near to the current time are more weighted, thus this method elaborates the identification of the parameters focusing more on the last errors. Typical λ values are 0.99, 0.95 and 0.90.

#### 5.2.2.1 Electrochemical Impedance Spectroscopy

Battery should represent Ohmic-capacitive effects due to its electrochemical properties, e.g. the ion diffusion dynamics in the cell's electrolyte and the electrons diffusion dynamics (faster) on the cell's electrodes. Consequently, it's important to define battery impedance which takes into account all these dynamics. So, battery impedance strongly depends on the sample time which internal resistance is estimated; the time duration of test and the frequency content of current signal which is supplied as input of battery model (its spectral density). In general, *Electrochemical Impedance Spectroscopy* (EIS) is conducted to analyze battery impedance when battery model is subjected to sinusoidal currents at various frequencies. Battery impedance is usually plotted in Nyquist diagram, where in *x*-axis is represented real impedance (resistive effects), and in *y*-axis negative imaginary impedance (capacitive effects). In Figure 5-12 is shown ideal lithium battery impedance.

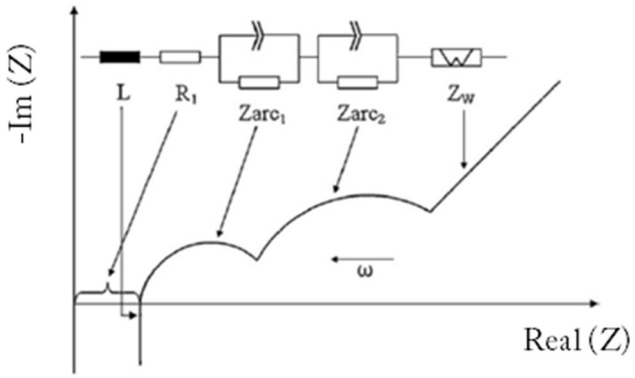


**Figure 5-12: Ideal impedance spectrum of a lithium-ion cell and all lumped parameters in series which compound impedance.**

Battery impedance is represented by an electrical circuit composed of passive elements connected in series which describe impedance behavior at various frequencies. In detail, these passive elements are described starting from low frequency:

- **Warburg impedance ($Z_W$):** it is present at very low frequency, with a linear trend with slope of 45° and it is usually simplified as a parallel of resistance and capacity. This impedance represents the phenomena of lithium diffusion in the porous active material of the electrodes.
- **$ZARC_2$ impedance:** it is shown by the second arc of a circle and represents the capacitive effect of the double layer interface and the resistance to the transfer of charges to the electrodes.
- **$ZARC_1$ impedance:** it is shown by the first arc of a circle; it is not always detected and represents the ohmic-capacitive effects of the *Solid Electrolyte Interphase* (SEI) formed during charge and discharge cycles on the anode surface.
- **Internal Resistance ($R_1$):** its value is identified in the intersection point between *x*-axis (Real(*Z*)) and impedance Nyquist diagram (called *zero-intercept Nyquist diagram point*). It represents the sum of resistors of current collectors, electrodes, electrolyte and SEI.

- **Inductive reactance ($L$):** it is present at very high frequency; battery presents inductive behavior due to the metal elements of the battery and cables.

In literature, complete EIS [21], [22], [23], [24] are measured in the frequency range from 1 mHz to 5 kHz, then current and voltage measurement are acquired in a sample frequency > 10 kHz.

### 5.2.3 Internal temperature

EIS measurement provides comprehensive information on battery impedance. Moreover, in literature, new methods are proposed to measure battery internal temperature based on EIS. Experimental test results in [25] prove that the zero-intercept Nyquist diagram frequency $f_0$ is exclusively related to the internal battery temperature; this relationship and does not depend on SOC and aging as shown in Figure 5-13. This method is useful in online application. Indeed, computing a $f_0$ – internal temperature function during EIS measurement in laboratory, BMS should have an online sensorless battery internal temperature information exciting battery with a current signal in an appropriate pass-band or exciting with a broadband current signal proposed in [26]. In [27] it is suggested to consider fixed impedance point at higher frequency than $f_0$. The advantage of this method is that measurement interferences, resulting from the current flowing through the battery can be avoided at these frequencies (not $f_0$). This gives higher signal-to-noise ratios (SNRs) and, consequently, more accurate temperature measurements.

An alternative sensorless method for battery internal temperature estimation is the Kalman filter observer based on adaptive thermal model [8], [28]. Indeed, battery thermal model should be described by an electrical circuit model as shown in Figure 5-14. Thermal and electrical processes represent exchanges of energy flows between two physical entities; so there is a strong correlation in the description of the two physical dynamics.

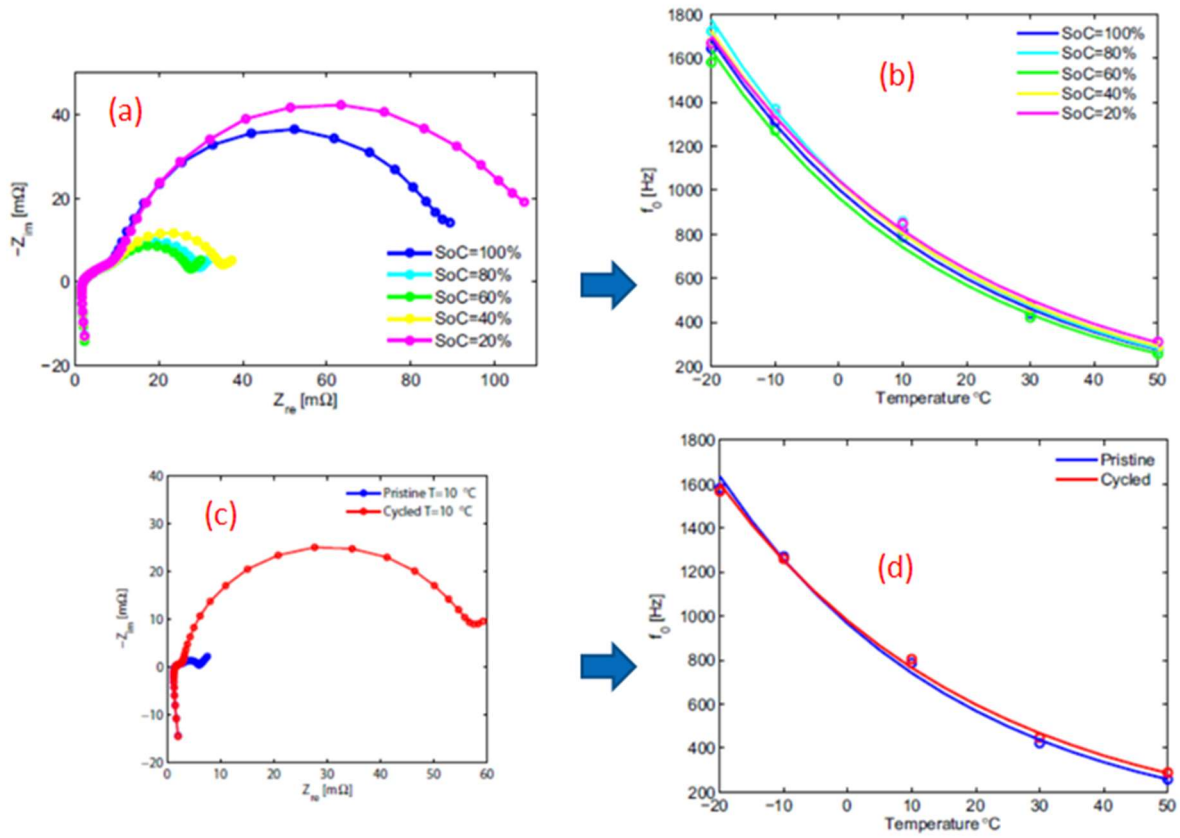


**Figure 5-13: Zero intercept frequency – NCA cell internal temperature results: (a) Nyquist plot of the impedance of new cell tested at -10°C at different SOC and (b) plot intercept frequency as a function of internal temperature; (c) Nyquist plot of**

impedance of new cell (Pristine) and aged cell (Cycled 600 times), finally (d) plot intercept frequency as a function of internal temperature [25].

After this consideration, the difference of temperature should be associated with a difference of electrical potential of two sources on a physical conductor; moreover the heat flow should be associated with the current flow exchanged between these. Battery thermal model shown in Figure 5-14 illustrates the dynamics of the exchange of heat flows from inside the battery to the outside. $T_{in}$ is the battery internal temperature; the amount of heat dissipated inside for Joule effect corresponds to the ideal current generator $Q_{th}$. Then, the transient heat exchange between internal and surface of battery is represented by the same electric dynamics of an RC group. It's composed by $C_{th,in}$, which is battery internal thermal capacity, and $R_{th,in}$ which is inversely proportional to heat conduction coefficient between internal and battery surface. $T_{sur}$ is battery surface temperature. Exchanges of heat flows between the surface of the battery and the surrounding temperature $T$ are represented by $R_{th,sur}$,$C_{th,sur}$ parameters. Battery thermal model's parameter can be identified using capacity test procedure defined in [9], [10], under different room temperature: in this case, internal and surface temperature should be measured; so parameters should be estimated minimizing performance index (Equation 5-2, Offline estimation method; or Equation 5-3, Recursive Least Square with Forgetting Factor method).

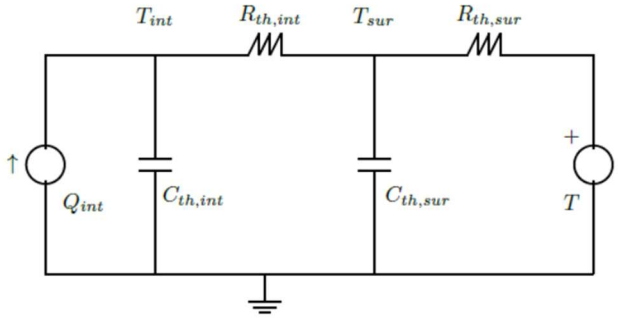


Figure 5-14: Battery thermal model.

## 5.3 State of Function

Results of battery model's parameter identification, state estimation and their calibration with battery model external input as current, temperature, voltage and internal input as SOC allow BMS to compute online battery State of Function. SOF is considered as a vector which uses information from actual battery SOC and SOH in order to define current and power limits which battery is constrained to guarantee its safety. Moreover, SOF should contain the effective energy (in *Ah*) actually stored by battery. Presuming $V_{max}$ and $V_{min}$ are the voltage limits, $I_{max,curr}^{charg}$ and $I_{max,curr}^{discharge}$ are the maximum current thresholds, the maximum available currents ($I_{max}^{charg}$ ,$I_{max}^{discharg}$ ), power ($P_{max}^{charg}$ ,$P_{max}^{discharge}$), efficiency ($\eta_{charg}$ ,$\eta_{discha}$ ), and finally energy stored are calculated by the following equations:

$$I_{max,volt}^{charg} = \frac{V_{max} - OCV}{R_0}$$

Equation 5-4: Maximum available current under the voltage limit in charging phase.

$$I_{max,volt}^{discharge} = \frac{OCV - V_{min}}{R_0}$$

Equation 5-5: Maximum available current under the voltage limit in discharging phase.

$$I_{max}^{charg} = \min(I_{max,volt}^{charg}, I_{max,curr}^{charge})$$

Equation 5-6: Maximum available current in charging phase.

$$I_{max}^{discharge} = \min(I_{max,volt}^{discharge}, I_{max,curr}^{discharge})$$

**Equation 5-7: Maximum available current in discharging phase.**

$$P_{max}^{charge} = I_{max}^{charge}(OCV + R_0 I_{max}^{charg})$$

**Equation 5-8: Maximum available Power in charging phase.**

$$P_{max}^{discharg} = I_{max}^{discharge}(OCV - R_0 I_{max}^{discharge})$$

**Equation 5-9: Maximum available Power in discharging phase.**

$$\eta_{charge} = \frac{OCV}{V}$$

**Equation 5-10: Efficiency in charging phase.**

$$\eta_{discharge} = \frac{V}{OCV}$$

**Equation 5-11: Efficiency in discharging phase**

$$Energy = \frac{SOC * C_{rated}}{100}$$

**Equation 5-12: Energy stored in the battery in *Ah.***

It's clearly noticeable that all components of SOF are predicted on the basis of battery state estimation $(SOC, OCV, R_0, C_{rated})$ which can be estimated online or through look-up table or surface function estimated in test laboratory.

# 6 Creating Real World related methods for electric vehicles

Testing cells and batteries components are conceived in order to be coherent or, at least, cautious in predicting performance and durability during real vehicle life. In the recent years, however, the methods for the assessment of performances of the whole vehicle have been deeply modified in order to enhance the overall representativeness in respect to real-world driving. These methods are critical especially for ICE vehicles; an analysis is presented highlighting the potential advantages of the introduction of similar methods in EV testing and development, mainly referring to the case studies proposed in the literature.

## 6.1 The use of Driving Cycle for vehicle performance assessment

According to UNECE regulation 101 [29], the homologation of any road vehicles is subjected to the evaluation of fuel/energy consumption and air emissions according to a procedure which is based on the use of a reference driving cycle. A driving cycle, as known, is a time-speed sequence representing typical vehicle mission [30], where "typical" means that it is built in such a way to be homogeneous to driving data obtained from acquisition campaign or from historical data [31] [32].
During the creation of a driving cycle the objective is, usually, to obtain a compromise between the need to maintain the representativeness of the original data (which can comprehend thousands of kilometres and hours of driving) and the need for a limited duration, which makes it compatible with test-bench verifications and/or driving sessions. Has shown in literature, the duration of most available driving cycle is below one hour [33].
In literature, hundreds of driving cycles are available, and they differ in terms of:

- Class of vehicles: M1/N1 classes, heavy vehicles, L vehicles all show different speed/acceleration distribution, mainly depending on their mass and their power to mass ratio
- Scopes: some cycles are supposed to be used for type approval; in parallel, many alternatives have been developed for applied research and context evaluation or for specific applications by institutes, manufacturers, researchers, depending on the scope of their activity
- Methods for compression: most are based on aggregation of sub-sequences (e.g. microtrips) using techniques for random walk creation or Montecarlo combination
- Evaluation of representativeness of the cycle in comparison with original data, which is done adopting a certain number of indicators (see Table 6-1) and studying the similarity with the same parameters calculated for the general data.

In case of electric vehicles, the evaluation of vehicle range and of energy consumption requires the repetition of the appropriate cycle until a low SOC status or other targets are reached [29]:
*Stopping the discharge occurs:*

*(a) When the vehicle is not able to run at 65 percent of the maximum Thirty minutes speed;*

*(b)Or when an indication to stop the vehicle is given to the driver by the standard onboard instrumentation; or*

*(c)After covering the distance of 100 km.*

Table 6-1 – Parameters describing driving cycle characteristics [34].

| Group | Parameter | Units |
|---|---|---|
| Distance related | Total distance | m |
| Time related | Total time | s |
| | Driving time | s |
| | Cruising time | s |
| | Drive time spent accelerating | s |
| | Drive time spent decelerating | s |
| | Time spent braking | s |
| | Standing time | s |
| | % of time driving | % |
| | % of cruising | % |
| | % of time accelerating | % |
| | % of time decelerating | % |
| | % of time braking | % |
| | % of time standing | % |
| Speed related | Average trip speed | km/h |
| | Average driving speed | km/h |
| | Standard deviation of speed | km/h |
| | Speed: 75th – 25th percentile | km/h |
| | Maximum speed | km/h |
| Acceleration related | Average acceleration | m/s2 |
| | Average positive acceleration | m/s2 |
| | Average negative acceleration | m/s2 |
| | Standard deviation of acceleration | m/s2 |
| | Standard deviation of positive acceleration | m/s2 |
| | Acceleration: 75th – 25th percentile | m/s2 |
| | Number of acceleration per km | [null]/km |
| Stop related | Number of stops | [null] |
| | Number of stops per km | [null]/km |
| | Average stop duration | s |
| | The average distance between stops | m |
| Dynamics related | Relative Positive Acceleration (RPA) | m/s3 |
| | Positive Kinetic Energy (PKE) | m/s2 |
| | Relative positive speed (RPS) | [null] |
| | Relative real speed (RRS) | [null] |
| | Relative square speed (RSS) | m/s |
| | Relative positive square speed (RRSS) | m/s |
| | Relative cubic speed (RCS) | m/s |
| | Relative positive cubic speed (RPCS) | m2/s2 |
| | Relative real cubic speed (RRCS) | m2/s2 |
| | Root mean square of acceleration (RMSA) | m2/s2 |

The main steps of driving cycle creation are shown in Figure 6-1, which represents the synthesis of a short cycle starting from a longer acquisition [35].

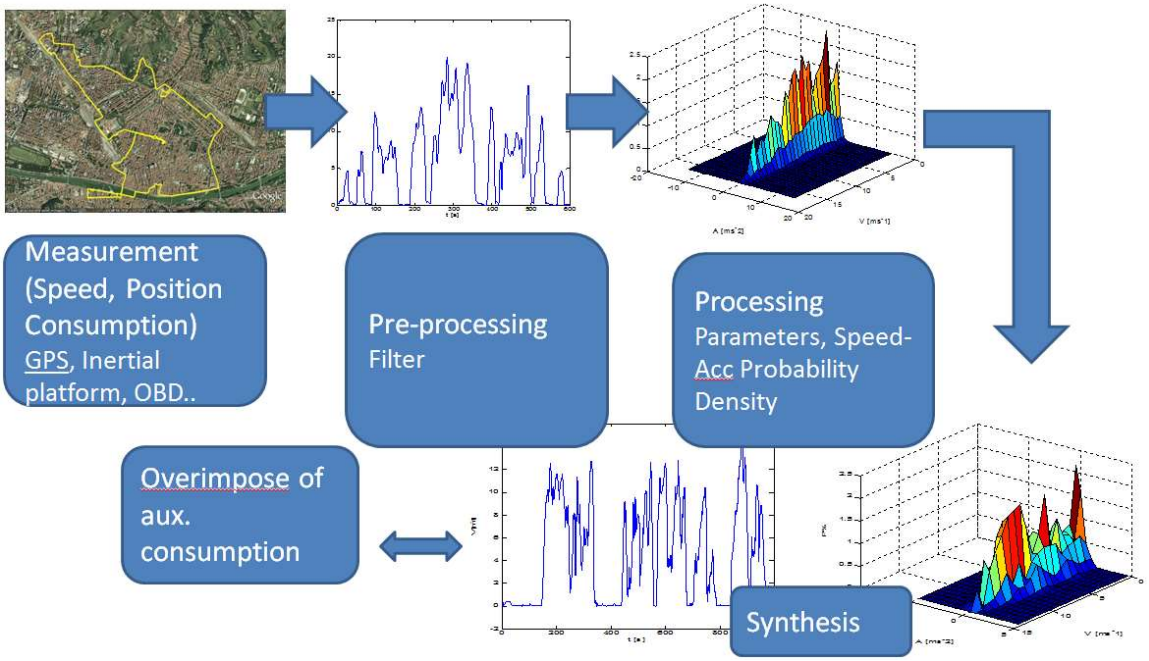


**Figure 6-1 – Driving cycle creation through the syntesis of a "short" cycle equivalent to a longer acquisition. The Velocity-Acceleration density matrix, represented as 3D plot, has been used in this case as the main reference for similarity verification.**

### 6.1.1 The transition from reference driving cycle to real-world assessment

According to the characteristics of the vehicle, the driving cycle together with additional context data (e.g. external temperature, use of auxiliary systems such as lighting and HVAC etc.) also determines the "power and current cycle" to which the battery cells are subjected due to the power used by powertrain and all the other vehicle systems (see Figure 6-2, Figure 6-3). Bench-tests of cells, therefore, are based on the reproduction of such current cycles at subsystem level [36]; in this case, the repetition of the known cycle for a large number of charge-discharge events is adopted.

The known limitation of this approach is the possibility of a polarization of results – in terms of energy/fuel consumption, emissions, overall vehicle set-up - due to the repeatability and the predictability of the cycle itself. This can happen for any kind of vehicle (including ICE/HEV/EV ones). The main consequences of such limitation are:

- Loss of representativeness of the results in comparison with real-world data
- Low capability of the cycles to generate those deviations from normality which could affect durability and reliability of the vehicle
- Scarce suitability of the cycles to be used for advanced vehicles calibration
    - E.g. for the tuning and optimization of the automatic transmission (ICE vehicles) or the development of energy management strategies (HEV vehicles) during the vehicle design phase [37].

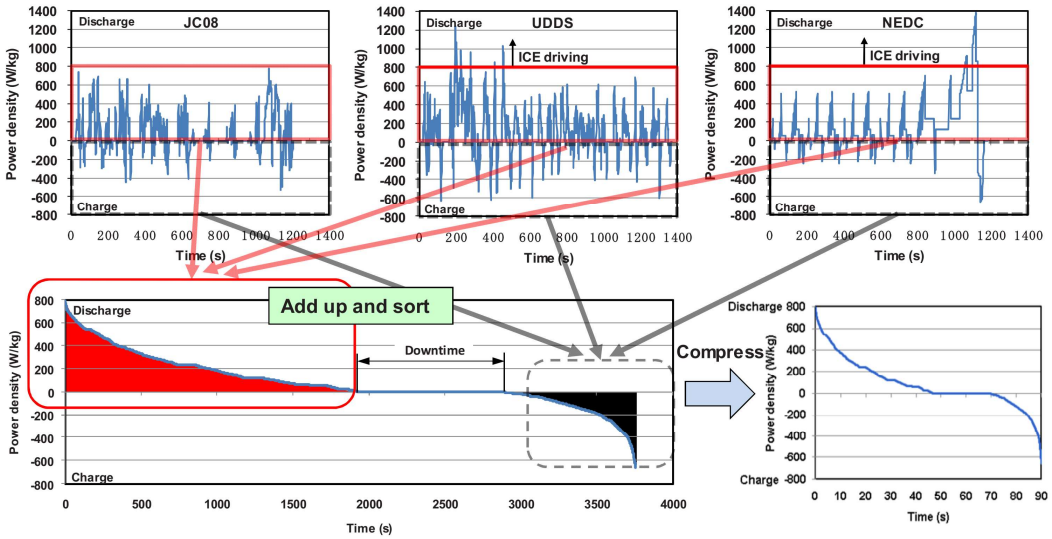


Figure 6-2 – Compression algorithm showing the transition from driving cycle (vehicle level) to "power cycle" (battery level) [36].

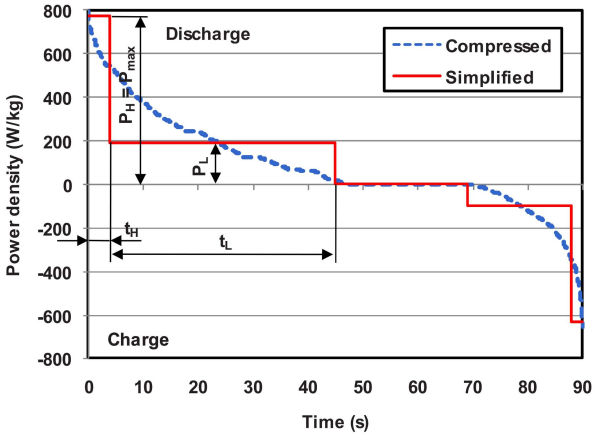


Figure 6-3 – Simplification of power density distribution to an equivalent simplified load profile [36].

For such reason, vehicle testing during development in most cases includes the use of tailored driving cycles [38] [39], together with a large number of road testing activities.
In parallel, a certain number of procedures have been presented in the literature to produced varied cycles, such as:

- Sequencing of more cycles (see Figure 6-4), also varying external temperature, to evaluate conditions similar to a long road test [40]; this approach, however, can be considered superseded by the introduction of WLTC, the most recent driving cycle adopted by EU regulation
- Variation of driving cycle through interrogation of a larger database [34].

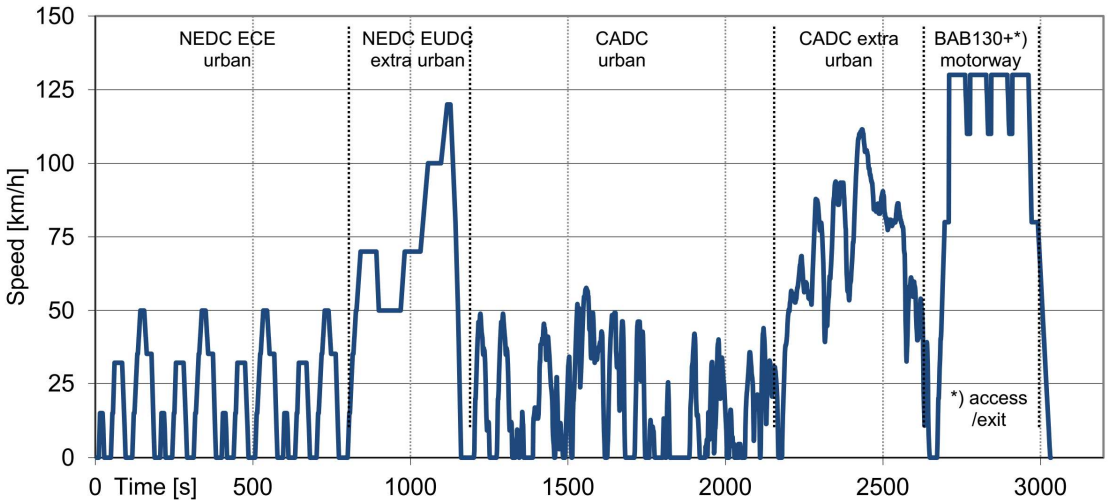


**Figure 6-4 – ECOTEST cycle proposal for estimation of vehicle consumption on various conditions [40].**

At a legislative level, a significant change has been introduced due to the recent came on the force of the Reg. 427/2016 [41], which prescribes:

- The use of the recently created WLTC cycle (all vehicles), which is based on naturalistic driving data and is supposed to be significantly improved in comparison with former reference cycle (NEDC)
- The Real-Driving-Emission (RDE) evaluation procedure for ICE vehicles.

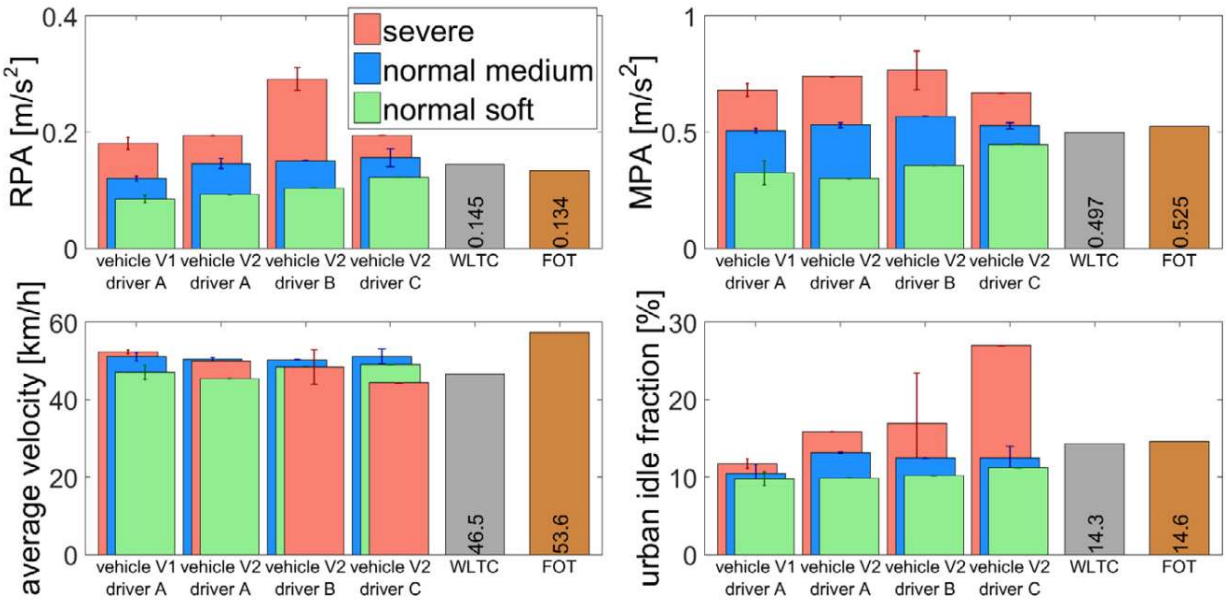


**Figure 6-5 - Driving Dynamics of the RDE trips for different vehicles and drivers over the same route [42].**

This latter point, in particular, is disruptive in comparison with typical procedures due to the fact that the vehicle under test has to be conducted on the open road in order to measure tailpipe emission directly in the using context, using a PEMS (Portable Emission Measurement System) device [43]. Due to the variability of open road driving, the protocol cannot impose any rigid time-speed sequence. The execution of the test can therefore vary depending to variables such as road morphology, traffic, the attitude of the driver, environmental conditions and any other element which can affect the use of the vehicle (see Figure 6-5.)

### 6.1.2 Peculiarities of RDE testing protocol

In order to achieve a certain homogeneity of the RDE tests, various prescription have to be respected in terms of road slope, speed, accelerations and other parameters; however, differently from predetermined driving cycles, such indicators can be verified only in terms of coherence with reference ranges, as clearly shown by an extract from the Regulation [41]:

*6. TRIP REQUIREMENTS*

*6.1. The shares of urban, rural and motorway driving, classified by instantaneous speed as described in points 6.3 to 6.5, shall be expressed as a percentage of the total trip distance.*

*6.2. The trip sequence shall consist of urban driving followed by rural and motorway driving according to the shares specified in point 6.6. The urban, rural and motorway operation shall be run continuously. Rural operation may be interrupted by short periods of urban operation when driving through urban areas. Motorway operation may be interrupted by short periods of urban or rural operation, e.g. when passing toll stations or sections of road work. If another testing order is justified for practical reasons, the order of urban, rural and motorway operation may be altered, after obtaining approval from the approval authority.*

*6.3. Urban operation is characterised by vehicle speeds up to 60 km/h.*

*6.4. Rural operation is characterised by vehicle speeds between 60 and 90 km/h.*

*6.5. Motorway operation is characterised by speeds above 90 km/h.*

*6.6. The trip shall consist of approximately 34 % urban, 33 % per cent rural and 33 % motorway operation classified by speed as described in points 6.3 to 6.5 above. "Approximately" shall mean the interval of ± 10 percent points around the stated percentages. The urban operation shall however never be less than 29 % of the total trip distance.*

*6.7. The vehicle velocity shall normally not exceed 145 km/h. This maximum speed may be exceeded by a tolerance of 15 km/h for not more than 3 % of the time duration of the motorway driving. Local speed limits remain in force at a PEMS test, notwithstanding other legal consequences. Violations of local speed limits per se do not invalidate the results of a PEMS test.*

*6.8. The average speed (including stops) of the urban driving part of the trip should be between 15 and 30 km/h. Stop periods, defined as vehicle speed of less than 1 km/h, shall account for at least 10 % of the time duration of urban operation. Urban operation shall contain several stop periods of 10 s or longer. The inclusion of one excessively long stop period that individually comprises >80 % of the total stop time of urban operation shall be avoided.*

*6.9. The speed range of the motorway driving shall properly cover a range between 90 and at least 110 km/h. The vehicle's velocity shall be above 100 km/h for at least 5 minutes.*

*6.10. The trip duration shall be between 90 and 120 minutes.*

*6.11. The start and the end point shall not differ in their elevation above sea level by more than 100 m.*

*6.12. The minimum distance of each operation: urban, rural and motorway, shall be 16 km.*

It is evident that – as an example – an interval of ± 10 percent points of distance driven in a certain context (urban/extra-urban) is a large tolerance. As a result, every single example of the vehicle is subjected to a test which differs from the others, aiming to catch the variability that a large fleet of the vehicle will experience when driven by the users. In practice, the tests are not exactly predictable neither fully reproducible.

### 6.1.3 Using the RDE approach for Electric and Hybrid Electric vehicles

Even if the RDE procedure is conceived to be functional to verification/type approval needs for a vehicle equipped with ICE motors, the approach proposed is relevant not only for HEV vehicles (to which it is also

dedicated), but also for EVs. EV powertrain systems appear to be less dependent on external factors in comparison with ICE ones; however, a few research questions arise:

- Would it be useful to adopt partially "unpredictable" test procedures for the development and testing phase of EVs?
- Which parameters would be affected by the execution of such tests?
- Which benefits are expected?
- In case of adoption of RDE-similar procedures, how should they differ from ICE RDE to better fit electric vehicles?
- How to build a power (current-voltage) correspondent RDE-type cycle to execute battery or cell test at bench level?
- Should RDE-like test be performed at road level (using the full vehicle) or at the component level, adopting pre-recorded cycles on the test bench? (realizing a kind of offline-RDE test)

As a preliminary evaluation, the transition from predetermined test reproduced in the loop to a naturalistic and/or randomized test could be functional to:

- The setup of energy management strategies at the vehicle level
  - Various sub-routines could be affected by the use of real-world varied cycles, starting from the interaction between regenerative braking and vehicle stability system (a possible factor which could cause a significant difference between expected data and naturalistic data)
- The verification of self-diagnostics procedures (e.g. for the evaluation of SOC and SOH using vehicle on-board devices)
  - RDE-like procedures would generate a varied Current-Voltage response from the cells, thus being a significant test for the assessment method itself
- The setup of battery thermal management system
  - to examine the reaction of the cells and, if present, of their cooling system in case occurrence of unusual but possible events; possible examples are:
    - The repetition of high peak power, which could induce a rapid temperature increase
    - The occurrence of contemporary intense loads (high traction power, the vehicle at full mass, high external temperature, HVAC at full power etc.)
- Estimation of cell ageing according to naturalistic data.

Looking at literature examples, similar approaches have been adopted in other industrial sectors, such as aerospace ( [44]); however, in these cases the test cycles have been obtained through a randomized sequence of discharging currents, a procedure which does not guarantee the realistic probability transition from one state to another.

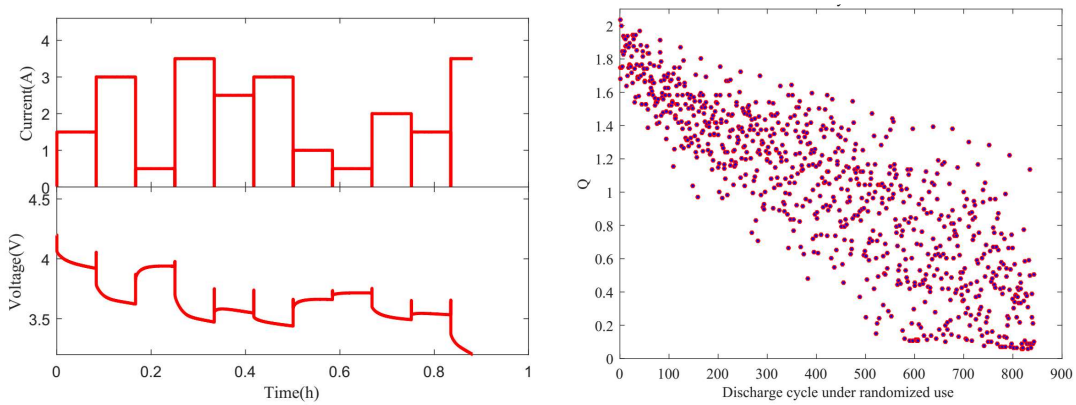


**Figure 6-6 – Example of randomized test for battery degradation characterization. Left: Current/Voltage profile a single randomized test. Right: capacity variation after the execution of various cycles.**

Other similar applications proposed ( [45] [46] [47]) are substantially coherent with the definition of RDE-like procedure. Various other studies have been proposed for the analysis of historical data and their use for the creation of pseudo-randomized vehicle mission, but most of them are related to the development of "smart" control strategies for energy management (a process continuously improved for HEV-PHEV, see [48]) rather than on the proposal of component testing methods and protocols. However, most of these studies adopt a method for which the transition from one power state to another is studied in detailed, due to the need to implement efficient energy management algorithm.

An early procedure which includes most of the points here exposed has been determined in former FP7 ASTERICS project ( [49] [35]), where the data acquired from the observation of EVs used in a naturalistic context have been processed not only for the creation of a single driving cycle, but also the whole data have been made available through a "driving cycle recombination tool" compatible with any Matlab model. The application is shown in Figure 6-7 ( [49]); it can be used to create a time-speed profile of any length rearranging former road acquisitions, binding together existing cycles and/or totally new ones (each row in the "cycle building table" correspond to a different sequence to be bound together with the others). The output of the request consists of a new time-speed driving cycle together with a rough assessment of energy consumption, assuming a certain reference vehicle (see Figure 6-8).


**Figure 6-7 - Driving cycle "binder" tool: main GUI screenshot.**

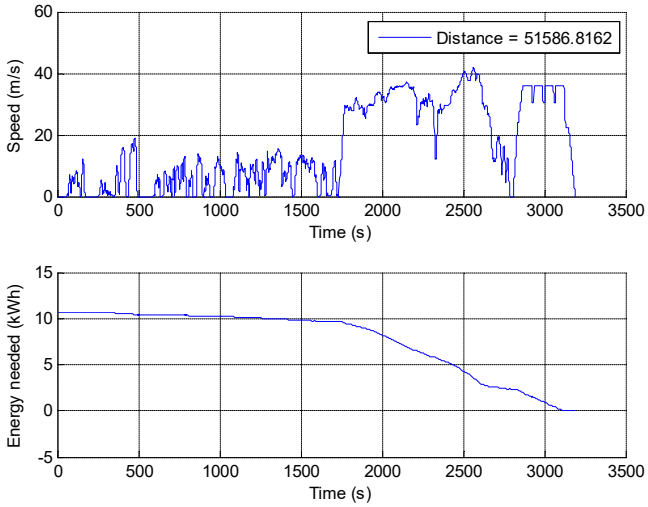


**Figure 6-8 – Typical output from "binder" tool. Upper plot: driving cycle. Lower plot: expected energy consumption.**

## 6.2 The inclusion of real-world data in the component testing application

In the present paragraph, a reference procedure for the application of RDE-like procedures to cell test-bench is proposed according to literature experiences. The objective is to create a set of data including various potential driving situations, preferably coming from real-world measurements. The approach is in accordance with the expected increasing availability of data coming from "big data" sources related to smartphone and Internet of Things application diffusion; such data need proper processing to exploit their potential in component testing-development.

To achieve the target, the main steps needed are:

1. Acquisition of "real world" driving data and creation of datasets
    a. From customers
    b. From testing campaign
    c. From simulation
    d. From ICT sources of any type
2. Processing of the data in order to identify their distributions in terms of:
    a. Frequency occurrence of certain driving situation and grouping of homogeneous events
        i. Through not pre-determined classes (e.g. using k-means algorithms, able to identify – within certain limits – existing clusters from a large group)
        ii. Through regression models, e.g. based on relevant external parameters related to the source (e.g. business/private customers; the city of origin; age/sex of drivers etc.)
    b. The probability of transition from a certain status to another different one
        i. Context transition: from urban to extra-urban/highway driving
        ii. Driving style transition: from stop-and-go (e.g. due to traffic) to fluent driving and vice-versa
    c. Identification of speed-acceleration matrix
    d. Identification of user habits, in terms of day-hour use, trip chaining and similar data
        i. To know its typical charging strategy (probability of occurrence of fast charging events, typical distance driven between two charges, day-by-day initial and final SOC distribution and other)
        ii. To synchronize related meteorological relevant data, with particular reference to external temperature

    e. Identification of vehicle accessory information, such as loaded mass and energy consumption from auxiliaries
3. Processing of the data, mostly recorded in terms of time/speed, switching from “speed” information to “power-current” information
    a. Calculation of power on the battery starting from dynamic data, assuming a proper calibrated simulation model
    b. If power is available, an adaptation of power level according to the context information available for the application (temperature, SOC, loaded mass)
4. Packing of the results in a proper data structure, which should be suitable for
    a. Interrogation of the database at any moment, to extract existing cycles from the database according to specific query
    b. Recombination of the data using a proper randomization method (e.g. random walk) and creation of totally new sequences, even if still coherent with the parameters defined at point 2.
5. Communication with external tools
    a. Simulation software, to use the processed data as input for simulation
    b. Test bench environment, to use the processed data directly to define the load

If such method is applied in case of durability test, the data sent to the external tools have to be stored for ex-post comparison. The final result of a similar test should include the calculation of overall parameters during the testing phase, such as C-rate distribution, distribution of power loads, of resulting SOC, of temperature distribution, thus summarizing in a few elements a large amount of data processed during various weeks and months of testing.

Figure 6-9 clarifies the whole approach. Assuming that a database of real-world driving data is available from the acquisition, the data are recombined creating a different mission profile for each battery charge-discharge event. Mission profile should include at least:

- A randomized driving cycle, varying its distance depending on the day of the year
- powertrain configuration (if it is dependent on the user, on the setting, on other external information)
- additional data related to mass transported by the vehicle mass and starting SOC, depending on last charging event
- ambient/environmental data such as temperature and wind.

Pseudo- randomized mission, obtained from Montecarlo extraction, can be applied on a model or on other emulation test-bench obtaining the power profile to be applied at cell or battery level.
Application of the method have been presented at simulation level ( [50]); a simulation plan equivalent to 3 years of use (1095 events of vehicle use) has been executed.

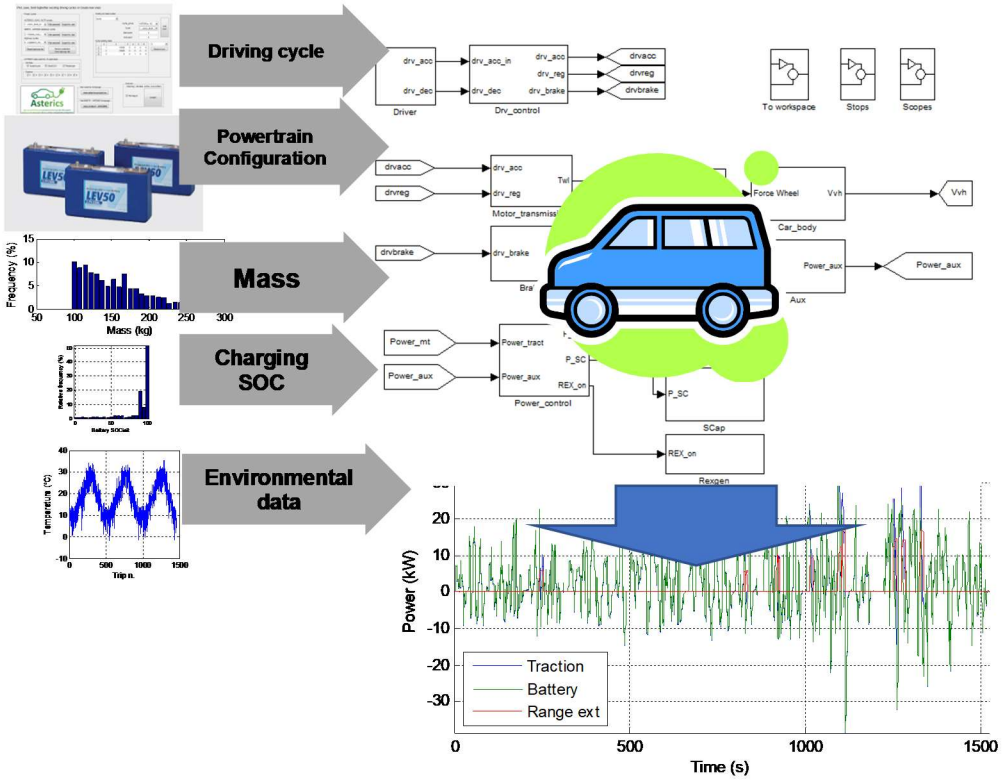


Figure 6-9 – Summary of the RDE-like approach for battery power profile creation (adapted from [50]).

## 6.3 Conclusion

In this chapter a brief introduction to real-world driving cycle according to recent vehicle regulation is presented. The adoption of methods for the acquisition, the treatment and the recombination of the data coming from road driving are suggested as a way to create new power/current profile to be proposed for cell and battery testing, aiming to switch from known sequence repetition to randomized mission creation. Similarly, to the RDE method for conventional vehicles, a better adherence to reality is expected in terms of durability, performance, efficiency assessment; however, the loss of full repeatability of the model is unavoidable. The implementation of the method requires the development of a database of real-world data, the proposal of a proper synthesis/recombination and data extraction method, and the assessment of battery power cycle starting from vehicle speed, so that a calibrated vehicle model and/or an emulation device is necessary.

# 7 References


[1] R. F. M. Wohlecker, "Battery Safety and Electric Vehicle Benchmarking.," *EGVI Expert Workshop on Testing of Electric Vehicle Performance and Safety, Brussels,* 2014.

[2] "ISO26262 “Road vehicles—Functional safety”," *ISO, Geneva,* 2011.

[3] "Electrically propelled road vehicles – Test specification for lithium-ion traction battery packs and systems Part 3: safety performance requirements," *The British Standards Institution,* 2014.

[4] C. Z. R. D. A. K. A. M. T. Debes, "Mulitiaxial Vibraion Testing of Inertia Force Related Components of EV.," *Proceedings of the 5th Symposium on Structural Durability in Darmstadt,* 2017.

[5] M. B.V., "Moog Replication – Application for signal editing, replication; sequence editing, playout, test, monitoring and control," *Nieuw-Vennep,* 2014.

[6] J. N. Matthias Rauschenbach, "A novel approach to the quantitative evaluation of reliability of complex systems within FMEA.," *DVM Workshop “Reliability of mechatronic and adaptronic systems”, Munich,* 2018.

[7] Elie Riviere, Pascal Venet, Ali Sari, Frederic Meniere, Yann Bultel,, "LiFePO4 Battery State of Health Online Estimation Using Electric Vehicle Embedded Incremental Capacity Analysis," in *2015 IEEE Vehicle Power and Propulsion Conference (VPPC),* , Montreal, QC, Canada., 2015.

[8] C. Zhang, K. Li, J. Deng and S. Song, "Improved Realtime State-of- Charge Estimation of LiFePO4 Battery Based on a Novel Thermoelectric Model," *IEEE Transactions on Industrial Electronics,* vol. 64, no. 1, pp. 654-663, 2017.

[9] "ISO 12405-1, “Electrically propelled road vehicles – test specification for lithium-ion traction battery packs and systems Part 1: high-power applications”," 2011.

[10] "ISO 12405-2, “Electrically propelled road vehicles – test specification for lithium-ion traction battery packs and systems Part 2: high-energy applications”," 2011.

[11] T. Huria, G. Ludovici, G. Lutzemberger, "State of charge estimation of high power lithium iron phosphate cells," *Journal of Power Sources,* vol. 249, pp. 92-102, 2014.

[12] D. U. S. Michael A. Roscher, "Dynamic electric behavior and open-circuit-voltage modeling of LiFePO4-based lithium ion secondary batteries," *Journal of Power Sources,* vol. 196, pp. 331-336, 2011.

[13] T. W. R. L. C. Z. Lei Pei, "Development of a voltage relaxation model for rapid open-circuit voltage prediction in lithium-ion batteries," *Journal of power source,* vol. 253, pp. 412-418, 2014.

[14] Y. S. N. C. J. L. X. H. Yonghuang Yea, "Electro-thermal modeling and experimental validation for lithium ion battery," *Journal of Power Sources,* vol. 199, pp. 227-238, 2012.

[15] Y. Maeda, A. Kurokawa, K. Morita, D. Imamura , "Analysis of the Relationship Between Actual Usage Conditions of Electric Vehicles and Battery Performance Degradation in the Real World," *JARI Research Journal,* 2016.

[16] T. G. J. M. Jakobus Groenewald, "Accelerated energy capacity measurement of lithium-ion cells to support future circular economy strategies for electric vehicles," *Renewable and Sustainable Energy Reviews,* vol. 69, pp. 98-111, 2017.

[17] L. P. L. B. M. P. A. P. Edoardo Locorotondo, "Online State Of Health Estimation of Lithium-Ion batteries based on improved Ampere-Count Method," in *IEEE Conference on environment and electrical engineering* , Palermo, 2018.

[18] W. Z. N. F. H. R.-E. ,. R. R. S. R. R. S. a. M.-Y. C. F. Baronti, "Parameter identification of Li-Po batteries in electric vehicles: A comparative study," in *IEEE International Symposium on Industrial Electronics*, Taipei, Taiwan, 2013.

[19] L. P. L. B. M. P. G. L. Edoardo Locorotondo, "Online identification of Thevenin equivalent circuit model parameters and estimation state Of Charge of Lithium-Ion batteries," in *IEEE Conference on environment and electrical engineering*, Paleromo, 2018.

[20] L. Ljung, "System Identification - Theory for the User," Prentice Hall, 1999.

[21] M. M. K. S. C. W. T. S.-G. D. S. D. Andrea, "Characterization of high-power lithium-ion batteries by electrochemical impedance spectroscopy. I. Experimental investigation," *Journal of Power Sources,* vol. 196, pp. 5334-5341, 2011.

[22] M. M. K. S. H. W. T. S.-G. D. S. D. Andrea, "Characterization of high-power lithium-ion batteries by electrochemical impedance spectroscopy. II: Modelling," *Journal of Power Sources,* vol. 196, pp. 5349-5356, 2011.

[23] S. K. D. U. S. Wladislaw Waag, "Experimental investigation of the lithium-ion battery impedance characteristic at various conditions and aging states and its influence on the application," *Applied Energy,* vol. 102, pp. 885-897, 2013.

[24] H.P.G.J. Beelen, L.H.J. Raijmakers, M.C.F. Donkers, P.H.L. Notten, H.J. Bergveld, "A comparison and accuracy analysis of impedance-based temperature estimation methods for Li-ion batteries," *Applied Energy,* vol. 175, pp. 128-140, 2016.

[25] L.H.J. Raijmakers, D.L. Danilov, J.P.M. van Lammeren, M.J.G. Lammers, P.H.L. Notten, "Sensorless battery temperature measurements based on electrochemical impedance spectroscopy," *Journal of Power Sources,* vol. 247, pp. 539-544, 2014.

[26] R. Al Nazer, V. Cattin, P. Granjon, Maxime Montaru, and M. Ranieri, "Broadband Identification of Battery Electrical Impedance for HEVs," *IEEE Transactions on vehicular technology,* vol. 62, 2013.

[27] L.H. J. Raijmakers, D.L. Danilov, J.P.M. van Lammeren, T.J.G. Lammers, H. Jan Bergveld, and P.H. L. Notten, "Non-Zero Intercept Frequency: An Accurate Method to Determine the Integral Temperature of Li-Ion Batteries," *IEEE Transactions on industrial eletronics,* p. 63, 2016.

[28] Lin X., Stefanopoulous A. G., Perez H. E., Siegel J.B., Li Y., Anderson R. D., "Quadruple adaptive observer of the core temperature in cylindrical Li-ion batteries and their health monitoring," in *American Control Conference*, 2012.

[29] UNECE, " Regulation No. 101 - Rev.3 - CO2 emission/fuel consumption," 2018. [Online]. Available: http://www.unece.org/fileadmin/DAM/trans/main/wp29/wp29regs/R101r3am3e.pdf. [Accessed 21 04 2018].

[30] J. R. Kenworthy, P. W. G. Newman and T. J. Lyons, "The ecology of urban driving I — methodology," *Transportation Research Part A: Policy and Practice,* vol. 26, pp. 263-272, 5 1992.

[31] H. Y. Tong and W. T. Hung, "A Framework for Developing Driving Cycles with On-Road Driving Data," *Transport Reviews,* vol. 30, pp. 589-615, 2010.

[32] J. D. K. Bishop, C. J. Axon and M. D. McCulloch, "A robust, data-driven methodology for real-world driving cycle development," *Transportation Research Part D: Transport and Environment,* vol. 17, pp. 389-397, 7 2012.

[33] T. J. Barlow, S. Latham, I. S. McCrae and P. G. Boulter, "A reference book of driving cycles for use in the measurement of road vehicle emissions," *A reference book of driving cycles for use in the measurement of road vehicle emissions,* vol. 1, pp. 1-280, 11 2009.

[34] L. Berzi, M. Delogu and M. Pierini, "Development of driving cycles for electric vehicles in the context of the city of Florence," *Transportation Research Part D: Transport and Environment,* vol. 47, pp. 299-322, 8 2016.

[35] R. C. B. H. B. L. Borgarello L., "A methodology to build vehicle “mission profile” - ASTERICS D1.4," 2013.

[36] M. Conte, F. V. Conte, I. D. Bloom, K. Morita, T. Ikeya and J. R. Belt, "Ageing Testing Procedures on Lithium Batteries in an International Collaboration Context," 2010.

[37] M. Montazeri, A. Fotouhi and A. Naderpour, "Driving segment simulation for determination of the most effective driving features for HEV intelligent control," *Vehicle System Dynamics,* vol. 50, pp. 229-246, 2012.

[38] L. Borgarello, E. Galliera, A. Avanzo and A. Fagiano, "Roller bench urban cycles identification for light commercial vehicles fuel consumption," *Italian Journal of Applied Statistics,* vol. 22, pp. 353-362, 2010.

[39] J. Lin and D. A. Niemeier, "Regional driving characteristics, regional driving cycles," *Transportation Research Part D: Transport and Environment,* vol. 8, pp. 361-381, 9 2003.

[40] B. Geringer and W. E. Tober, "Battery Electric Vehicles in Practice, Costs, Range, Environment, Convenience

- 2nd extended and corrected edition," 2012.

[41] E. Commission, *Commission Regulation (EU) 2016/427 of 10 March 2016 amending Regulation (EC) No 692/2008 as regards emissions from light passenger and commercial vehicles (Euro 6) (Text with EEA relevance),* 2016.

[42] J. Gallus, U. Kirchner, R. Vogt and T. Benter, "Impact of driving style and road grade on gaseous exhaust emissions of passenger vehicles measured by a Portable Emission Measurement System (PEMS)," *Transportation Research Part D: Transport and Environment,* vol. 52, pp. 215-226, 5 2017.

[43] T. Donateo and M. Giovinazzi, "Building a cycle for Real Driving Emissions," *Energy Procedia,* vol. 126, pp. 891-898, 9 2017.

[44] J. Yu, B. Mo, D. Tang, J. Yang, J. Wan and J. Liu, "Indirect State-of-Health Estimation for Lithium-Ion Batteries under Randomized Use," *Energies,* vol. 10, p. 2012, 12 2017.

[45] B. Bole, C. S. Kulkarni and M. Daigle, "Adaptation of an Electrochemistry-based Li-Ion Battery Model to Account for Deterioration Observed Under Randomized Use," 2014.

[46] L. Ungurean, G. Cârstoiu, M. V. Micea and V. Groza, "Battery state of health estimation: a structured review of models, methods and commercial devices," *International Journal of Energy Research,* vol. 41, pp. 151-181, 2 2017.

[47] K. P. Divakarla, S. Nalakath, M. Drennan, R. Ahmed, A. Emadi and S. Razavi, "Battery characterization and state-of-charge prediction for different journey conditions with the help of the journey mapping concept," in *IECON 2015 - 41st Annual Conference of the IEEE Industrial Electronics Society*, 2015.

[48] S. J. Moura, H. K. Fathy, D. S. Callaway and J. L. Stein, "A stochastic optimal control approach for power management in plug-in hybrid electric vehicles," *Control Systems Technology, IEEE Transactions on,* vol. 19, pp. 545-555, 2011.

[49] P. M. Berzi L., "A tool to build vehicle “mission profile” - ASTERICS D1.5," 2014.

[50] L. Berzi, M. Delogu and M. Pierini, "A comparison of electric vehicles use-case scenarios: Application of a simulation framework to vehicle design optimization and energy consumption assessment," in *2016 IEEE 16th International Conference on Environment and Electrical Engineering (EEEIC)*, 2016.

[51] "Deliverable D7.2".

[52] P. Shen , M. Ouyang, L. Lu, J. Li, "The Co-estimation of State of Charge, State of Health, and State of Function for Lithium-Ion Batteries in Electric Vehicles," *IEEE Transactions on vehicular technology,* vol. 67, 2018.

[53] V. Schwarzer and R. Ghorbani, "Drive Cycle Generation for Design Optimization of Electric Vehicles," *IEEE Transactions on Vehicular Technology,* vol. 62, pp. 89-97, 2013.

[54] L. Miegeville, P. Guerin and D. Dreulle, "Investigation of Correlations between Driving Patterns and Power Demand of Auxiliary Devices Aboard Military Vehicles," in *IEEE Vehicle Power and Propulsion Conference (VPPC)*, 2014.

[55] T. Kok, A. Morris, H. Scott and D. Baglee, "The Use of Markov Chain Analysis for Rule-Based Power and Energy Management Optimisation in Electric Vehicles," in *European Battery, Hybrid and Fuel Cell Electric Vehicle Congress*, Brussels, 2015.

[56] G. Souffran, L. Miegeville and P. Guerin, "Simulation of Real-World Vehicle Missions Using a Stochastic Markov Model for Optimal Powertrain Sizing," *IEEE Transactions on Vehicular Technology,* vol. 61, pp. 3454-3465, 2012.

# 8 Acknowledgement

The author(s) would like to thank the partners in the project for their valuable comments on previous drafts and for performing the review.

**Project partners:**

| Partner no. | Partner organisation name | Short Name |
|---|---|---|
| **1** | AVL List GmbH | AVL |
| **2** | Centro Richerche Fiat SCpA | CRF |
| **3** | FORD Otomotiv Sanayi Anonim sirketi | FO |
| **4** | Renault Trucks SAS | RT-SAS |
| **5** | AVL Software and Functions GmbH | AVL-SFR |
| **6** | Robert Bosch GmbH | Bosch |
| **7** | SIEMENS INDUSTRY SOFTWARE NV | SIE-NV |
| **8** | SIEMENS Industry Software SAS | SIE-SAS |
| **9** | Uniresearch BV | UNR |
| **10** | Valeo Equipements Electroniques Moteurs | Valeo |
| **11** | Commissariat à l'Energie Atomique et aux Energies Alternatives | CEA |
| **12** | LBF Fraunhofer | FhG-LBF |
| **13** | FH Joanneum Gesellschaft M.B.H. | FHJ |
| **14** | National Institute of Chemistry | NIC |
| **15** | University Ljubljana | UL |
| **16** | University Florence | UNIFI |
| **17** | University of Surrey | US |
| **18** | Das Virtuelle Fahrzeug Forschungsgesellschaft mbH | VIF |
| **19** | Vrije Universiteit Brussel | VUB |



This project has received funding from the European Union's Horizon 2020 research and innovation programme under grant agreement No 769506.

# 9 Appendix B (Abbreviations and Definitions)

## 9.1 Abbreviations

| Abbreviated term | Definition |
|---|---|
| **BEV** | Battery Electric Vehicle |
| **BOL** | Battery Electric Vehicle |
| **$C_{actre}$** | Actual Reference Capacity |
| **CC** | Constant Current |
| **CHA** | Charge |
| **$C_{nom}$** | Nominal Capacity |
| **C-Rate** | Current Rate |
| **CU** | Checkup |
| **CV** | Constant Voltage |
| **CVL** | Maximum voltage |
| **DVL** | Minimum voltage |
| **EIS** | Electrochemical Impedance Spectroscopy |
| **EOCV** | End of Charge Voltage |
| **EODV** | End of Discharge Voltage |
| **EOL** | End of Life |
| **EOT** | End of Test |
| **HPPC** | Hybrid pulse power characterization |
| **IPIT** | Impedance Parameter Identification Test |
| **OCV** | Open Circuit Voltage |
| **PAU** | Pause |
| **RT** | Room temperature |

| | |
|---|---|
| **S-CHA** | Standard Charge |
| **SOH** | State of Health (First Life) |
| **ΔC** | Capacity Fade |